

# Capturing impurities from oil and gas using deep eutectic solvents

**Citation for published version (APA):**

Warrag, S. E. E. (2018). *Capturing impurities from oil and gas using deep eutectic solvents*. [Phd Thesis 1 (Research TU/e / Graduation TU/e), Chemical Engineering and Chemistry]. Technische Universiteit Eindhoven.

**Document status and date:**

Published: 03/07/2018

**Document Version:**

Publisher's PDF, also known as Version of Record (includes final page, issue and volume numbers)

**Please check the document version of this publication:**

- A submitted manuscript is the version of the article upon submission and before peer-review. There can be important differences between the submitted version and the official published version of record. People interested in the research are advised to contact the author for the final version of the publication, or visit the DOI to the publisher's website.
- The final author version and the galley proof are versions of the publication after peer review.
- The final published version features the final layout of the paper including the volume, issue and page numbers.

[Link to publication](#)

**General rights**

Copyright and moral rights for the publications made accessible in the public portal are retained by the authors and/or other copyright owners and it is a condition of accessing publications that users recognise and abide by the legal requirements associated with these rights.

- Users may download and print one copy of any publication from the public portal for the purpose of private study or research.
- You may not further distribute the material or use it for any profit-making activity or commercial gain
- You may freely distribute the URL identifying the publication in the public portal.

If the publication is distributed under the terms of Article 25fa of the Dutch Copyright Act, indicated by the "Taverne" license above, please follow below link for the End User Agreement:

[www.tue.nl/taverne](http://www.tue.nl/taverne)

**Take down policy**

If you believe that this document breaches copyright please contact us at:

[openaccess@tue.nl](mailto:openaccess@tue.nl)

providing details and we will investigate your claim.

# Capturing Impurities from Oil and Gas Using Deep Eutectic Solvents

PROEFSCHRIFT

ter verkrijging van de graad van doctor aan de Technische Universiteit Eindhoven, op  
gezag van de rector magnificus prof.dr.ir. F.P.T. Baaijens,  
voor een commissie aangewezen door het College voor Promoties, in het openbaar te  
verdedigen op dinsdag 3 juli 2018 om 16:00 uur

door

Samah Esam-Eldin Warrag

Geboren te Gainesville, Florida,  
Verenigde Staten van Amerika

Dit proefschrift is goedgekeurd door de promotoren en de samenstelling van de promotiecommissie is als volgt:

voorzitter:	prof.dr.ir. E.J.M. Hensen
1 <sup>e</sup> promotor:	prof.dr.ir. M. van Sint Annaland
2 <sup>e</sup> promotor:	prof.dr.ir. C.J. Peters (Colorado School of Mines)
Copromotor(en):	prof.dr.ir. M.C. Kroon (Khalifa University of Science and Technology, Petroleum Institute University and Research Center)
leden:	prof.dr. I.J. Siepmann (University of Minnesota) prof.dr.ir. B. Schuur (Universiteit Twente) prof.dr.ir. R. Tuinier
adviseur(s):	dr. M. Mooijer-van den Heuvel (Shell Global Solutions International BV)

*Het onderzoek of ontwerp dat in dit proefschrift wordt beschreven is uitgevoerd in overeenstemming met de TU/e Gedragscode Wetenschapsbeoefening.*



A catalogue record is available from the Eindhoven University of Technology Library.

ISBN: 978-90-386-4522-3

Printed by: Gildeprint <http://www.gildeprint.nl/nl/>

This research project was funded by the Petroleum Institute Research Center (PIRC) through a grant entitled “Advanced PVT-Properties and Molecular Modeling of Complex Fluids in Support of Safe and Green Hydrocarbon Production” (Project Code: LTR14009), United Arab Emirates, Abu Dhabi

*To*

*My parents*

*My grandparents*

*My husband*

*My siblings*

## Summary

### *Capturing Impurities from Oil and Gas Using Deep Eutectic Solvents*

In broad terms, chemical engineers design processes to produce and transform matters. Starting with laboratory experimentation, followed by implementation of the technology in plant-scale production. The chemical engineering profession was established in the 19<sup>th</sup> century. During that era, liquid solvents such as toluene, benzene, dichloromethane, acetonitrile, methanol, ethanol, and other solvents generally known as ‘volatile organic compounds’ (VOCs) were already known and applied for controlling reactions, performing separations and processing materials. Despite their efficiency, hydrogen-bonding ability and a wide range of polarity, these solvents suffer from toxicity, flammability, and relatively narrow liquidus region, ranging from 75 to perhaps 200 °C, and therefore undesirably volatile at several processes’ conditions. Within these constraints, chemical engineers have contributed to design processes, making numerous valuable products and breakthrough inventions that have immeasurably improved the world. Nevertheless, according to Allen and Shonnard, 20 million ton of VOCs is discharged into the atmosphere each year as a result of industrial processing operations leading to global climate change, poor air quality, and adverse health impact. And operationally, the volatility of the VOCs may lead to complicated and often costly solvent recovery. This poses a new challenge to chemical engineers; providing valuable products, while at the same time significantly reduce the economical and environmental impact.

A few decades ago, a novel class of solvents has emerged, the so-called ionic liquids (ILs). The most pronounced property of ILs is that they essentially have negligible vapor pressure “non-volatile” and thus reduced emissions, remarkable solvation properties, low flammability and tunable physicochemical properties. Thus, ILs have been widely investigated as alternatives to VOCs. Moreover, many of ILs are liquids over large temperature ranges, from below ambient to well over 300 °C, which opens up the possibility for their use under unique processing conditions. The discovery of ILs was the key to inspire chemical engineers to investigate novel process designs with increased efficiency and that are more environmentally benign. However, the synthesis of ILs involves several costly synthetic steps that often result in by-products and waste generation which hampered their utilization on an industrial scale.

In 2003, a new generation of solvents, the so-called deep eutectic solvents (DESs), was reported for the first time. DESs are composed of at least one hydrogen bond donor (HBD) and at least one hydrogen bond acceptor (HBA), which can be associated with each other via hydrogen bond interactions to form a mixture with a melting temperature far below that of its constituents. The hydrogen bonding interactions contribute to a large extent to the low vapor pressure that is usually observed in DESs. In that sense, DESs were known as analogous to ILs. However, DESs can simply be prepared by mixing low cost, readily available and often biodegradable starting materials HBD and HBA with no further

purification. Beside the low volatility “wide liquidus range”, low production cost, simple synthesis process, and good biocompatibility, the physicochemical properties of the DESs can be designed by altering the HBA and HBD to suit the considered application. The attractive properties of DESs being environmentally friendly with reduced economical impact were the driving force for many chemical engineers to consider DESs as alternatives for both VOCs and ILs in several applications.

DESs were investigated in a wide range of applications such as chemical synthesis, biochemistry, separation technologies, electrochemistry, and catalysis amongst other processes. In this thesis, the performance of DESs for the capture of impurities from oil and gas was investigated. The main objective was to propose a novel solution to some industrial challenges in the purification of oil and gas, and in particular, the extraction of mercury, CO<sub>2</sub> capture from flue gases, and oil desulfurization. A series of equilibrium experiments were performed to assess the workability of the DESs for the different applications from a thermodynamics point of view.

On a commercial scale mercury is captured from liquid/gaseous hydrocarbon streams via adsorption in activated carbon beds. Due to the high cost associated with this approach, researchers have considered other technologies such as: chemical absorption, reactive absorption and extraction using ILs. These methods were found to be either inefficient or expensive. Therefore, in this work, the removal of elemental mercury using DESs from oil was considered. Four DESs were investigated including choline chloride: urea, choline chloride: ethylene glycol, choline chloride: levulinic acid and betaine: levulinic acid, using a molar ratio of 1:2 in all cases. Their performance for mercury extraction was assessed experimentally using saturated solutions in *n*-dodecane as the oil model. The effect of the solvent to feed ratios and temperature was studied. An extraction efficiency above 80% was obtained for all four DESs. The efficiency of the DESs together with their low cost made them a very attractive solvent for mercury capture from oil.

Moreover, the application of DESs as absorbents for CO<sub>2</sub> capture from flue gas was studied. Typically, post-combustion capture of CO<sub>2</sub> in power plants involves the use of VOCs such as monoethanolamine (MEA). As mentioned earlier, the use of VOCs is associated with environmental and economic concerns. Finding alternatives that can be nonvolatile and efficient is highly desirable. Two DESs constituted of tetrahexylammonium bromide as HBA and either ethylene glycol or glycerol as HBD were investigated as sustainable absorbents for CO<sub>2</sub> capture. The phase behavior of CO<sub>2</sub> with the DESs was measured using a gravimetric magnetic suspension balance operating in the static mode at 293.2 and 298.2 K and pressures up to 2 MPa. The CO<sub>2</sub> solubilities in the studied DES were found to be lower than the benchmark solvents. Nonetheless, DESs are a promising class of absorbents because of their low cost starting materials and preparation, their environmentally friendly character, and their tunability which allows further optimization for CO<sub>2</sub> capture.

Catalytic hydrodesulfurization is the common process that is used in the industry to achieve low sulfur concentrations in oil fuels. However, it is usually conducted at relatively high pressure and temperature resulting in an expensive and energy-consuming process. Aiming to reduce the energy



requirements of this separation, liquid–liquid extraction is considered. VOCs and ILs have been widely studied for extractive desulfurization of oil fuels. Nonetheless, they either raised safety and environmental concerns due to their volatilities (in the case of VOCs) or being not economically attractive (in the case of ILs). Therefore, desulfurization of oil fuels using DESs was studied in this work. Six DESs based on tetraethylammonium chloride, tetrahexylammonium bromide and methyltriphenylphosphonium bromide as HBAs and polyols (ethylene glycol and glycerol) as HBDs have been experimentally investigated for the extraction of sulfur derivatives from two aliphatic hydrocarbons, *n*-hexane and *n*-octane, via liquid-liquid equilibrium (LLE). The objective of this study was to provide insights on: (i) the LLE for {*n*-alkane + thiophene + DESs} systems, (ii) the effect of type/length of the *n*-alkane, (iii) the influences and/or characteristics of the HBAs, such as the different chain length of the alkyl group and the functional group on the ammonium cation, (iv) the influences and/or characteristics of the HBDs, particularly the type of the polyol on the extraction of thiophene from an {*n*-alkane + thiophene} mixture. To evaluate the separation capability of the studied DESs, the solute distribution ratio and the selectivity were calculated from the experimental LLE data and compared to relevant literature data. Moreover, the extraction mechanism of the thiophene using DESs was explained using the *COnductor-like Screening MOdel for Real Solvents (COSMO-RS)*. Furthermore, the phase behavior of the LLE ternary systems {*n*-alkane + thiophene + DES} was predicted using Perturbed-Chain Statistical Associating Fluid Theory (PC-SAFT). It was concluded that DESs are promising candidates for extractive desulfurization of fuels and that PC-SAFT serves as an appropriate approach for predictive solvent screening in order to obtain thermodynamically optimal DESs.

A sensitivity analysis of the liquid extraction column for the separation of thiophene from {*n*-hexane + thiophene} mixtures using DESs, was performed via Aspen Plus<sup>®</sup>. Four different DESs composed of tetraethylammonium chloride, tetrahexylammonium bromide and as HBA and polyols (ethylene glycol and glycerol) as HBD were selected for this extraction. The influences of the solvent-to-feed ratio and the number of equilibrium stages on (i) the thiophene recovery, (ii) the *n*-alkane recovery, (iii) the mass fraction of the thiophene in the extract stream, and (iv) the mass fraction of the *n*-alkane in the raffinate stream, were studied. It was found that with tetraethylammonium chloride:ethylene glycol (1:2) DES, a recovery of the *n*-alkane and thiophene greater than 98% can be achieved in an extraction column of 10 equilibrium stages or more with a solvent-to-feed ratio of 3 or more.

To conclude, DESs are still a new field of research. More in-depth fundamental studies and more experimental data are highly desirable, such as characterization data, phase behavior and molecular interactions within the DES. The promising results described in this thesis are encouraging and merit further research and optimization for their use in various separation processes in the oil and gas industry, as well as in other chemical and process industries

## Table of Contents

Summary .....	I
1 INTRODUCTION.....	1
1.1 Problem definition and motivation.....	2
1.2 Scope of the thesis.....	5
1.3 References .....	7
2 BACKGROUND.....	9
2.1 Introduction to ionic liquids .....	10
2.1.1 Properties of ionic liquids.....	11
2.1.2 Future perspectives.....	12
2.2 Introduction to deep eutectic solvents (DESs).....	12
2.2.1 Properties of deep eutectic solvents.....	14
2.2.2 Applications of DESs.....	15
2.2.3 Challenges and future perspectives .....	20
2.3 Abbreviations .....	20
2.4 References .....	22
3 MERCURY CAPTURE FROM <i>n</i> -DODECANE USING DEEP EUTECTIC SOLVENTS.....	27
3.1 Introduction .....	28
3.2 Experimental procedures.....	29
3.2.1 Materials and DES preparation .....	29
3.2.2 DES characterization.....	30
3.2.3 Mercury extraction experiments.....	31
3.3 Results and discussion.....	31
3.3.1 DES characterization.....	31
3.3.2 Mercury extraction efficiencies.....	34
3.4 Conclusions .....	36
3.5 References .....	37
3.6 Appendix <i>Chapter 3</i> .....	40
4 THE SOLUBILITY OF CO <sub>2</sub> IN TETRAHEXYLAMMONIUM-BASED DEEP EUTECTIC SOLVENTS .....	46
4.1 Introduction .....	47
4.2 Experimental procedures.....	48
4.2.1 Chemicals .....	48
4.2.2 DES Preparation.....	49
4.2.3 CO <sub>2</sub> Absorption.....	49
4.3 Results and discussion.....	50
4.3.1 CO <sub>2</sub> Absorption data.....	50

4.3.2	Henry's law constant .....	52
4.3.3	Enthalpy of Absorption .....	54
4.4	Conclusions .....	55
4.5	References .....	56
4.6	Appendix <i>chapter 4</i> .....	58
5	OIL DESULFURIZATION USING DEEP EUTECTIC SOLVENT AS EXTRACTANT VIA LIQUID-LIQUID EXTRCACION .....	60
5.1	Introduction .....	61
5.2	Experimental and modeling procedures .....	63
5.2.1	Chemicals .....	63
5.2.2	Preparation of the DESs .....	63
5.2.3	Experimental determination of the LLE data .....	64
5.2.4	COSMO-RS .....	65
5.3	Results and discussion .....	66
5.3.1	Solubility test .....	66
5.3.2	Ternary LLE experiments .....	67
5.3.3	Literature comparisons .....	72
5.3.4	Extraction mechanism .....	75
5.3.5	DES regeneration .....	76
5.4	Conclusions .....	76
5.5	References .....	78
5.6	Appendix <i>Chapter 5</i> .....	82
6	PREDICTION OF THE LIQUID-LIQUID EQUILIBRIUM DATA OF { <i>n</i> -ALKANES + THIOPHENE + DES} SYSTEMS USING THE PERTURBATED CHAIN-STATISTICAL ASSOCIATING FLUID THEORY (PC-SAFT) .....	90
6.1	Introduction .....	91
6.2	PC-SAFT .....	93
6.2.1	Modeling approach .....	94
6.3	Results and discussion .....	95
6.3.1	Pure components .....	95
6.3.2	Binary systems .....	97
6.3.3	Ternary systems .....	100
6.4	Conclusions .....	104
6.5	References .....	106
7	EXTRACTION OF THIOPHENE FROM { <i>n</i> -HEXANE + THIOPHENE} MIXTURES USING DEEP EUTECTIC SOLVENTS: A SENSITIVITY ANALYSIS .....	108
7.1	Introduction .....	109
7.2	Procedure .....	109

7.3	Results and discussion.....	110
7.4	Conclusions .....	115
7.5	References .....	117
7.6	Appendix chapter 7 .....	118
8	CONCLUSIONS & RECOMMENDATIONS .....	119
8.1	Conclusions .....	120
8.2	Recommendations .....	123
	ABOUT THE AUTHOR.....	125
	CONTRIBUTIONS AND PUBLICATIONS .....	126
	ACKNOWLEDGEMENTS .....	128

## 1 INTRODUCTION

*The separation of impurities from oil and gas involves several energy-intensive and costly processes, as well as the use of different volatile organic compounds. Existing separation process could be improved by considering as extracting agents a new generation of low volatility solvents so-called deep eutectic solvents (DESs). Their superior solvent characteristics suggest that their applicability for oil and gas separation processes is promising.*

## **1.1 Problem definition and motivation**

Since the industrial revolution in the 18<sup>th</sup> century, the world has witnessed severe changes in energy generation and demand. Traditionally, energy is generated by the combustion of fossil fuels that are mainly derived from coal, crude oil and natural gas. Nevertheless, the growth of the world population, the economic development, the advanced technologies, industry and transportation resulted in an increasing global demand for the energy. The past decades have seen a shift towards renewable energy from wind, waves, solar and nuclear power generation. However, the dependence on fossil fuels for power generation remains the greatest. It is well known that the combustion of fossil fuels produces large volumes of greenhouse gases, primarily CO<sub>2</sub>, that are released to the atmosphere damaging the environment and leads to man-made climate change and global warming. The problem is compounded as we continue to consume more energy, to meet the global demand that is expected to increase by 30 % in 2040 according to the world energy outlook.<sup>1</sup> Although the combustion of fossil fuel is a major contributor to the environmental concerns, the transport section, forestry, building and waste are also contributors to a certain percentage. The sector shares of global greenhouse emissions in 2004 are shown in Figure 1.<sup>2,3</sup> Thus, to respond to global warming and climate change either we need an energy supply that has low carbon release or we need to find ways to use less energy, in another words to develop more sustainable and energy efficient processes.

Recent decades have seen a growing awareness towards green and sustainable process designs. The development of sustainable process designs allows achieving a range of energy-related goals, such as climate stabilization, cleaner air and reducing energy security risks (see Figure 2). Based on the sustainable development scenario projected by the International Energy Agency (IEA) in 2040, the low-carbon sources share 40 % in the energy mix, the oil and coal demand will noticeably decline, over 60 % of the energy will be generated from renewables, and 15% will be nuclear power as well as a contribution from carbon capture and storage of 6%.<sup>1</sup> To achieve the energy goals, substantial research efforts should be invested in obtaining safer, energy efficient, environmentally benign, and economically viable processes.

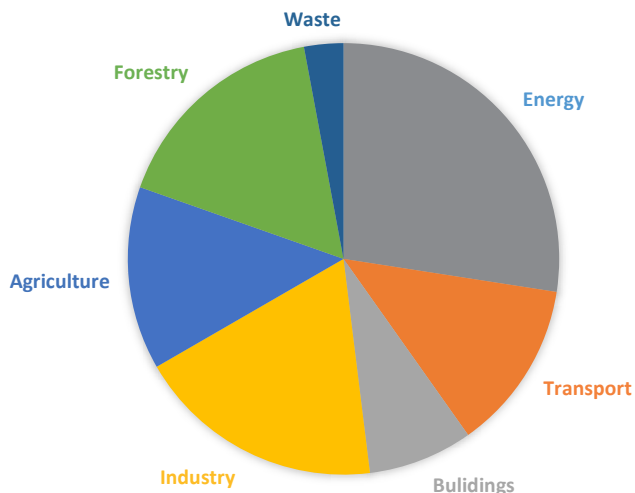


**Figure 1:** GHG emissions by sector in 2004 <sup>2,3</sup>

Zooming into the problem of the heavy energy consumption, separation technologies account for 22% of all in-plant industrial energy use (approximately 4,500 TBtu/yr) in the United States.<sup>4</sup> Moreover, solvents comprise 2/3 of all industrial emissions and 1/3 of all the volatile organic compounds (VOCs) emissions.<sup>5</sup> The development of novel separation technologies is critical in achieving global energy reduction goals. One of the greatest opportunities for energy reduction lies in replacing energy-intensive separation processes with energy-efficient separation processes. The hope to capture these opportunities is tied to extensive research efforts that are directed towards the development of enhanced separation materials, technologies, solvents, etc. The availability of appropriate separation agents and/or methods is often critical to the successful realization of a new engineering or process concept. The success or failure of many industrial energy efficiency concepts, particularly depends on the selection of suitable separation materials and/or methods. Materials development is essential to achieve major improvements in separation technology, necessary for raw materials utilization and waste reduction (or reuse).

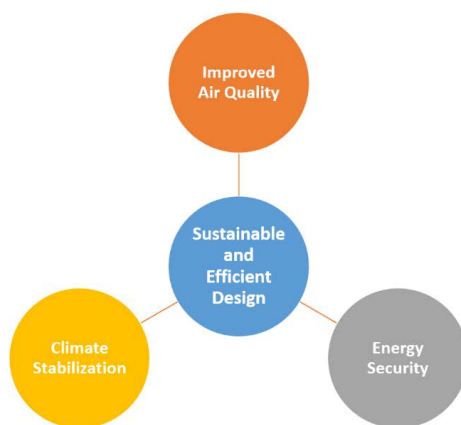


**Figure 2:** The development of sustainable process designs

On the path of the development of energy-efficient, cost-effective and environmentally benign separation processes, low volatility solvents, such as ionic liquids (ILs)<sup>6</sup> and deep eutectic solvents (DESs)<sup>7</sup>, have been a hot research topic. The low volatility of this class of solvents has promoted them as great candidates for replacing the conventional volatile VOCs that are involved in several separation processes, as for example in liquid-liquid extraction, absorption and extractive distillation. VOCs have been commercially utilized as solvents for decades and are still in use. However, several drawbacks, such as volatility leading to solvent losses, flammability, corrosiveness and degradation have been reported. The major drawback from an industrial viewpoint is the solvent recovery. Due to the volatility of the VOCs, the solvent recovery is an expensive step, solvent losses are common to occur with an extra energy consumption penalty. Moreover, the use of VOCs is often accompanied with several environmental concerns and operational risks.

It can be concluded that the use of low volatility solvents in separation processes may hold the promise for a solution of the issues and drawbacks associated with the use of VOCs. In the last decades, ionic liquids were successfully considered as potential candidates for the replacement of VOCs in various separation applications. The negligible vapor pressure is an added value in terms of environmental concerns and energy saving in the solvent recovery step. However, the synthesis of ILs involves several synthesis steps that often result in by-products and waste generation. Other aspects that have been reported are their toxicity and poor biodegradability<sup>8,9</sup>.

In 2003, a new generation of sustainable solvents was discovered, the so-called deep eutectic solvents. DESs are composed of at least one hydrogen bond donor (HBD) and at least one hydrogen bond acceptor (HBA), which can be associated with each other via hydrogen bond interactions to form a mixture with a melting temperature far below that of its constituents.<sup>10-15</sup> DESs are arising as promising alternatives to ILs that provide similar properties (i.e. low vapor pressure and low flammability) while



avoiding some drawbacks. They can be prepared in high purity, simply by mixing low-cost HBD and HBA compounds that are mostly naturally occurring and biodegradable.

The separation of impurities from oil and gas involves several energy-intensive and costly processes, as well as the use of different VOCs. As an example, the removal of sulfur and sulfur derivatives from crude oil is conventionally achieved by catalytic hydrodesulfurization.<sup>16,17</sup> This process is conducted at elevated temperature and pressure leading to high operation costs.<sup>18</sup> Also, mercury capture from oil and gas poses an operational and economic challenge. The mature approaches for mercury capture suffer from either being less efficient or less economically viable.<sup>19-21</sup> Another example is CO<sub>2</sub> capture from natural gas. Industrially, CO<sub>2</sub> is captured from natural gas via absorption using amine solutions.<sup>22</sup> The volatility of the amines is a major issue as it leads to solvent losses and high energy consumption for regeneration. Moreover, the toxicity of the amine-based solutions and their evaporative losses are environmentally undesirable.

In this thesis, the potential for application of DESs in separation processes in oil and gas treating, and particularly capturing mercury, CO<sub>2</sub> capture and desulfurization will be investigated from a thermodynamic point of view.

## 1.2 Scope of the thesis

In this thesis, the performance of DESs to capture impurities from oil and gas is investigated. The main objective is to propose a novel solution to some industrial challenges in the purification of oil and gas from a thermodynamics point of view. After the introduction given in this chapter (*Chapter 1*), a background will be developed in *Chapter 2*, where the ILs and DESs will be introduced. And finally, the application of DESs in separation processes of oil and gas treating will be reviewed.

In *Chapter 3*, a new technology using deep eutectic DESs for elemental mercury (Hg<sup>0</sup>) extraction from hydrocarbons is demonstrated. Four DESs are investigated including choline chloride:urea, choline chloride:ethylene glycol, choline chloride:levulinic acid and betaine:levulinic acid, where the molar ratio is 1:2 in all cases. Their performance for mercury extraction is assessed using saturated solutions in *n*-dodecane as the model oil. The effect of the solvent ratios and temperature is studied.

In *Chapter 4*, two DESs constituted of tetrahexylammonium bromide as HBA and either ethylene glycol or glycerol as HBDs are investigated as sustainable absorbents for CO<sub>2</sub> capture. The phase behavior of CO<sub>2</sub> with the DESs is measured using a gravimetric magnetic suspension balance operating in the static mode at 293.2 K and 298.2 K and pressures up to 2 MPa. The CO<sub>2</sub> solubilities in the studied DES are compared with those in conventional physical solvents to assess the potential of DESs for CO<sub>2</sub> capture.

In *Chapter 5*, six DESs based on tetraethylammonium chloride, tetrahexylammonium bromide and methyltriphenylphosphonium bromide as hydrogen bond acceptors (HBAs) and polyols (ethylene glycol and glycerol) as hydrogen bond donors (HBDs) are studied for the extraction of sulfur derivatives from two aliphatic hydrocarbons via liquid-liquid extraction (LLE). The effects of the aliphatic hydrocarbon type/length and the nature of the HBA and the HBD are investigated. The performance of the DESs is compared to the relevant literature, and the extraction mechanism of the thiophene using DESs is explained using the *COnductor-like Screening MOdel for Real Solvents (COSMO-RS)*<sup>23</sup>. In addition, the phase behavior of the LLE ternary systems {*n*-alkane + thiophene + DES} is described using Perturbed-Chain Statistical Associating Fluid Theory (PC-SAFT).<sup>24</sup> The results are presented in *Chapter 6*, showing that DESs are promising candidates for extractive desulfurization of fuels and that PC-SAFT serves as an appropriate approach for predictive solvent screening in order to obtain thermodynamically optimal DESs.

A sensitivity analysis of the liquid extraction column for the separation of thiophene from *n*-alkanes using DESs, is performed via Aspen Plus<sup>®</sup>, presented in *Chapter 7*. Finally, in *Chapter 8*, the conclusions and recommendations for future research are highlighted.

### 1.3 References

- (1) International Energy Agency. World Energy Outlook 2017 <https://www.iea.org/weo2017/>.
- (2) Intergovernmental Panel on Climate Change. *Mitigation of Climate Change: Contribution of Working Group III to the Fourth Assessment Report of the Intergovernmental Panel on Climate Change*; Cambridge University Press: New York, 2007.
- (3) Olivier, J. G. J.; Van Aardenne, J. A.; Dentener, F. J.; Pagliari, V.; Ganzeveld, L. N.; Peters, J. A. H. W. Recent Trends in Global Greenhouse Gas Emissions: regional Trends 1970–2000 and Spatial Distribution of Key Sources in 2000. *Environ. Sci.* **2005**, *2* (2–3), 81–99.
- (4) U.S. Department of Energy. Materials for Separation Technologies: Energy and Emission Reduction Opportunities. **2005**.
- (5) Brennecke, J. F.; JMagginn, E. Ionic Liquids: Innovative Fluids for Chemical Processing. *AIChE J.* **2001**, *47* (11), 2384–2389.
- (6) Pena-Pereira, F.; Namieśnik, J. Ionic Liquids, and Deep Eutectic Mixtures: Sustainable Solvents for Extraction Processes. *ChemSusChem* **2014**, *7* (7), 1784–1800.
- (7) Abbott, A. P.; Capper, G.; Davies, D. L.; Rasheed, R. K.; Tambyrajah, V. Novel Solvent Properties of Choline Chloride/urea Mixtures. *Chem. Commun. (Camb)*. **2003**, No. 1, 70–71.
- (8) Peric, B.; Sierra, J.; Martí, E.; Cruañas, R.; Garau, M. A.; Arning, J.; Bottin-Weber, U.; Stolte, S. (Eco)toxicity and Biodegradability of Selected Protic and Aprotic Ionic Liquids. *J. Hazard. Mater.* **2013**, *261*, 99–105.
- (9) Thuy Pham, T. P.; Cho, C. W.; Yun, Y. S. Environmental Fate and Toxicity of Ionic Liquids: A Review. *Water Research*. 2010, pp 352–372.
- (10) Carolin Ruß, a B. K. Low Melting Mixtures in Organic Synthesis – an Alternative to Ionic Liquids? Carolin. *Green Chem.* **2010**, *4* (8), 1166–1169.
- (11) Dai, Y.; Van Spronsen, J.; Witkamp, G. J.; Verpoorte, R.; Choi, Y. H. Ionic Liquids and Deep Eutectic Solvents in Natural Products Research: Mixtures of Solids as Extraction Solvents. *J. Nat. Prod.* **2013**, *76* (11), 2162–2173.
- (12) Domínguez de María, P.; Maugeri, Z. Ionic Liquids in Biotransformations: From Proof-of-Concept to Emerging Deep-Eutectic-Solvents. *Curr. Opin. Chem. Biol.* **2011**, *15* (2), 220–225.
- (13) Francisco, M.; Van Den Bruinhorst, A.; Kroon, M. C. Low-Transition-Temperature Mixtures (LTTMs): A New Generation of Designer Solvents. *Angew. Chemie - Int. Ed.* **2013**, *52* (11), 3074–3085.

- 
- (14) Zhang, Q.; De Oliveira Vigier, K.; Royer, S.; Jérôme, F. Deep Eutectic Solvents: Syntheses, Properties, and Applications. *Chem. Soc. Rev.* **2012**, *41* (21), 7108–7146.
  - (15) Smith, E. L.; Abbott, A. P.; Ryder, K. S. Deep Eutectic Solvents (DESs) and Their Applications. *Chem. Rev.* **2014**, *114* (21), 11060–11082.
  - (16) Brunet, S.; Mey, D.; Perot, G.; Bouchy, C.; Diehl, F. On the Hydrodesulfurization of FCC Gasoline: A Review. *Appl. Catal. A Gen.* **2005**, *278* (2), 143–172.
  - (17) Shafi, R.; Hutchings, G. J. Hydrodesulfurization of Hindered Dibenzothiophenes: An Overview. *Catal. Today* **2000**, *59* (3), 423–442.
  - (18) Debajyoti, B. Design Parameters for a Hydro Desulfurization (HDS) Unit for Petroleum Naphtha at 3500 Barrels per Day. *World Sci. News* **2015**, *3*, 99–111.
  - (19) Granite, E. J.; Pennline, H. W.; Hargis, R. a. Novel Sorbents for Mercury Removal from Flue Gas. *Ind. Eng. Chem. Res.* **2000**, *39*, 1020–1029.
  - (20) Eckersley, N. Advanced Mercury Removal Technologies. *Hydrocabon Process.* **2010**, No. January, 29–35.
  - (21) Hiroshi Nishino, Toshio Aibe, K. N. Process for Removal of Mercury Vapor and Adsorbant Therefor. US Patent 4500327 A, 1985.
  - (22) A. J. Kidnay, W. R. Parrish, D. G. M. *Fundamental of Natural Gas Processing*, Second edi.; CRC PressINC, 2011.
  - (23) Klamt, A. Conductor-like Screening Model for Real Solvents: A New Approach to the Quantitative Calculation of Solvation Phenomena. *J. Phys. Chem.* **1995**, *99*, 2224–2235.
  - (24) Gross, J.; Sadowski, G. Perturbed-Chain SAFT: An Equation of State Based on a Perturbation Theory for Chain Molecules. *Ind. Eng. Chem. Res.* **2001**.

## 2 BACKGROUND

*This chapter has been published in: S.E.E. Warrag, C.J. Peters, M.C. Kroon "Deep Eutectic Solvents for Highly Efficient Separations in Oil and Gas Industries" Current Opinion in Green and Sustainable Chemistry, 2017, 5, 55–60.*

*Low volatility solvents have captured great scientific attention as a new, 'green' and sustainable class of tailor-made solvents. This chapter aims to provide an introduction about the low volatility solvents: ionic liquids (ILs) and deep eutectic solvents (DESs). Moreover, selected applications of DESs in separation processes of oil and gas will be reviewed, such as dearomatization, desulfurization, the removal of glycerol from biofuel and natural gas sweetening.*

## 2.1 Introduction to ionic liquids

Ionic liquids (ILs) have been a research interest in different scientific fields such as chemical synthesis, biochemistry, separation technologies, electrochemistry, catalysis, and other areas.<sup>1</sup> ILs are generally defined as molten salts with a melting point below 373 K.<sup>2,3</sup> Most of them have melting points around or below room temperature, usually known as room temperature ionic liquids (RTILs). ILs contain charged cations and anions held together via ionic bonds, which contribute to the very low vapor pressure that is usually observed in them. One of the earliest RTIL was ethylammonium nitrate “melting point of 285 K” that was reported in 1914 by Paul Walden.<sup>4</sup> Later in the 1970s, ILs were developed as potential electrolytes in batteries. They were based on alkyl substituted imidazolium and pyridinium cations, with a halide or tetrahalogenoaluminate anions.<sup>5,6</sup> And since then, ILs have been widely investigated for various applications. ILs have unique physical and chemical properties such as thermal stability, viscosity, and polarity that can be tailored by altering the combination of the cations and the anions.<sup>3</sup> Figure 1 presents the common cations and anions found in the literature. However, these represent only a limited options of an almost infinite number of possible cations and anions that may form ILs. The negligible volatility of ILs has promoted them as great candidates for replacing the conventional volatile organic solvents (VOCs). The label ‘green’ is often associated with ILs due to their negligible vapor pressure and low flammability, which are an added values in terms of environmental concerns. However, the synthesis of ILs involves several synthesis steps that often result in by-products and waste generation. Other aspects that have been reported are the toxicity and poor biodegradability<sup>7,8</sup>. Therefore, the ‘greenness’ of ILs has been overlooked and misinterpreted.<sup>9</sup> Also, the high cost associated with the synthesis has limited their industrial application.

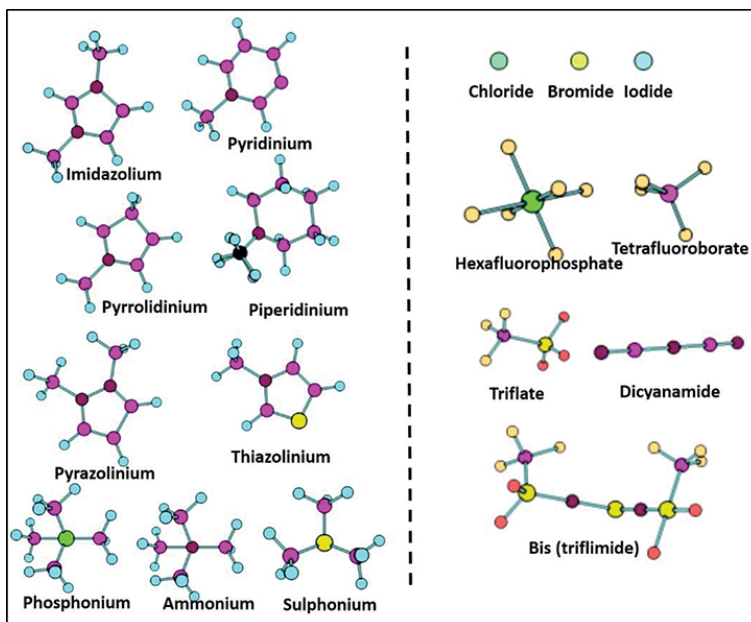


Figure 1: Common cations and anions of ionic liquids<sup>10</sup>

### 2.1.1 Properties of ionic liquids

Several reviews<sup>11,12</sup> and databases<sup>13</sup> collected physicochemical properties data of various ILs. In this section, the main properties of the ILs will be outlined.

**Melting point:** The melting point is highly affected by the ILs constituents: the cations and anions. Most of the ILs remain liquid at room temperature. They possess a high degree of asymmetry that defeats packing and thus reduces the lattice energy and inhibits crystallization.<sup>14</sup>

**Volatility:** The most pronounced property in the ILs is their low vapor pressure at room temperature. As mentioned earlier, the cations and anions are held together via strong ionic bonds that contribute to lowering the volatility. This character of ILs made them excellent alternatives for volatile organic compounds.

**Viscosity:** ILs are generally more viscous compared to conventional VOCs. The viscosity is highly affected by the molecular weight and the intermolecular interactions. And similar to other physicochemical properties, the anions and cations of the IL play a role in its viscosity. Literature suggested that the flat shape of the anion contributes to a lower viscosity of the ILs.<sup>15</sup> While the longer the alkyl chain length in the cation, the higher the viscosity for the same anion.<sup>16</sup> According to Brennecke

et.al., ionic liquids (excluding those that form liquid crystals) are Newtonian fluids.<sup>14</sup> Moreover, it was reported that the viscosity significantly decreases with an increase in temperature.<sup>17</sup>

**Thermal stability:** ILs are known to be highly thermally stable with a wide liquid range, from below ambient to well over 573 K to 673 K,<sup>14</sup> which suggests they could be used under unique processing conditions. Again, this property strongly depends on the structure of the IL. The thermal stability was found to be more dependent on anions than on the cations.<sup>16</sup>

**Other properties:** The toxicity of two imidazolium-based ILs with [PF<sub>6</sub><sup>-</sup>] and [BF<sub>4</sub><sup>-</sup>] anions was studied. It was found that both ILs are equally toxic to ecosystems and the toxicity of ILs increases with increasing alkyl chain length of the cation.<sup>18</sup> The biodegradability of ILs was reported in some studies.<sup>19–21</sup> However, toxicological data and information on the biodegradability of the ILs are still scarce in the open literature. Further investigations are highly needed.

### 2.1.2 Future perspectives

The attractive properties of ILs particularly, the ability to tailor properties by the choice of the anion, cation and substituents, offer a great opportunity to revolutionize industrial processes. Through the years of research, many ILs-based industrial applications are now a reality. For example, Clariant and Petronas announced the commercialization of a new solid-supported ionic liquid (SSIL) mercury removal technology.<sup>22</sup> SSIL effectively removes mercury from natural gas. Nonetheless, the usage of ILs for practical applications on an industrial scale is still in its early stages. Further research should be directed towards the design and development of ILs.

## 2.2 Introduction to deep eutectic solvents (DESs)

In 2003, a new generation of sustainable solvents was described, the so-called deep eutectic solvents (DESs).<sup>23</sup> DESs are composed of at least one hydrogen bond donor (HBD) and at least one hydrogen bond acceptor (HBA), which can be associated with each other via hydrogen bond interactions to form a mixture with a melting temperature far below that of its constituents<sup>24–29</sup>. And each DES possess unique physiochemical properties. Abbot et al.<sup>23</sup> reported the formation of a eutectic mixture of choline chloride and urea at 285 K, which is considerably lower than that of either of the constituents (melting points: choline chloride = 575 K and urea = 406 K) (see Figure 2). For some DESs, a melting point is not found, but instead, a glass transition temperature is obtained. Thus, these DESs are known as low-transition-temperature mixtures (LTTMs)<sup>27</sup>.



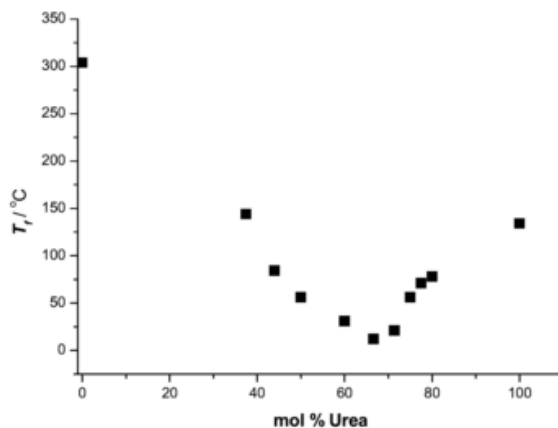


**Figure 2:** Melting point of choline chloride/urea mixtures as a function of composition<sup>23</sup>

DESs can be prepared in high purity, simply by mixing low-cost HBD and HBA compounds that are mostly naturally occurring. Typical HBAs can be choline chloride, quaternary ammonium salts, halide salts, phosphonium salts, amino acids and sugars. While typical HBDs can be urea, amines, carboxylic acids, hydroxyl acids, alcohols and polyols. The structures of some HBDs and HBAs are shown in Figure 3. The pictures of the dog and his keeper might seem funny, however, it provides an analogy of the strong bond between the dog and his keeper, and the hydrogen bond between the HBA and the HBD, that result in a unique match with entirely different characteristics.

DESs have several attractive properties, such as low vapor pressure, low flammability, thermal stability, wide liquid range, high solvation properties, often biodegradable and low-cost. More interestingly, the desired physicochemical properties of DESs can be achieved by perceptive and adequate selection of the DES constituents and their ratios, making them ‘objective-oriented’ solvents.<sup>26–28</sup> Due to these characteristics, DESs have attracted significant interest as promising alternatives for VOCs and ILs as ‘greener’ solvents. It is worth mentioning that the ‘greenness’ and sustainability of the DESs is also bounded by the choice of the constituents. The number of papers on DESs has increased exponentially in the last few years, with 1671 entries up to now (Scopus, February 2018).

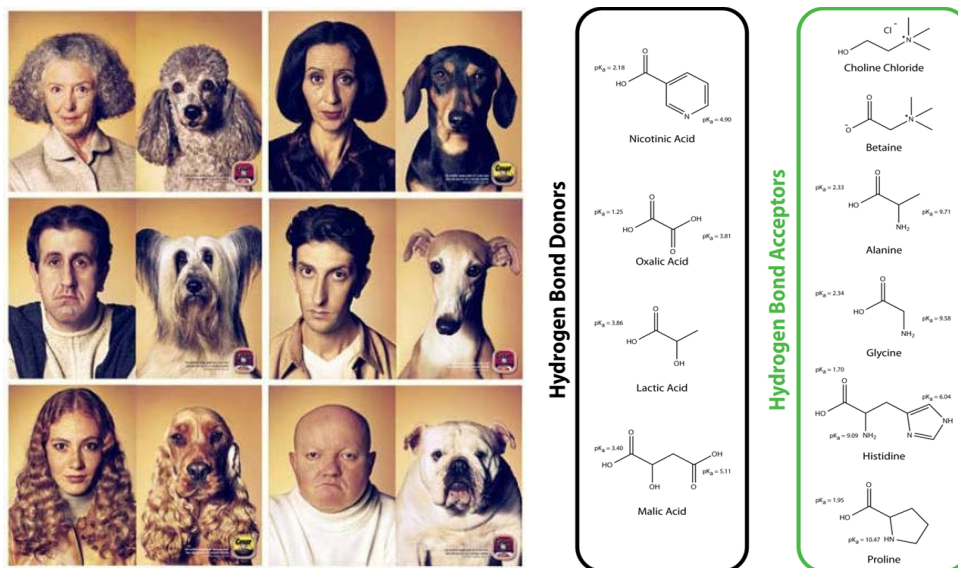


Figure 3: Examples of the HBAs and HBDs

### 2.2.1 Properties of deep eutectic solvents

DESs have been acknowledged as analogous to ILs. Despite the mutual essential characteristics between them including low vapor pressure, low flammability, thermal stability, wide liquid range, high solvation properties, they should be differentiated from each other. ILs are entirely composed of ions, while DES is simply a mixture of a HBA and a HBD with a melting point lower than that of its individual constituents. DESs have many advantages over ILs, including low production cost, simple synthesis process, and good biocompatibility when using quaternary ammonium salts.<sup>30–32</sup> The main characteristics of the DESs are summarized below.

**Freezing Point:** the freezing point of the DESs is dependent on the strength of molecular interactions between the HBA and the HBD and therefore the nature of the constituents and the mixing molar ratios. For instance, Zhang et al. highlighted that the freezing point depression of choline salts based-DES (HBA) with urea exhibit the following order:  $F^- > NO_3^- > Cl^- > BF_4^-$ .<sup>33</sup> Also, the mixture of choline chloride with urea in a molar ratio of 1:1 and 1:2, exhibit a freezing point  $>50^\circ C$  and  $12^\circ C$ , respectively. As for the HBD, it has been found that for quaternary ammonium salts and carboxylic acids, the lower the molecular weight of the acid, the larger the depression in the freezing point.<sup>34</sup>

**Liquid range:** the liquid range can be defined as the range between the freezing point of the DES and the decomposition temperature. Generally, DESs are in the range of 400-500 K.<sup>35</sup>

**Density and viscosity:** Both properties are essential for process design purposes. Most of the DESs show a density between 1.0 and 1.35 g/cm<sup>3</sup> at room temperature and atmospheric pressure. The density of the DESs depend on HBD and HBA nature, and the molar ratio between them. Also it was found to decrease linearly with temperature.<sup>35</sup> The viscosity of the DESs depend on the same factor, however, the effect of the temperature on the viscosity is significant and sharply decrease with a temperature increase. Similar to ILs, the major drawback of this class of solvents is their high viscosity.<sup>35</sup>

### 2.2.2 Applications of DESs

DESs have demonstrated excellence in several research fields such as chemical synthesis, biochemistry, separation technologies, electrochemistry, catalysis and other fields.<sup>27,33,35-37</sup> In this chapter selected applications of DESs in separation processes for oil and gas treating will be discussed such as: dearomatization, desulfurization, the removal of glycerol from biofuel and natural gas sweetening.

#### 2.2.2.1 Applications in separation processes of oil

In the quest of exploring more sustainable approaches for producing clean oil fuels, the suitability of DESs in several applications related to separation technologies in oil processing has been investigated by scientists worldwide. It is well known that the aromatic content in fuels is a double-edged sword. On the one hand, it can enhance the fuel lubricity and density, therefore, its heat content. But, on the other hand, they are an environmental concern and cause of plugging problems in cryogenic downstream processing at sufficiently high concentrations.<sup>38</sup> Optimization of the aromatic content is an industrial challenge as they form azeotropes with aliphatic hydrocarbons. DESs have demonstrated an excellent extraction performance of different aromatic compounds from aliphatic hydrocarbons.<sup>39-42</sup> Table 1 summarizes selected studies on dearomatization using DESs. Phosphonium-based DESs have been applied to the systems heptane/toluene and hexane/benzene mixtures.<sup>39,41</sup> It was found that the temperature has a clear effect on the extraction of the aromatic. An increase in temperature enhanced the extraction of the aromatic. Interestingly, the DES has not been detected in the hydrocarbon-rich layer. This is remarkable as it prevents solvent losses during the extraction process. Gonzalez *et al.*<sup>40</sup> have studied the removal of benzene from hexane using the most popular DESs, which are the choline chloride-based. The DESs proved to have a much higher selectivity than the commercially used solvent (sulfolane). Also, no DES was detected in the hexane phase. The tetrahexylammonium bromide DESs were applied to a similar system by Rodriguez *et al.*<sup>42</sup> and they found that the DESs performance is also comparable to commercial solvents but in contrast, the temperature has a minor effect on the extraction. Commonly, solvents like sulfolane and ethylene glycol are used as extractants for this application<sup>43</sup>. Both solvents are volatile, toxic and flammable. Therefore, it can

be concluded that the use of DESs as replacements for dearomatization fulfills the principle of green extraction that has been stated as: “Green extraction is based on the discovery and design of extraction processes which will reduce energy consumption, allow the use of alternative solvents and renewable natural products, and ensure a safe and high-quality extract/product”<sup>44</sup>.

Following a similar conceptual line of dearomatization, DESs have been used for the removal of sulfur-containing aromatics such as thiophenes from fuels. The combustion of organosulfur-containing fuels is a major source of SO<sub>x</sub> and H<sub>2</sub>S. In response to the established regulations of the European Union (EU) and US Environmental Protection Agency (EPA) regarding SO<sub>x</sub> emissions, the reduction of sulfur concentrations in fuels is of utmost importance.<sup>45</sup> Similarly, the use of volatile organic solvents for desulfurization is an environmental concern. Deep extractive desulfurization of fuels has been recently performed using green carboxylic acid based DESs.<sup>46</sup> Benzothiophene, dibenzothiophene and thiophene were efficiently removed from octane. It was found that the efficiency is insensitive to the extraction temperature and that after three extraction cycles, deep desulfurization can still be attained (up to 98% efficiency). Remarkably, regeneration of the DES has been performed using methyl *tert*-butyl ether as back-extractant and the DES extraction property was completely recovered. From the NMR spectrum of the fresh DES and the regenerated DES it was observed that the DES structure did not change, thus the recyclability is guaranteed. The study also suggested that the extraction was driven by the hydrogen bond interaction of DESs with the sulfur atom in thiophenes.

Few other studies have also demonstrated the excellent efficiency of DESs in deep desulfurization with a possibility of regeneration of the DESs (see Table 1)<sup>47–50</sup>. Deep desulfurization of fuels using DESs will provide a promising green and inexpensive option with a potential for industrial application.

One of the earliest attempts in the oil purification field using DESs was the removal of glycerol from biofuels, particularly ‘biodiesel’<sup>51</sup>. Biodiesel is a renewable and clean-burning fuel that is made from vegetable oils and/or animal fats. Biodiesel generates less toxic pollutants and greenhouse gases than fossil diesel. It is predominantly consisting of long- alkyl (methyl, ethyl, or propyl) esters and typically produced by catalyzed transesterification. Glycerol is an undesirable by-product of transesterification as it increases the fuel viscosity, leading to damages in the high-pressure injection system of the diesel engine. In principle, water is used to wash off the glycerol from the biodiesel. However, it has been reported that water washing results in a considerable product loss and the waste water discharge is environmentally undesirable<sup>52</sup>. Abbott *et al.*<sup>51</sup> have approached this issue in two manners: first, they tried the so-called *in situ* eutectic extraction by adding a pure quaternary ammonium salt to crude biodiesel that is able to form a eutectic mixture with the glycerol. This approach was not successful. The authors believed that it might be due to the enthalpy of formation of the eutectic mixture. Second, they prepared a DESs of ammonium salts as a HBA and glycerol as a HBD

in 1:2 molar ratio. Remarkable removal of glycerol up to 99% has been achieved. They have also studied the recovery of the ammonium salt (choline chloride) by adding a co-solvent (1-butanol). The analysis showed that 25% of the choline chloride has been recovered upon recrystallization.

Afterward, the group of Shahbaz *et al.*<sup>53</sup> reported the extraction of free glycerol and the reduction of total glycerol contents from palm-oil-based biodiesel samples using non-glycerol based DESs. Interestingly, all the DESs have successfully removed the free glycerol with an efficiency of >99%. Another interesting aspect of the study is the recyclability of the DES. The DES can be used for three consecutive batches with negligible loss of the extraction capability. In another paper, the removal of residual transesterification catalyst (KOH) by DESs has been reported<sup>54</sup>. Table 1 summarizes the highlighted studies. The capability of green and sustainable DESs to extract glycerol and the residual catalyst with a possibility of recycling provides a promising route for the purification of biofuels in an efficient and environmentally friendly approach.

**Table 1:** Selected applications of DESs for oil separation processes. The DES are presented as HBA:HBD in molar ratio, T is the temperature in K. (The abbreviations are explained at the end of the chapter.)

Impurity	Oil Model	Extraction Method	DESs	T (K)	Ref.
<b>Dearmatization</b>					
Benzene	Hexane	LLE	THABr:EG, THABr:GL in 1:2	298	42
			THABr:EG, THABr:GL in 1:2	308	
Benzene	Hexane	LLE	MTPPBr:EG in 1:4,1:6,1:8	300	39
			MTPPBr:EG in 1:4,1:6,1:8	308	
			MTPPBr:EG in 1:4,1:6,1:8	318	
Toluene	Heptane	LLE	TBPBr:EG,TBPBr:Sol in 1:2, 1:4,1:6,1:8	313	41
			TBPBr:EG,TBPBr:Sol in 1:2, 1:4,1:6,1:8	323	
			TBPBr:EG,TBPBr:Sol in 1:2, 1:4,1:6,1:8	333	
Benzene	Hexane	LLE	ChCl:LA, ChCl:GL in 1:2	298	40
				308	
				318	
<b>Desulfurization</b>					
Benzothiophene, Dibenzothiophene or Thiophene	Octane	LLE	TBABr:FA in 1:1	293-323	46
Benzothiophene	Octane	LLE	ChCl:MA/GL/EG/Pr, TMAC:GL/EG/PAA, TBAC:MA/GL/TEG/EG/PAA/CA/Pr/PEG in 1:2	298	47

Dibenzothiophene and Thiophene	Octane, Decane, Cyclohexane, isooctane and toluene in 30%, 30%, 30%, 10% respectively	LLE	TBPBr: stannous chloride dihydrate in 1:1	303-343	48
3-Methylthiophene, Benzothiophene or Dibenzothiophene	Heptane	LLE	Chlorinated paraffins-52:AICl <sub>3</sub> :Toluene/Bezene/p-xylene/ o-xylene/Ethylbenzene in 1:6:18	293	49
Thiophene	Heptane	LLE	TBABr:EG/TEG, MTPPBr:EG in 1:4 and TBABr:Sul in 1:7	298	50
<b>Purification of biofuels</b>					
Glycerol	Soy bean oil	LLE	AChCl/TPABr/EACl/ChCl/Cl <sub>2</sub> EMe <sub>3</sub> :Gly in 1:2	313	51
Glycerol	Palm oil	LLE	ChCl:EG in 1:1.7, 1:2, 1:2.23 , 1:2.45 and ChCl:TFAA in 1:1.5, 1:1.7, 1:1.94, 1:2.45	298	53
KOH	Palm oil	LE	ChCl:Gly in 1:1, 1:2, 1:3, ChCl:EG in 1:75, 1:2, 1:2.5, ChCl:TFAA in 1:1.75, 1:2, 1:2.5 MTPPBr:Gly in 1:2, 1:3,1:4 MTPPBr:EG in 1:3, 1:4, 1:5 MTPPBr:TEG IN 1:3, 1:4, 1:5	298	54

### 2.1.1.1 Applications in natural gas sweetening

Natural gas mainly consists of methane (CH<sub>4</sub>), but it also contains undesired acid gases such as carbon dioxide (CO<sub>2</sub>) and hydrogen sulfide (H<sub>2</sub>S). The removal of CO<sub>2</sub> from natural gas streams in a so-called sweetening process is crucial, not only for environmental concerns as it is a 'greenhouse gas', but also because the presence of CO<sub>2</sub> may cause problems during transportation, such as gas hydrate formation that can clog pipelines. Moreover, the presence of CO<sub>2</sub> reduces the heating value of natural gas<sup>55</sup>. The use of a volatile organic solvent such as monoethanolamine (MEA) for CO<sub>2</sub> capture in power plants is also an environmental concern. Moreover, amines are corrosive solvents that degrade with time, leading to solvent losses and high energy consumption for regeneration. The solubility of CO<sub>2</sub> in ILs and DESs has been widely studied with the objective to exploit a class of solvents that are both non-volatile and efficient to replace amines. In a comprehensive study, the solubility of CO<sub>2</sub> in DESs has been measured in a temperature range of 308-318 K and pressures up to 2 MPa in a series of tetramethylammonium chloride, tetraethylammonium chloride and tetrabutylammonium chloride as HBA and lactic acid as HBD in 1:2 molar ratio.<sup>56</sup> The results suggested that the solubility of CO<sub>2</sub> increased with increasing pressure and decreased with increasing temperature, so that the DESs can be regenerated by pressure-swing absorption (PSA). However, the regeneration was not reported in the paper. Also, the higher the alkyl chain length, the higher the solubility. This is presumably due to the larger free volume available for absorption. The reported solubilities are only slightly lower than that of

the fluorinated ILs, which are known for their high CO<sub>2</sub> absorption capacity (and their high toxicity). It worth mentioning that the order of magnitude of the diffusion coefficients is ( $10^{-11}$ – $10^{-10}$  m<sup>2</sup>·s<sup>-1</sup>) is also comparable to the CO<sub>2</sub> diffusivities in fluorinated ILs (e.g., [bmim][PF<sub>6</sub>]<sup>56</sup>). In another paper of this group, the influence of the molar ratio of HBA:HBD of the DES tetrabutylammonium chloride: lactic acid has been tested. It was found that the solubility decreased with increasing HBD concentration. The authors believe that this can be due to the lower amount of salt in the DES, and thus a lower free volume available for absorption<sup>57</sup>. In contrast, Lu *et al.*<sup>58</sup> reported the solubilities of CO<sub>2</sub> in choline chloride as HBA and levulinic acid or furfuryl alcohol as HBD in a molar ratio of 1:3, 1:4 and 1:5. They observed that the solubility increased with increasing concentration of the HBD.

Ali *et al.*<sup>59</sup> have attempted adding ammonium salts to monoethanolamine, diethanolamine and triethanolamine to induce an amine-based DES formation. No DES characterization data were reported, but it was found that the amine-based DESs have the highest CO<sub>2</sub> adsorption capacity in comparison to the polyols DESs such as ethylene glycol or glycerol. However, the corrosivity of the amine is still a concern.

Trivedi *et al.*<sup>60</sup> synthesized DESs that capture CO<sub>2</sub> via carbamate formation upon reaction between their hydrogen bonding donor units and CO<sub>2</sub>. Monoethanolamine (MEA) was reacted with hydrochloric acid (HCl) in equimolar amounts to produce a monoethanolamine hydrochloride salt [MEA.Cl] that is considered as HBA. Similarly, hydrochloride salts of urea, thioacetamide and triethanolamine were prepared. The HBAs were properly mixed with ethylenediamine (EDA) as HBD in different molar ratios to form a DES (see Table 2). The authors reported the thermogravimetric properties of the mixture that proved the depression of the freezing point due to hydrogen bonding interactions. Among the tested DESs, [MEA.Cl][EDA] in a molar ratio of 1:3 is found to uptake 33.7 wt% of CO<sub>2</sub>. Also, the DES showed a stable absorption performance in the presence of 10 wt% of water and a decent tolerance against temperature rise. The DESs could successfully be recycled at a temperature of 100 °C and could be reused for five consecutive cycles with the same performance. The corrosion penetration rate was quantified for [MEA.Cl][EDA] and found to be more corrosion-resistant than the pure EDA. However, the corrosive character of the [MEA.Cl][EDA] is not desirable in terms of greenness.

Other research groups have studied the solubility of CO<sub>2</sub> in DESs<sup>61–63</sup>. Table 2 summarizes selected studies on CO<sub>2</sub> capture using DESs. The highlighted studies have all agreed that an increase in pressure increases the solubility, while the opposite is observed in the case of increasing temperature. The mechanism of CO<sub>2</sub> capture, whether it depends on the free volume or on the molecular interactions of the CO<sub>2</sub> and the DES, is still a debate. Nevertheless, the results are promising and with further research and optimization, DESs can be a low-cost and sustainable alternative for natural gas sweetening solvents.

**Table 2:** Selected applications of DESs for gas sweetening. The DES are presented as HBA:HBD in molar ratio, T is the temperature in kelvin and P is the pressure in MPa. (The abbreviations are explained at the end of the chapter.)

Absorbate	DES	T (K)	P (MPa)	Ref.
CO <sub>2</sub>	TMACI/TEACI/TBACI:LA in 1:2, TBACI:LA in 1:3	308 - 318	Up to 2 MPa	<sup>56,57</sup>
CO <sub>2</sub>	ChCl:LevA/FurA in 1:3, 1:4, 1:5	303-333	Up to 0.6 MPa	<sup>58</sup>
CO <sub>2</sub>	ChCl:TEG in 1:4, ChCl:EG in 1:4, 1:8, ChCl:Urea in 1:2.5, 1:4, ChCl:Gly in 1:3, 1:8, ChCl:MEA/DEA in 1:6, BTPPCl:Gly in 1:12, BTPPBr:EG 1:12, MTPPBr:EA in 1:6, 1:7, 1:8, TBABr: MEA/DEA in 1:6, TBABr:TEA in 1:3	298	0.1 Mpa	<sup>59</sup>
CO <sub>2</sub>	MEA.Cl:EDA in 1:1, 1:2, 1:3 and 1:4, TEA.Cl:EDA in 1:3, Urea.Cl:EDA in 1:3, TAE.Cl:EDA in 1:3	308 - 363	0.1 MPa	<sup>60</sup>
CO <sub>2</sub>	ChCl:LA in 1:2	303 - 348	Up to 9 MPa	<sup>62</sup>
CO <sub>2</sub>	ChCl:Urea, ChCl:EG in 1:2 and ChCl:MalA:EG in 1.3:1:2.2	309 - 329	Up to 0.16 MPa	<sup>61</sup>

### 2.2.3 Challenges and future perspectives

DESs are a new class of tailor-made solvents that are simply prepared from low-cost and natural building blocks. The choice of the starting materials determines their physical and chemical properties. Also, it contributes to a large extent to their ‘greenness’ and sustainable characteristics. DESs are still a new field of research. In-depth fundamental studies and experimental data are highly needed, including characterization data, phase behavior and understanding of the molecular interactions within the DES. However, promising results were found for different fields of applications. Like ILs, the thermal stability of the DESs is still a challenge due to the sensitivity of the hydrogen bonding interactions towards temperature. The regeneration/recyclability of the DES has been reported in very few applications and there is a need for further studies. As sustainable solvents, DESs are expected to play a significant role in the future. The economic value, efficiency, cleanness and renewability of DESs are all very attractive properties for large scale deployment in the field of oil and gas processing.

## 2.3 Abbreviations

LLE	Liquid liquid extraction
DES	Deep eutectic solvent
IL	Ionic liquid
HBA	Hydrogen bond acceptor
HBD	Hydrogen bond donor
THABr	Tetrahexylammonium bromide
EG	Ethylene glycol
Gly	Glycerol
MTPPBr	Methyltriphenylphosphonium bromide
TBPBr	Tetrabutylphosphonium bromide
Sul	Sulfolane



---

ChCl	Choline chloride
LA	Lactic acid
TBABr	Tetrabutylammonium bromide
FA	Formic acid
MA	Malonic acid
Pr	Propionate
TMACl	Tetramethylammonium chloride
PAA	Phenylacetic acid
TBACl	Tetrabutylammonium chloride
TEG	Triethylene glycol
CA	Caproic acid
PEG	Polyethylene glycol
AChCl	Acetylcholine
TPABr	Tetrapropylammonium bromide
EACl	Ethylammonium chloride
Cl <sub>2</sub> EMe <sub>3</sub>	2-Chloroethyltrimethylammonium chloride
TFAA	Trifluoroacetamide
TEACl	Tetraethylammonium chloride
MalA	Malic acid
LevA	Levulinic acid
FurA	Furfuryl acid
MEA	Monoethanolamine
DEA	Diethanolamine
TEA	Triethanolamine
BTPPCl	Benzyltriphenylphosphonium chloride
BTPPBr	Butyltriphenylphosphonium bromide
MEA.Cl	Monoethanolamine hydrochloride
TEA.Cl	Triethanolamine hydrochloride
Urea.Cl	Urea hydrochloride
TEA.Cl	Thioacetamide hydrochloride
EDA	Ethanediamine

## 2.4 References

- (1) Pena-Pereira, F.; Namieśnik, J. Ionic Liquids and Deep Eutectic Mixtures: Sustainable Solvents for Extraction Processes. *ChemSusChem* **2014**, *7* (7), 1784–1800.
- (2) Gordon, C. M. New Developments in Catalysis Using Ionic Liquids. *Appl. Catal. A Gen.* **2001**, *222* (1–2), 101–117.
- (3) Welton, T. Ionic Liquids in Catalysis. *Coord. Chem. Rev.* **2004**, *248* (21–24), 2459–2477.
- (4) Walden, P. Molecular Weights and Electrical Conductivity of Several Fused Salts, *Bulletin of the Russian Academy of Sciences*, 1914.
- (5) Chum, H. L.; Koch, V. R.; Miller, L. L.; Osteryoung, R. A. Electrochemical Scrutiny of Organometallic Iron Complexes and Hexamethylbenzene in a Room Temperature Molten Salt. *J. Am. Chem. Soc.* **1975**, *97* (11), 3264–3265.
- (6) Wilkes, J. S.; Levisky, J. A.; Wilson, R. A.; Hussey, C. L. Dialkylimidazolium Chloroaluminate Melts: A New Class of Room-Temperature Ionic Liquids for Electrochemistry, Spectroscopy and Synthesis. *Inorg. Chem.* **1982**, *21* (3), 1263–1264.
- (7) Peric, B.; Sierra, J.; Martí, E.; Cruañas, R.; Garau, M. A.; Arning, J.; Bottin-Weber, U.; Stolte, S. (Eco)toxicity and Biodegradability of Selected Protic and Aprotic Ionic Liquids. *J. Hazard. Mater.* **2013**, *261*, 99–105.
- (8) Thuy Pham, T. P.; Cho, C. W.; Yun, Y. S. Environmental Fate and Toxicity of Ionic Liquids: A Review. *Water Research*. 2010, pp 352–372.
- (9) Deetlefs, M.; Seddon, K. R. Assessing the Greenness of Some Typical Laboratory Ionic Liquid Preparations. *Green Chem.* **2010**, *12* (1), 17–30.
- (10) Devaki, S. J.; Sasi, R. Ionic Liquids/Ionic Liquid Crystals for Safe and Sustainable Energy Storage Systems. In *Progress and Developments in Ionic Liquids*; InTech, 2017; pp 313–336.
- (11) Ghandi, K. A Review of Ionic Liquids, Their Limits and Applications. *Green Sustain. Chem.* **2014**, *4* (1), 44–53.
- (12) Aparicio, S.; Atilhan, M.; Karadas, F. Thermophysical Properties of Pure Ionic Liquids: Review of Present Situation. *Ind. & Eng. Chem. Res.* **2010**, *49* (20), 9580–9595.
- (13) Zhang, S.; Sun, N.; He, X.; Lu, X.; Zhang, X. Physical Properties of Ionic Liquids: Database and Evaluation. *J. Phys. Chem. Ref. Data* **2006**, *35* (4), 1475–1517.
- (14) Brennecke, J. F.; Maginn, E. Ionic Liquids: Innovative Fluids for Chemical Processing. *AIChE J.* **2001**, *47* (11), 2384–2389.

- 
- (15) Zhou, Z.-B.; Matsumoto, H.; Tatsumi, K. Structure and Properties of New Ionic Liquids Based on Alkyl- and Alkenyltrifluoroborates. *Chemphyschem* **2005**, *6* (7), 1324–1332.
- (16) Singh, V. V.; Nigam, A. K.; Batra, A.; Boopathi, M.; Singh, B.; Vijayaraghavan, R. Applications of Ionic Liquids in Electrochemical Sensors and Biosensors. *Int. J. Electrochem.* **2012**, *2012*, 1–19.
- (17) Okoturo, O. O.; VanderNoot, T. J. Temperature Dependence of Viscosity for Room Temperature Ionic Liquids. *J. Electroanal. Chem.* **2004**, *568* (1–2), 167–181.
- (18) Keskin, S.; Kayrak-Talay, D.; Akman, U.; Hortaçsu, Ö. A Review of Ionic Liquids towards Supercritical Fluid Applications. *Journal of Supercritical Fluids*. 2007, pp 150–180.
- (19) Romero, A.; Santos, A.; Tojo, J.; Rodríguez, A. Toxicity and Biodegradability of Imidazolium Ionic Liquids. *J. Hazard. Mater.* **2008**, *151* (1), 268–273.
- (20) Docherty, K. M.; Dixon, J. K.; Kulpa, C. F. Biodegradability of Imidazolium and Pyridinium Ionic Liquids by an Activated Sludge Microbial Community. *Biodegradation* **2007**, *18* (4), 481–493.
- (21) Atefi, F.; Garcia, M. T.; Singer, R. D.; Scammells, P. J. Phosphonium Ionic Liquids: Design, Synthesis and Evaluation of Biodegradability. *Green Chem.* **2009**, *11* (10), 1595.
- (22) Abai, M.; Atkins, M. P.; Hassan, A.; Holbrey, J. D.; Kuah, Y.; Nockemann, P.; Oliferenko, A. A.; Plechkova, N. V.; Rafeen, S.; Rahman, A. A.; et al. An Ionic Liquid Process for Mercury Removal from Natural Gas. *Dalt. Trans.* **2015**, *44* (18), 8617–8624.
- (23) Abbott, A. P.; Capper, G.; Davies, D. L.; Rasheed, R. K.; Tambyrajah, V. Novel Solvent Properties of Choline Chloride/urea Mixtures. *Chem. Commun. (Camb)*. **2003**, No. 1, 70–71.
- (24) Carolin Ruß, a B. K. Low Melting Mixtures in Organic Synthesis – an Alternative to Ionic Liquids? Carolin. *Green Chem.* **2010**, *4* (8), 1166–1169.
- (25) Dai, Y.; Van Spronsen, J.; Witkamp, G. J.; Verpoorte, R.; Choi, Y. H. Ionic Liquids and Deep Eutectic Solvents in Natural Products Research: Mixtures of Solids as Extraction Solvents. *J. Nat. Prod.* **2013**, *76* (11), 2162–2173.
- (26) Domínguez de María, P.; Maugeri, Z. Ionic Liquids in Biotransformations: From Proof-of-Concept to Emerging Deep-Eutectic-Solvents. *Curr. Opin. Chem. Biol.* **2011**, *15* (2), 220–225.
- (27) Francisco, M.; Van Den Bruinhorst, A.; Kroon, M. C. Low-Transition-Temperature Mixtures (LTTMs): A New Generation of Designer Solvents. *Angew. Chemie - Int. Ed.* **2013**, *52* (11), 3074–3085.

- 
- (28) Zhang, Q.; De Oliveira Vigier, K.; Royer, S.; Jérôme, F. Deep Eutectic Solvents: Syntheses, Properties and Applications. *Chem. Soc. Rev.* **2012**, *41* (21), 7108–7146.
- (29) Smith, E. L.; Abbott, A. P.; Ryder, K. S. Deep Eutectic Solvents (DESs) and Their Applications. *Chem. Rev.* **2014**, *114* (21), 11060–11082.
- (30) Hayyan, M.; Looi, C. Y.; Hayyan, A.; Wong, W. F.; Hashim, M. A. In Vitro and in Vivo Toxicity Profiling of Ammonium-Based Deep Eutectic Solvents. *PLoS One* **2015**, *10* (2).
- (31) Radošević, K.; Cvjetko Bubalo, M.; Gaurina Srček, V.; Grgas, D.; Landeka Dragičević, T.; Redovniković, R. I. Evaluation of Toxicity and Biodegradability of Choline Chloride Based Deep Eutectic Solvents. *Ecotoxicol. Environ. Saf.* **2015**, *112*, 46–53.
- (32) Hayyan, M.; Hashim, M. A.; Hayyan, A.; Al-Saadi, M. A.; AlNashef, I. M.; Mirghani, M. E. S.; Saheed, O. K. Are Deep Eutectic Solvents Benign or Toxic? *Chemosphere* **2013**, *90* (7), 2193–2195.
- (33) Zhang, Q.; De Oliveira Vigier, K.; Royer, S.; Jérôme, F. Deep Eutectic Solvents: Syntheses, Properties and Applications. *Chem. Soc. Rev.* **2012**, *41* (21), 7108.
- (34) Abbott, A. P.; Boothby, D.; Capper, G.; Davies, D. L.; Rasheed, R. K. Deep Eutectic Solvents Formed between Choline Chloride and Carboxylic Acids: Versatile Alternatives to Ionic Liquids. *J. Am. Chem. Soc.* **2004**, *126* (29), 9142–9147.
- (35) García, G.; Aparicio, S.; Ullah, R.; Atilhan, M. Deep Eutectic Solvents: Physicochemical Properties and Gas Separation Applications. *Energy & Fuels* **2015**, *29* (4), 2616–2644.
- (36) Tang, B.; Row, K. H. Recent Developments in Deep Eutectic Solvents in Chemical Sciences. *Monatshfte fur Chemie* **2013**, *144* (10), 1427–1454.
- (37) Troter, D. Z.; Todorović, Z. B.; Đokić-Stojanović, D. R.; Stamenković, O. S.; Veljković, V. B. Application of Ionic Liquids and Deep Eutectic Solvents in Biodiesel Production: A Review. *Renew. Sustain. Energy Rev.* **2016**, *61*, 473–500.
- (38) Althuluth, M.; Rodriguez, N. R.; Peters, C. J.; Kroon, M. C. The Ionic Liquid 1-Ethyl-3-Methylimidazolium Tris(pentafluoroethyl)trifluorophosphate as Alternative Extractant for BTEX Separation. *Fluid Phase Equilib.* **2015**, *405*, 17–24.
- (39) Kareem, M. A.; Mjalli, F. S.; Hashim, M. A.; AlNashef, I. M. Liquid-Liquid Equilibria for the Ternary System (Phosphonium Based Deep Eutectic Solvent-Benzene-Hexane) at Different Temperatures: A New Solvent Introduced. *Fluid Phase Equilib.* **2012**, *314*, 52–59.
- (40) Gonzalez, A. S. B.; Francisco, M.; Jimeno, G.; De Dios, S. L. G.; Kroon, M. C. Liquid-Liquid Equilibrium Data for the Systems {LTTM+benzene+hexane} and {LTTM+ethyl

- Acetate+hexane} at Different Temperatures and Atmospheric Pressure. *Fluid Phase Equilib.* **2013**, *360*, 54–62.
- (41) Kareem, M. A.; Mjalli, F. S.; Hashim, M. A.; Hadj-Kali, M. K. O.; Bagh, F. S. G.; Alnashef, I. M. Phase Equilibria of Toluene/heptane with Tetrabutylphosphonium Bromide Based Deep Eutectic Solvents for the Potential Use in the Separation of Aromatics from Naphtha. *Fluid Phase Equilib.* **2012**, *333*, 47–54.
- (42) Rodriguez, N. R.; Requejo, P. F.; Kroon, M. C. Aliphatic–Aromatic Separation Using Deep Eutectic Solvents as Extracting Agents. *Ind. Eng. Chem. Res.* **2015**, *54* (45), 11404–11412.
- (43) Ali, S. H.; Lababidi, H. M. S.; Merchant, S. Q.; Fahim, M. A. Extraction of Aromatics from Naphtha Reformate Using Propylene Carbonate. *Fluid Phase Equilib.* **2003**, *214* (1), 25–38.
- (44) Chemat, F.; Vian, M. A.; Cravotto, G. Green Extraction of Natural Products: Concept and Principles. *Int. J. Mol. Sci.* **2012**, *13* (7), 8615–8627.
- (45) Portney, P. R. Economics and the Clean Air Act. *J. Econ. Perspect. Fall* **1990**, *4* (4), 173–181.
- (46) Li, J. J.; Xiao, H.; Tang, X. D.; Zhou, M. Green Carboxylic Acid-Based Deep Eutectic Solvents as Solvents for Extractive Desulfurization. *Energy and Fuels* **2016**, *30* (7), 5411–5418.
- (47) Li, C.; Li, D.; Zou, S.; Li, Z.; Yin, J.; Wang, A.; Cui, Y.; Yao, Z.; Zhao, Q. Extraction Desulfurization Process of Fuels with Ammonium-Based Deep Eutectic Solvents. *Green Chem.* **2013**, *15* (10), 2793–2799.
- (48) Gano, Z. S.; Mjalli, F. S.; Al-wahaibi, T.; Al-wahaibi, Y. The Novel Application of Hydrated Metal Halide ( $\text{SnCl}_2 \cdot 2\text{H}_2\text{O}$ ) – Based Deep Eutectic Solvent for the Extractive Desulfurization of Liquid Fuels. *Int. J. Chem. Eng. Appl.* **2015**, *6* (5), 367–271.
- (49) Tang, X. dong; Zhang, Y. fen; Li, J. jing; Zhu, Y. qiang; Qing, D. yong; Deng, Y. xin. Deep Extractive Desulfurization with Arenium Ion Deep Eutectic Solvents. *Ind. Eng. Chem. Res.* **2015**, *54* (16), 4625–4632.
- (50) Hadj-Kali, M. K.; Mulyono, S.; Hizaddin, H. F.; Wazeer, I.; El-Blidi, L.; Ali, E.; Hashim, M. A.; AlNashef, I. M. Removal of Thiophene from Mixtures with *N*-Heptane by Selective Extraction Using Deep Eutectic Solvents. *Ind. Eng. Chem. Res.* **2016**, *55* (30), 8415–8423.
- (51) Abbott, A. P.; Cullis, P. M.; Gibson, M. J.; Harris, R. C.; Raven, E. Extraction of Glycerol from Biodiesel into a Eutectic Based Ionic Liquid. *Green Chem.* **2007**, *9* (8), 868.
- (52) Berrios, M.; Skelton, R. L. Comparison of Purification Methods for Biodiesel. *Chem. Eng. J.* **2008**, *144* (3), 459–465.

- 
- (53) Shahbaz, K.; Mjalli, F. S.; Hashim, M. A.; Al Nashef, I. M. Using Deep Eutectic Solvents for the Removal of Glycerol from Palm Oil-Based Biodiesel. *Journal of Applied Sciences*. 2010, pp 3349–3354.
- (54) Shahbaz, K.; Mjalli, F. S.; Hashim, M. A.; Alnashef, I. M. Eutectic Solvents for the Removal of Residual Palm Oil-Based Biodiesel Catalyst. *Sep. Purif. Technol.* **2011**, *81* (2), 216–222.
- (55) A. J. Kidnay, W. R. Parrish, D. G. M. *Fundamental of Natural Gas Processing*, Second edi.; CRC PressINC, 2011.
- (56) Zubeir, L. F.; Lacroix, M. H. M.; Kroon, M. C. Low Transition Temperature Mixtures as Innovative and Sustainable CO<sub>2</sub> Capture Solvents. *J. Phys. Chem. B* **2014**, *118* (49), 14429–14441.
- (57) Zubeir, L. F.; Held, C.; Sadowski, G.; Kroon, M. C. PC-SAFT Modeling of CO<sub>2</sub> Solubilities in Deep Eutectic Solvents. *J. Phys. Chem. B* **2016**, *120* (9), 2300–2310.
- (58) Lu, M.; Han, G.; Jiang, Y.; Zhang, X.; Deng, D.; Ai, N. Solubilities of Carbon Dioxide in the Eutectic Mixture of Levulinic Acid (or Furfuryl Alcohol) and Choline Chloride. *J. Chem. Thermodyn.* **2015**, *88*, 72–77.
- (59) Ali, E.; Hadj-Kali, M. K.; Mulyono, S.; Alnashef, I.; Fakeeha, A.; Mjalli, F.; Hayyan, A. Solubility of CO<sub>2</sub> in Deep Eutectic Solvents: Experiments and Modelling Using the Peng-Robinson Equation of State. *Chem. Eng. Res. Des.* **2014**, *92* (10), 1898–1906.
- (60) Trivedi, T. J.; Lee, J. H.; Lee, H. J.; Jeong, Y. K.; Choi, J. W. Deep Eutectic Solvents as Attractive Media for CO<sub>2</sub> Capture. *Green Chem.* **2016**, *18* (9), 2834–2842.
- (61) Mirza, N. R.; Nicholas, N. J.; Wu, Y.; Mumford, K. A.; Kentish, S. E.; Stevens, G. W. Experiments and Thermodynamic Modeling of the Solubility of Carbon Dioxide in Three Different Deep Eutectic Solvents (DESs). *J. Chem. Eng. Data* **2015**, *60* (11), 3246–3252.
- (62) Francisco, M.; van den Bruinhorst, A.; Zubeir, L. F.; Peters, C. J.; Kroon, M. C. A New Low Transition Temperature Mixture (LTTM) Formed by Choline Chloride+lactic Acid: Characterization as Solvent for CO<sub>2</sub> Capture. *Fluid Phase Equilib.* **2013**, *340*, 77–84.
- (63) Sarmad, S.; Mikkola, J.-P.; Ji, X. Carbon Dioxide Capture with Ionic Liquids and Deep Eutectic Solvents: A New Generation of Sorbents. *ChemSusChem* **2017**, *10* (2), 324–352.

### 3 MERCURY CAPTURE FROM *n*-DODECANE USING DEEP EUTECTIC SOLVENTS

*Parts of this chapter have been published in: S. E. E. Warrag, D.J.G.P. van Osch, E. O. Fetisov, D. B. Harwood, M. C. Kroon, J. I. Siepmann, C. J. Peters "Mercury Capture from Petroleum Using Deep Eutectic Solvents", Industrial & Engineering Chemistry Research, 2017. (Submitted)*

*Parts of this chapter have been published in: S. E. E. Warrag, M. C. Kroon, C. J. Peters "Mercury Capture from Petroleum Using Deep Eutectic Solvents", Patent ref. no.: A149669WO*

*Mercury capture is a major challenge in petroleum and natural gas processing. Recently, ionic liquids (ILs) have been introduced as mercury extractants from oil and gas. ILs yield very high mercury extraction efficiencies (> 95%) from hydrocarbons, but their drawbacks include complex synthesis, toxicity, and difficult regeneration after mercury capture. In this chapter, a new technology using deep eutectic solvents (DESs) for elemental mercury ( $Hg^0$ ) extraction from hydrocarbons is demonstrated. DESs are an innovative class of designer solvents exhibiting similar properties as ILs, such as low vapor pressure and low flammability, but DESs are formed from inexpensive hydrogen-bond donor and acceptor compounds that are often biodegradable. In this work, four DESs are investigated including choline chloride:urea, choline chloride:ethylene glycol, choline chloride:levulinic acid, and betaine:levulinic acid, where the molar ratio is 1:2 in all cases. The DESs are tested for their thermal stability, density, and viscosity. Their performance for mercury extraction is assessed using saturated solutions in *n*-dodecane as the model oil. It is found that solvent to feed ratios of 1:1 and 2:1 at temperatures of 303.15 and 333.15 K and atmospheric pressure yield extraction efficiencies greater than 80% for all four DESs.*

### 3.1 Introduction

Energy efficient, economically feasible and environmentally friendly processes for the production of fuels and chemical feedstocks are highly needed. In particular, carbon dioxide capture and natural gas sweetening technologies have garnered significant research efforts over the past two decades.<sup>1-3</sup> On the other hand, comparatively little effort has been directed towards mercury (Hg) capture due to its very small concentration that varies between 0.01 ppb and 10 ppm, depending on the geological location of the oil/gas reservoir.<sup>4</sup> Mercury in crude oil/natural gas is present in different toxic species: elemental mercury ( $\text{Hg}^0$ ) is most prevalent, but mercuric halides (mostly,  $\text{HgCl}_2$ ), organic mercury compounds ( $\text{RHgR}'$  and  $\text{RHgCl}$ ) and mercury-sulfur complexes can also be found.<sup>4</sup> Beyond mercury's health and safety risks for the biosphere, mercury is also a major problem in oil and gas processing units as it deposits in the cryogenic units forming amalgams with different metals (e.g., aluminum) that lead to equipment degradation, and it poisons many catalysts.<sup>4</sup> Additionally, Hg emissions are a major environmental concern and are classified as hazardous air pollutants.<sup>5</sup> Owing to mercury's adverse environmental effects, as well as the operational issues in the oil and gas processing industry, it is rendered mandatory to develop an efficient removal process.

Several technologies are commercially available for mercury capture from liquid/gaseous hydrocarbon streams based on either amalgamation,<sup>6</sup> physical adsorption,<sup>7</sup> chemical adsorption or reactive absorption.<sup>8</sup> The most mature technologies are adsorption on activated carbon and on sulfur/transition metal sulfides impregnated on a solid support, such as activated carbon, alumina, zeolite or silica.<sup>8-10</sup> Due to the sensitivity of sulfur to moisture in organic systems, the latter is less suitable for application in liquid streams.<sup>9</sup> Some other technologies employ regenerative molecular sieves impregnated with silver, but this is an expensive option compared to activated carbon beds.<sup>9</sup> Recently, Clariant and Petronas announced the commercialization of a new solid-supported ionic liquid (SSIL) mercury removal technology.<sup>11</sup> SSIL effectively removes elemental, organic and inorganic mercury from natural gas.<sup>12</sup> Other ILs also show promise as mercury capture technology,<sup>12-15</sup> but ILs are a relatively expensive class of solvents, and economical regeneration approaches have not yet been reported.

As highlighted in *Chapter 2*, DESs have already been utilized in a number of separations relevant to oil and gas industries, such as desulfurization,<sup>16</sup> dearomatization,<sup>16</sup> gas separation<sup>17</sup> and water reclamation<sup>18</sup>. Additionally, the application of DES-functionalized carbon nanotube adsorbents for mercury removal has been studied.<sup>19</sup> In this chapter, the first use of DESs as extracting agents for the removal of mercury from Hg-containing liquid hydrocarbons is reported. The selection of an extraction solvent for mercury from hydrocarbon liquids depends on four factors: (i) its strong affinity for solvating various mercury species, (ii) its low mutual solubility with hydrocarbons, (iii) its thermal stability, and (iv) its regenerability. Here, the first three factors are addressed. DESs are very polar and, hence, their mutual solubility with aliphatic hydrocarbons is expected to be very low.<sup>20</sup> *n*-Dodecane was selected to



represent the aliphatic hydrocarbons in petroleum. It is known that halogen (particularly, Cl) and nitrogen containing ILs exhibit excellent extraction efficiency for mercury.<sup>15</sup> Mancini *et al.*<sup>21</sup> studied the mechanism of the removal of mercury ions from aqueous solutions using hydrophobic/Cl-containing ILs in the absence of chelating agent and suggested that  $\text{Hg}^{2+}$  ions are transferred to the IL phase through the formation of polyanion species  $\text{HgCl}_n^{-n+2}$  (where  $n$  is 1 to 4) and then extraction by the IL. Cheng *et al.*<sup>22</sup> evaluated the extraction of  $\text{Hg}^0$  from flue gas using 1-alkyl-3-methylimidazolium chloride ILs and identified the formation of a complex  $[\text{IL cation}]\text{HgCl}_3$  on a solid adsorbent by means of Raman and UV-Vis spectroscopies. Thus, salt based/polar DESs are expected to be good candidates for this application. Therefore, the selected DESs were (i) choline chloride:urea (**DES-1**), (ii) choline chloride:ethylene glycol (**DES-2**), (iii) choline chloride:levulinic acid (**DES-3**), and (iv) betaine:levulinic acid (**DES-4**), where the molar ratio is 1:2 in all four cases. **DES-4** was chosen to test the influence of replacing a salt-based HBA with a zwitter-ionic HBA. These DESs were tested for their thermal stability by observing their degradation, and for their transport properties by determining glass transition temperatures and measuring viscosities. **DES-1** and **DES-2** are widely used and their densities and viscosities have been reported previously.<sup>23–26</sup> The densities and viscosities of **DES-3** and **DES-4** were determined in this work at temperatures from 298.15 to 333.15 K and atmospheric pressure. The extraction efficiency for the system [dodecane +  $\text{Hg}^0$  + DES] was determined by direct solvent-feed extraction in ratios of 1:1 and 2:1 at  $T = 303.15$  and 333.15 K and atmospheric pressure. These experimental operating conditions were chosen based on the conventional processing temperatures for the Hg adsorbent beds.<sup>9</sup>

## 3.2 Experimental procedures

### 3.2.1 Materials and DES preparation

The chemical compounds used in this work, along with their sources and purities, are reported in Table 1. The choline chloride was dried under vacuum prior to use. The other chemicals were used as obtained.

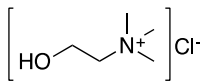
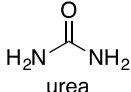
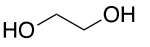
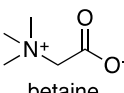
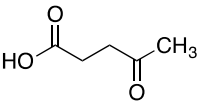
**Table 1:** Chemicals used in this work.

Chemical	Purity (wt %)	Source
Choline chloride	$\geq 98$	Sigma-Aldrich
Urea	$\geq 98$	Sigma-Aldrich
Ethylene glycol	$\geq 99.8$	Sigma-Aldrich
Levulinic acid	$\geq 98$	Sigma-Aldrich
Betaine	$\geq 98$	Sigma-Aldrich
Dodecane	$\geq 99$	Merck
Mercury	Extra pure	Merck

The molecular structures of the constituents for the four DESs are provided in Table 2. Here, the DESs were prepared in 50 g batches using a 1:2 molar ratio for HBA:HBD. The constituents were weighed using a Sartorius ED 224S analytical balance with a precision of  $\pm 0.1$  mg, then added together

in a closed 100 mL glass bottles and mixed thoroughly using a Vortex mixer (VWR). The mixtures were stirred at 323.15 K in an oil bath with a temperature controller (IKA ETS-D5, uncertainty =  $\pm 0.1$  K), until a homogeneous clear liquid was formed. Three DESs were prepared with choline chloride as the HBA and the HBDs were urea, ethylene glycol, and levulinic acid. A fourth DES was prepared from betaine and levulinic acid.

**Table 2:** Molecular structure of the constituents for the DESs investigated here.

HBA	HBD
 <p>choline chloride</p>	 <p>urea</p>
	 <p>ethylene glycol</p>
 <p>betaine</p>	 <p>levulinic acid</p>

### 3.2.2 DES characterization

The water content,  $w$ , of each DES was determined using the Karl Fischer titration method (899 Coulometer, Metrohm Karl Fischer). Three measurements were carried out for each DES to obtain its water content. The specific density,  $\rho$ , and the dynamic viscosity,  $\eta$ , of **DES-3** and **DES-4** were measured over a temperature range from 298.15 to 333.15 K in steps of 5 K at atmospheric pressure using an Anton Paar SVM 3000 Stabinger Viscometer, with instrumental uncertainties of  $\pm 0.01$  K for the temperature and  $\pm 0.0005$  g cm<sup>-3</sup> for the specific density, and a relative uncertainty of  $\pm 0.35\%$  for the dynamic viscosity.

The degradation temperatures,  $T_{\text{deg}}$ , for each DES were obtained using a thermogravimetric analyzer (TGA 4000, PerkinElmer). The weighing precision and sensitivity of the balance are  $\pm 0.01\%$  and 1  $\mu\text{g}$ , respectively. The instrumental uncertainty in temperature is  $\pm 1$  K. The thermographs of the DESs (9-10 mg each) were obtained using the following heating protocol: First, the sample was heated from ambient temperature to 313 K at a heating rate of 5 K min<sup>-1</sup> in a ceramic crucible under a continuous nitrogen flow of 20 cm<sup>3</sup> min<sup>-1</sup> and a gas pressure of 0.2 MPa. Then, the sample was held for 120 min at 313 K. Finally, the change in mass was scanned by heating from 313 K to 673 K at a rate of 5 K min<sup>-1</sup>. Two thermographs were obtained for each DES.

Differential scanning calorimetry (TA Instruments, DSC Q100) was used to determine the glass transition temperature,  $T_g$ , of the DES with a scanning rate of 5 K min<sup>-1</sup> and temperature range from 193.15 K to 303.15 K. The instrumental uncertainty in  $T$  is  $\pm 0.1$  K. The calorimeter precision and sensitivity are  $\pm 0.1$  % and 0.2  $\mu$ W, respectively.

The structure of the DESs was verified by proton and carbon nuclear magnetic resonance (NMR) spectroscopy using a Bruker 400 MHz spectrometer (Appendix, Figures 4 to 11).

### 3.2.3 Mercury extraction experiments

25 mL of *n*-dodecane (>99% purity) was saturated with elemental mercury (extra pure) at ambient conditions to a concentration of approximately 4 mg kg<sup>-1</sup>. The saturated *n*-dodecane solution was added to the DESs using both a 1:1 and 2:1 solvent-to-feed mass ratio. The mixtures were initially mixed for a short time using a Vortex mixer followed by shaking the solutions for 2 h using an incubating shaker (IKA KS 4000i) at temperatures of 303.15 and 333.15 K. The mixtures were left to settle for 30 min until liquid–liquid coexistence was visually observed with the *n*-dodecane and DES being the upper and lower phases, respectively. A sample from the *n*-dodecane phase was taken using a syringe without disturbing the equilibrium interface. The *n*-dodecane sample was then analyzed for its mercury content using a Milestone Direct Mercury Analyzer DMA-80 pyrolysis/AA analyzer. A sample of the *n*-dodecane phase (20–30 mg) was introduced in the DMA-80, in which the sample was initially dried at  $T = 573$  K and then thermally decomposed at  $T = 1123$  K in an oxygen flow (200 mL min<sup>-1</sup>) and a gas pressure of 4 bar. The combustion products were carried off and further decomposed in a hot catalyst bed at  $T = 873$  K. The mercury vapors were trapped on a gold amalgamator and subsequently desorbed at  $T = 1173$  K. Finally, the mercury content is determined using atomic absorption spectrophotometry at 254 nm.

## 3.3 Results and discussion

### 3.3.1 DES characterization

Figure 1 illustrates the temperature dependencies ( $298.15 \text{ K} \leq T \leq 333.15 \text{ K}$ ) of the specific density,  $\rho$ , and of the dynamic viscosity,  $\eta$ , for **DES-3** and **DES-4** (the numerical data are provided in the Appendix, Table 4). Over this 35 K temperature range, the specific densities are well described by linear fits as follows:

**DES-3:**

$$\rho = (-0.652 \pm 0.002) [\text{kg m}^{-3}\text{K}^{-1}] T + (1331.2 \pm 0.5) [\text{kg m}^{-3}]$$

**DES-4:**

$$\rho = (-0.723 \pm 0.004) [\text{kg m}^{-3}\text{K}^{-1}] T + (1373.4 \pm 1.1) [\text{kg m}^{-3}]$$

The standard deviations of the experimental data from the corresponding linear fits are 0.124 and 0.116 kg m<sup>-3</sup> for **DES-3** and **DES-4**, respectively.

The viscosity is a key property for selecting a proper absorbent candidate because it is related to the mass transfer rate of the solute from the feed to the solvent. As illustrated in Figure 1, the viscosities of **DES-3** and **DES-4** decrease sharply over the temperature range investigated here. Although the two DESs share a common HBD compound, DES-4 with the zwitter-ionic HBA yields  $\eta$  values exceeding those of DES-3 with the ionic HBA by factors ranging from 2.5 at 333.15 K to 4.8 at 298.15 K. The Vogel–Fulcher–Tammann (VFT) equation is widely used to describe the temperature dependence of the dynamic viscosity for DESs.<sup>27,28</sup> Here we also observe a good description of the  $\eta$  values by the VFT equation as follows:

**DES-3:**

$$\eta = (0.126 \pm 0.012) [\text{mPa s}] \exp \left[ \frac{(857 \pm 24) [\text{K}]}{T - (186 \pm 2) [\text{K}]} \right]$$

**DES-4:**

$$\eta = (0.059 \pm 0.006) [\text{mPa s}] \exp \left[ \frac{(1078 \pm 20) [\text{K}]}{T - (190 \pm 1) [\text{K}]} \right]$$

The standard deviations of the experimental data from the corresponding VFT fits are 0.042 and 0.282 mPa s for **DES-3** and **DES-4**, respectively.

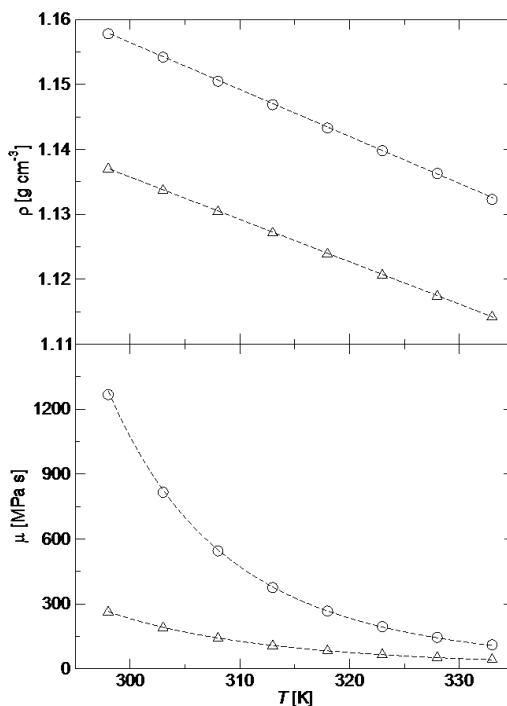


**Figure 1:** Experimental data for the specific density (top) and the dynamic viscosity (bottom) for DES-3 (triangles) and DES-4 (circles) as function of temperature. The dashed lines show linear fits for the specific density and VFT fits for the dynamic viscosity. The statistical uncertainties are smaller than the symbol size.

Knowledge of the thermal stability range is important to assess the viability of an extraction solvent. The thermographs for the four DESs are depicted in Figure 2. As can be seen, the thermal degradation proceeds in two major steps for **DES-2**, **DES-3**, and **DES-4**, but only one broad step for **DES-1**. Conventionally, the degradation temperature,  $T_{\text{deg}}$ , is determined from the intersection of the extrapolated tangent where the weight loss starts (the first derivative equals to zero) and the slope of the weight loss at the inflection point (the peak of the first derivative).<sup>29</sup> The same method was applied here using the inflection point for the first step in the thermographs, and the results are presented in Table 3. Since any absorbed water is likely to evaporate first as the heating protocol is started, the water content was also determined and found to range from 1510 ppm for **DES-1** to 7150 ppm for **DES-3**. The thermograph for **DES-2** showed a 3% decrease in weight after keeping the sample at  $T = 313.15$  K for 2 h which can only be attributed to the evaporation of volatile impurities because the moisture content was low. **DES-2** also is thermally least stable with  $T_{\text{deg}} = 386$  K, whereas the  $T_{\text{deg}}$  values of the other three DESs are above 440 K. Thus, all four DESs are thermally stable at the operating temperature of the extraction experiments.

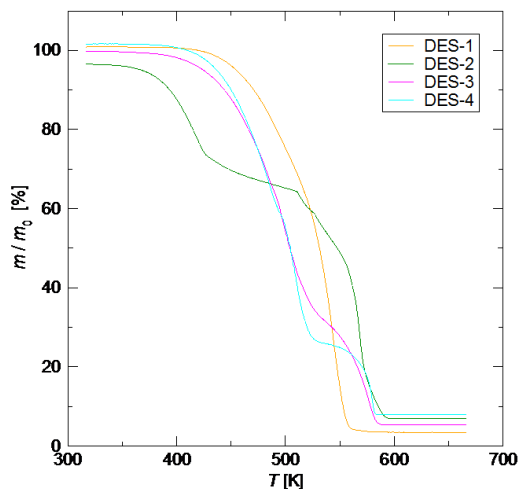


**Figure 2:** Thermographs of the four DESs obtained with a heating rate of  $5 \text{ K min}^{-1}$ .

The glass transition temperatures were also determined for the four DESs using differential scanning calorimetry. The half-step glass transition temperature method<sup>28</sup> was adopted here, and  $T_g$  values range from 205 K for **DES-1** to 245 K for **DES-2** (see Table 3).

**Table 3:** Water content ( $w$ ), degradation temperature ( $T_{deg}$ ), and glass transition temperature ( $T_g$ ) of the four DESs.

DESs	$w$ [ppm]	$T_{deg}$ [K]	$T_g$ [K]
DES-1	$1510 \pm 20$	$455.4 \pm 0.5$	205.15
DES-2	$1870 \pm 20$	$386.0 \pm 1.5$	245.15
DES-3	$7150 \pm 40$	$445.1 \pm 1.3$	243.15
DES-4	$6690 \pm 40$	$443.4 \pm 0.1$	214.15

### 3.3.2 Mercury extraction efficiencies

The extraction performance for the system [*n*-dodecane +  $\text{Hg}^0$  + DES] was evaluated for solvent to feed ratios of 1:1 and 2:1 at  $T = 303.15$  and  $333.15$  K and atmospheric pressure. No color change was noticed when the DESs were mixed with the *n*-dodecane solution and the mercury was transferred from the non-polar alkane phase to the polar DES phase. The initial and final mercury concentrations in the *n*-dodecane solution,  $C_i$  and  $C_f$ , respectively, were measured in triplicate for each sample, and each extraction experiment was done in duplicate (numerical data are provided in the Appendix, Table 5). The extraction efficiencies,  $E$ , were calculated as follows:

$$E = (C_i - C_f)/C_i$$

The results are displayed in Figure 3 (tables with numerical data are provided in the Appendix, Table 5). It should be noted that the statistical uncertainties are fairly large, as one should expect for extraction experiments using very dilute solute concentrations. At 303.15 K, the two extraction experiments yield consistent  $C_f$  values when the same feed solution was used. At 333.15 K, however, the  $C_f$  values for **DES-1** show significant scatter despite the use of the same feed solution. Increasing the solvent-to-feed ratio is found to increase the extraction efficiency only for six of the eight cases, but even in those cases the increase in  $E$  falls within the statistical uncertainties.

All four solvents yield extraction efficiencies in excess of 80% for both temperatures and both solvent:feed ratios. Overall, 9 out of 16  $E$  values fall into the range from 87 to 93%, and  $E$  values tend to be somewhat higher at  $T = 333.15$  K with 3 out of 8 satisfying  $E \geq 95\%$ . Particularly, **DES-3** extracts more than 97% of the mercury at 333.15 K, but here a feed solution with an unusually high  $C_i$  value was used. The good extraction performance for **DES-1**, **DES-2**, and **DES-3** can likely be attributed to the coordination of mercury by Cl anions, but coordination by electronegative oxygen atoms of the solvent may also play a role. For the zwitter-ionic **DES-4**, coordination by the carboxylate group may provide a favorable environment for mercury. An affinity of Hg atoms to solvate in acidic mediums has been described previously.<sup>30</sup> Gibbs free energies of transfer were also estimated from the concentration data (see Appendix, Table 5) and are found to range from  $-4$  to  $-14$  kJ mol<sup>-1</sup> (with uncertainties being less than 2 kJ mol<sup>-1</sup>); thus, solvation in the DESs is clearly much preferred over solvation in a petroleum oil, but the uncertainties preclude a detailed ranking of the DESs investigated here.

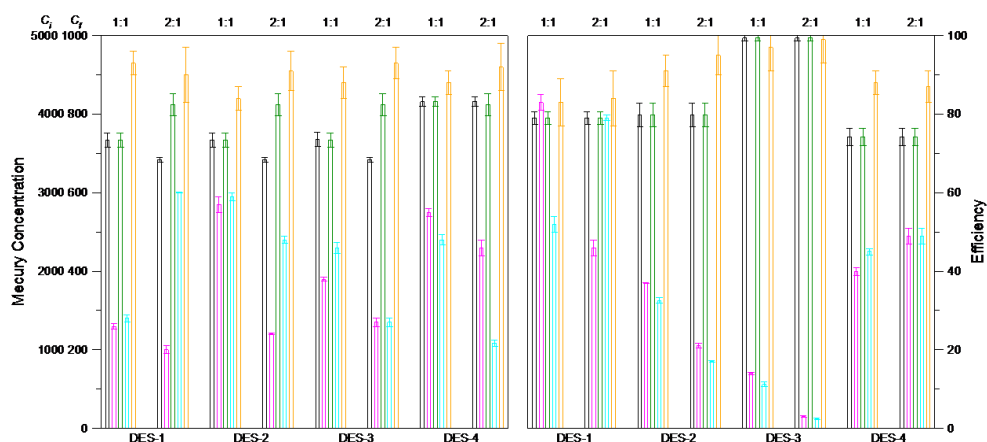


**Figure 3:** Extraction performance data for the four DESs at 303.15 K (left) and 333.15 K (right). The  $C_i$  values in [ $\mu\text{g kg}^{-1}$ ] for the two extraction experiments performed for each solvent and feed ratio are shown as black and green bars using the outer tick labels on the left. The corresponding  $C_f$  values in [ $\mu\text{g kg}^{-1}$ ] are shown as magenta and cyan bars using the inner tick labels on the left side. The  $E$  values averaged over the two extraction experiments are shown as orange bars using the tick labels on the right side.

### 3.4 Conclusions

In this chapter, the first application of DESs for the removal of elemental mercury ( $\text{Hg}^0$ ) from liquid petroleum was described. The DESs were composed of either choline chloride or betaine as the hydrogen-bond acceptor, and either urea, ethylene glycol or levulinic acid as the hydrogen-bond donor. These compounds are widely available or can be synthesized from bio-renewable resources. For example, choline chloride is an additive in chicken feed and levulinic acid can be derived from degradation of cellulose. All four DESs were found to be very good extraction solvents with extraction efficiencies exceeding 80% for 1:1 and 2:1 solvent:feed ratios and Gibbs free energies of transfer from *n*-dodecane to DES being negative (i.e., favorable) with a magnitude from about 4 to 14  $\text{kJ mol}^{-1}$ .



### 3.5 References

- (1) Sanz-Pérez, E. S.; Murdock, C. R.; Didas, S. A.; Jones, C. W. Direct Capture of CO<sub>2</sub> from Ambient Air. *Chem. Rev.* **2016**, *116* (19), 11840–11876.
- (2) Abanades, J. C.; Arias, B.; Lyngfelt, A.; Mattisson, T.; Wiley, D. E.; Li, H.; Ho, M. T.; Mangano, E.; Brandani, S. Emerging CO<sub>2</sub> Capture Systems. *Int. J. Greenh. Gas Control* **2015**, *40*, 126–166.
- (3) Shah, M. S.; Tsapatsis, M.; Siepmann, J. I. Hydrogen Sulfide Capture: From Absorption in Polar Liquids to Oxide, Zeolite, and Metal-Organic Adsorbents and Membranes. *Chem. Rev.* **2017**, *117*, 9755–9803.
- (4) Wilhelm, S. M.; Bloom, N. Mercury in Petroleum. *Fuel Process. Technol.* **2000**, *63* (1), 1–27.
- (5) Portney, P. R. Economics and the Clean Air Act. *J. Econ. Perspect. Fall* **1990**, *4* (4), 173–181.
- (6) Markovs, J.; Heights, Y.; Cintins, P. E.; Plaines, D. Purification of Fluid Streams Containing Mercury. US Patent 4874525, 1989.
- (7) Li, L.; Li, X.; Lee, J.-Y.; Keener, T. C.; Liu, Z.; Yao, X. The Effect of Surface Properties in Activated Carbon on Mercury Adsorption. *Ind. Eng. Chem. Res.* **2012**, *51* (26), 9136–9144.
- (8) Granite, E. J.; Pennline, H. W.; Hargis, R. a. Novel Sorbents for Mercury Removal from Flue Gas. *Ind. Eng. Chem. Res.* **2000**, *39*, 1020–1029.
- (9) Eckersley, N. Advanced Mercury Removal Technologies. *Hydrocarbon Process.* **2010**, No. January, 29–35.
- (10) Hiroshi Nishino, Toshio Aibe, K. N. Process for Removal of Mercury Vapor and Adsorbant Therefor. US Patent 4500327 A, 1985.
- (11) Rogers, R. D.; Holbrey, J.; Rodriguez, H. Process for Removing Metals from Hydrocarbons. WO 2010/116165 A2, 2010.
- (12) Abai, M.; Atkins, M. P.; Hassan, A.; Holbrey, J. D.; Kuah, Y.; Nockemann, P.; Oliferenko, A. a; Plechkova, N. V; Rafeen, S.; Rahman, A. a; et al. An Ionic Liquid Process for Mercury Removal from Natural Gas. *Dalt. Trans.* **2015**, *44* (18), 8617–8624.
- (13) Ji, L.; Thiel, S. W.; Pinto, N. G. Room Temperature Ionic Liquids for Mercury Capture from Flue Gas. *Ind. Eng. Chem. Res.* **2008**, *47* (21), 8396–8400.
- (14) Ji, L.; Thiel, S. W.; Pinto, N. G. Pyrrolidinium Imides: Promising Ionic Liquids for Direct Capture of Elemental Mercury from Flue Gas. *Water, Air, Soil Pollut. Focus* **2007**, *8* (3–4), 349–358.

- 
- (15) Rogers, R. D.; Holbrey, J. Ionic Liquid Solvents of Perhlide Type for Metals and Metal Compounds. US 20120090430A, 2012.
- (16) Warrag, S. E. E.; Peters, C. J.; Kroon, M. C. Deep Eutectic Solvents for Highly Efficient Separations in Oil and Gas Industries. *Curr. Opin. Green Sustain. Chem.* **2017**, *5*, 55–60.
- (17) Garcia, G.; Aparicio, S.; Ullah, R.; Atilhan, M. Deep Eutectic Solvents: Physicochemical Properties and Gas Separation Applications. *Energy & Fuels* **2015**, *29*, 2616–2644.
- (18) Mahto, A.; Mondal, D.; Poliseti, V.; Bhatt, J.; Nidhi, M. R.; Prasad, K.; Nataraj, S. K. Sustainable Water Reclamation from Different Feed Streams by Forward Osmosis Process Using Deep Eutectic Solvents as Reusable Draw Solution. *Ind. Eng. Chem. Res.* **2017**, *56*, 14623–14632.
- (19) Alomar, M. K.; Alsaadi, M. A.; Jassam, T. M.; Akib, S.; Ali Hashim, M. Novel Deep Eutectic Solvent-Functionalized Carbon Nanotubes Adsorbent for Mercury Removal from Water. *J. Colloid Interface Sci.* **2017**, *497*, 413–421.
- (20) Smith, J. G. *Organic Chemistry*, second.; Timp, T., Ed.; New york, 2008.
- (21) Mancini, M. V.; Spreti, N.; Di Profio, P.; Germani, R. Understanding Mercury Extraction Mechanism in Ionic Liquids. *Sep. Purif. Technol.* **2013**, *116*, 294–299.
- (22) Cheng, G.; Bai, B.; Zhang, Q.; Cai, M. Hg<sup>0</sup> Removal from Flue Gas by Ionic liquid/H<sub>2</sub> O<sub>2</sub> .*J. Hazard. Mater.* **2014**, *280*, 767–773.
- (23) Abbott, A. P.; Capper, G.; Gray, S. Design of Improved Deep Eutectic Solvents Using Hole Theory. *Chemphyschem* **2006**, *7* (4), 803–806.
- (24) D’Agostino, C.; Harris, R. C.; Abbott, A. P.; Gladden, L. F.; Mantle, M. D. Molecular Motion and Ion Diffusion in Choline Chloride Based Deep Eutectic Solvents Studied by <sup>1</sup>H Pulsed Field Gradient NMR Spectroscopy. *Phys. Chem. Chem. Phys.* **2011**, *13*, 21383–21391.
- (25) Abbott, A. P.; Harris, R. C.; Ryder, K. S. Application of Hole Theory to Define Ionic Liquids by Their Transport Properties. *J. Phys. Chem. B* **2007**, *111* (18), 4910–4913.
- (26) Shahbaz, K.; Mjalli, F. S.; Hashim, M. A.; Al Nashef, I. M. Using Deep Eutectic Solvents for the Removal of Glycerol from Palm Oil-Based Biodiesel. *Journal of Applied Sciences*. 2010, pp 3349–3354.
- (27) Rodriguez, N. R.; Requejo, P. F.; Kroon, M. C. Aliphatic–Aromatic Separation Using Deep Eutectic Solvents as Extracting Agents. *Ind. Eng. Chem. Res.* **2015**, *54* (45), 11404–11412.
- (28) Zubeir, L. F.; Lacroix, M. H. M.; Kroon, M. C. Low Transition Temperature Mixtures as

- Innovative and Sustainable CO<sub>2</sub> Capture Solvents. *J. Phys. Chem. B* **2014**, *118* (49), 14429–14441.
- (29) Vyazovkin, S. Thermogravimetric Analysis. In *Characterization of Materials*; 2012; pp 1–12.
- (30) ShamsiJazeyi, H.; Kaghazchi, T. Investigation of Nitric Acid Treatment of Activated Carbon for Enhanced Aqueous Mercury Removal. *J. Ind. Eng. Chem.* **2010**, *16* (5), 852–858.

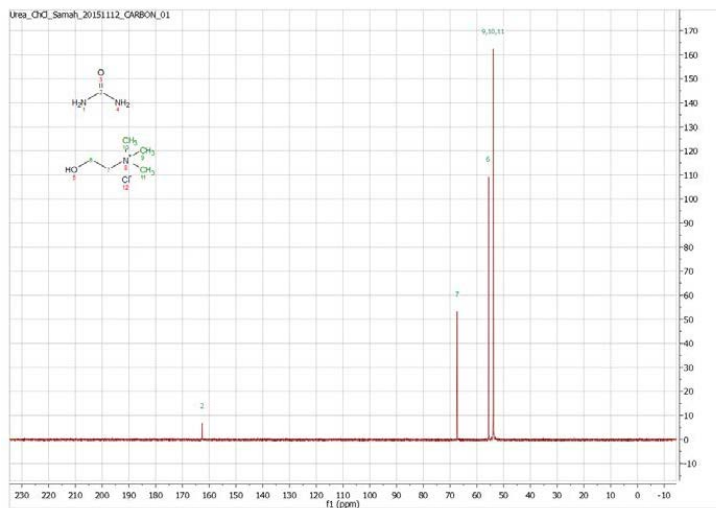
### 3.6 Appendix Chapter 3

#### DES Structure

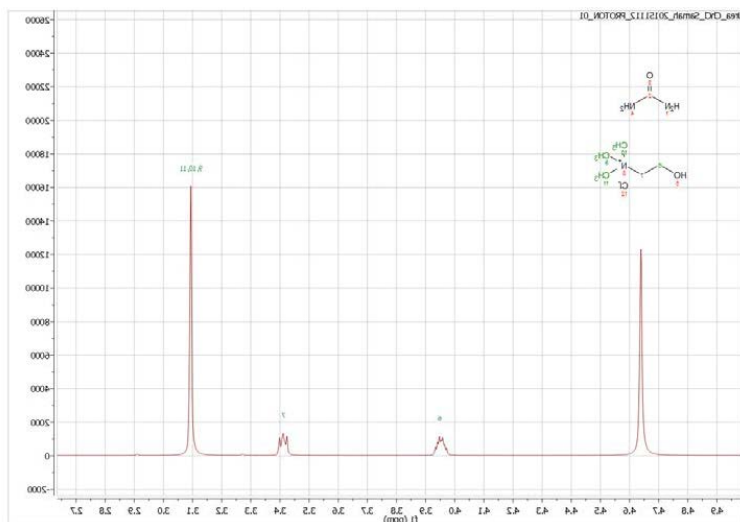
NMR analyses were performed to investigate whether the constituents of the DES reacted with each other. For all four DESs deuterated water (D<sub>2</sub>O) was used as NMR solvent. Precision tubes (8”) from the brand Wilmad with an outer diameter of 5 mm were used. The <sup>1</sup>H NMRs were recorded in 64 scans with a relaxation time of 3s. The <sup>13</sup>C NMRs were taken in 1024 scans with a relaxation time of 5s. Fourier transformation was automatically performed with the recording software VnmrJ, and MestreNova (version 9.1.0-14011) was used for the analysis of the spectra. The spectra were analyzed as measured.

All <sup>13</sup>C NMR spectra showed the same number of peaks at the approximate position as theoretically predicted with ChembiDraw (version 14.0.0.117). The <sup>1</sup>H NMR spectra showed the proper peaks except for the peaks of the acids and alcohol. These could not be measured since these hydrogens will be exchanged with the deuteriums of the deuterated water. Predictions made with ChembiDraw were used to check the shifts if condensations would occur. No big shifts were observed.

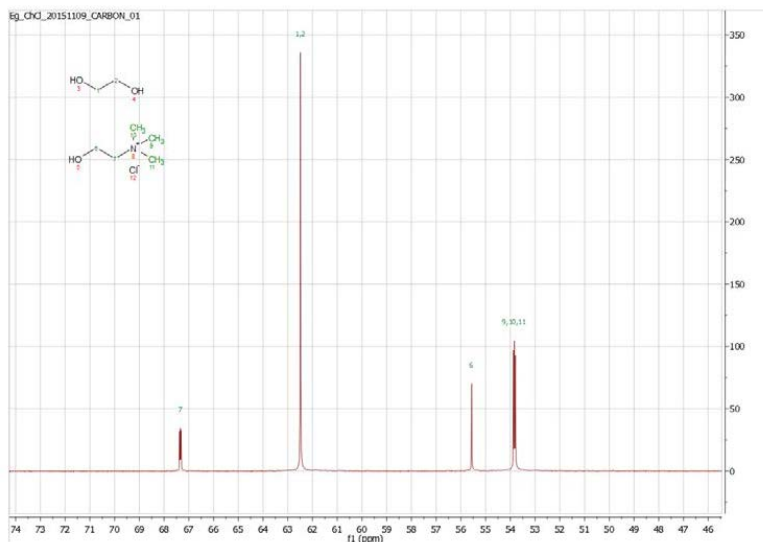
From the combination of only small shifts in the <sup>1</sup>H NMR spectra and no extra peaks in the <sup>13</sup>C NMR spectra, it is concluded that no reaction between the constituents of the DES has occurred.

**Choline chloride: Urea (1:2) (DES-1)****Carbon (DES-1)**

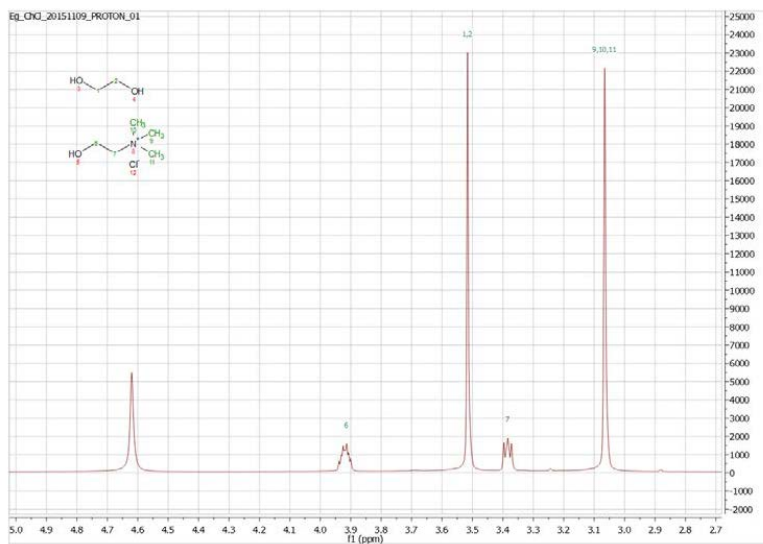
**Figure 4:**  $^{13}\text{C}$  NMR spectrum of DES-1 constituted of choline chloride and urea in a 1:2 molar ratio

**Proton (DES-1)**

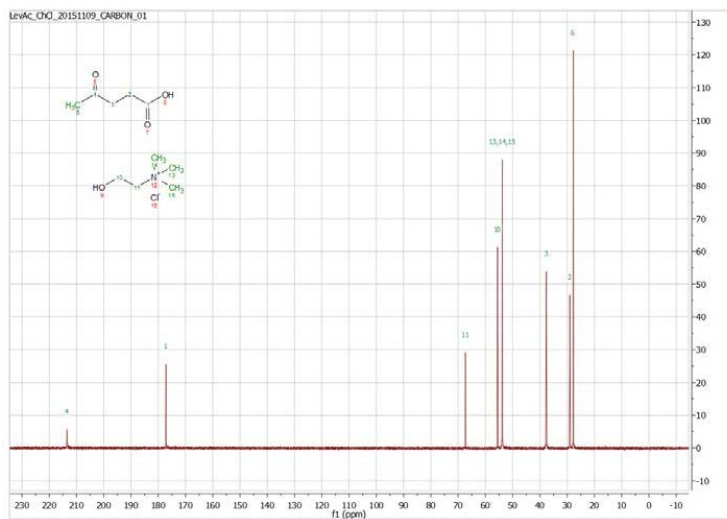
**Figure 5:**  $^1\text{H}$  NMR spectrum of DES-1 constituted of choline chloride and urea in a 1:2 molar ratio

**Carbon (DES-2)**

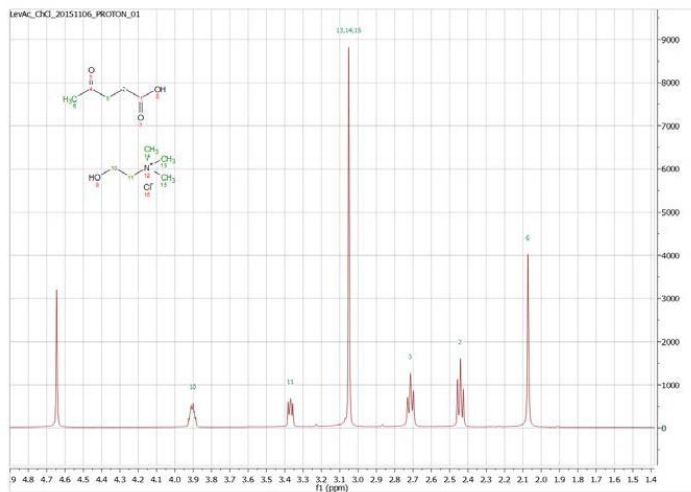
**Figure 6:** <sup>13</sup>C NMR of DES-2 constituted of choline chloride and ethylene glycol in a 1:2 molar ratio

**Proton (DES-2)**

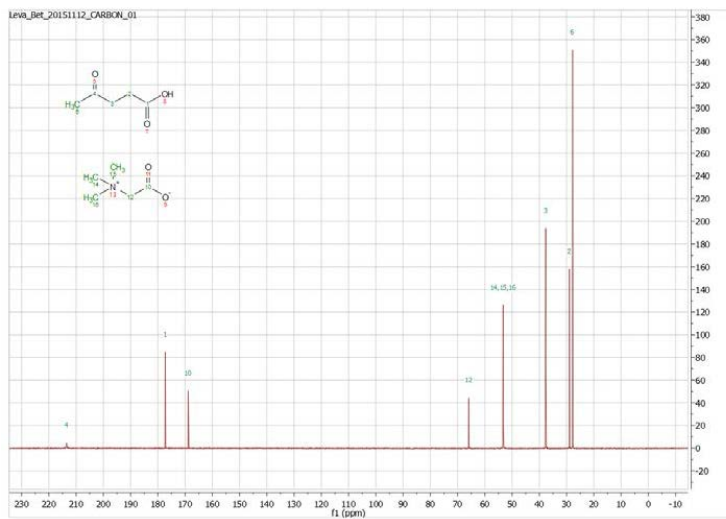
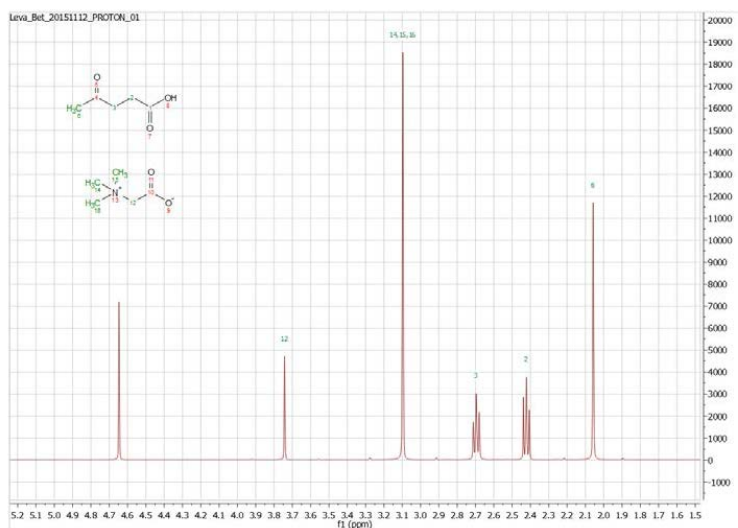
**Figure 7:** <sup>1</sup>H NMR spectrum of DES-2 constituted of choline chloride and ethylene glycol in a 1:2 molar ratio

**Choline chloride: levulinic acid (1:2) (DES-3)****Carbon (DES-3)**

**Figure 8:** <sup>13</sup>C NMR spectrum of DES-3 constituted of choline chloride and levulinic acid in a 1:2 molar ratio

**Proton (DES-3)**

**Figure 9:** <sup>1</sup>H NMR spectrum of DES-3 constituted of choline chloride and levulinic acid in a 1:2 molar ratio

**Betaine: levulinic acid (1:2) (DES-4)****Carbon (DES-4)****Figure 10:**  $^{13}\text{C}$  NMR spectrum of DES-4 constituted of betaine and levulinic acid in a 1:2 molar ratio**Proton (DES-4)****Figure 11:**  $^1\text{H}$  NMR spectrum of DES-4 constituted of betaine and levulinic acid in a 1:2 molar ratio



### Experimental Density and Viscosity Data

**Table 4:** Experimental densities and viscosities of DES-3 and DES-4 at different temperatures and at atmospheric pressure. The standard deviations are estimated from replicate measurements.

$T$	DES-3		DES-4	
	$\rho$	$\eta$	$\rho$	$\eta$
	[K]	[kg m <sup>-3</sup> ]	[mPa s]	[kg m <sup>-3</sup> ]
298.15	1137.0 ± 0.1	262.8 ± 0.4	1157.8 ± 0.1	1267 ± 2
303.15	1133.7 ± 0.1	189.7 ± 0.3	1154.2 ± 0.1	816 ± 2
308.15	1130.4 ± 0.1	140.7 ± 0.2	1150.5 ± 0.1	544.9 ± 0.8
313.15	1127.1 ± 0.1	106.7 ± 0.1	1146.9 ± 0.1	375.7 ± 0.5
318.15	1123.9 ± 0.1	82.6 ± 0.1	1143.3 ± 0.1	267.0 ± 0.3
323.15	1120.6 ± 0.1	65.22 ± 0.07	1139.8 ± 0.1	194.8 ± 0.2
328.15	1117.4 ± 0.1	52.43 ± 0.06	1136.3 ± 0.1	145.57 ± 0.07
333.15	1114.2 ± 0.1	42.72 ± 0.03	1132.3 ± 0.1	111.16 ± 0.02

### Extraction Experiment Data

**Table 5:** Concentrations obtained for two extraction experiments (labeled by superscripts A and B), and derived efficiencies, and Gibbs free energies of transfer. The standard deviations are estimated from replicate measurements and error propagation.

DES #	$T$	Ratio	$C_i^A$	$C_r^A$	$C_i^B$	$C_r^B$	$E$	$\Delta G$
	[K]		[ $\mu\text{g kg}^{-1}$ ]	[ $\mu\text{g kg}^{-1}$ ]	[ $\mu\text{g kg}^{-1}$ ]	[ $\mu\text{g kg}^{-1}$ ]	[%]	[kJ mol <sup>-1</sup> ]
DES-1	303.15	1:1	3670 ± 90	260 ± 10	3670 ± 90	280 ± 10	93 ± 3	-7.7 ± 0.2
DES-1	303.15	2:1	3420 ± 30	200 ± 10	4120 ± 140	600 ± 10	90 ± 7	-5.3 ± 1.8
DES-1	333.15	1:1	3950 ± 80	830 ± 20	3950 ± 80	520 ± 20	83 ± 6	-5.8 ± 1.1
DES-1	333.15	2:1	3950 ± 80	460 ± 20	3950 ± 80	790 ± 10	84 ± 7	-4.2 ± 1.3
DES-2	303.15	1:1	3670 ± 90	570 ± 20	3670 ± 90	590 ± 10	84 ± 3	-5.5 ± 0.1
DES-2	303.15	2:1	3420 ± 30	240 ± 10	4120 ± 140	480 ± 10	91 ± 5	-5.4 ± 1.0
DES-2	333.15	1:1	3990 ± 150	370 ± 10	3990 ± 150	330 ± 10	91 ± 4	-7.9 ± 0.3
DES-2	333.15	2:1	3990 ± 150	210 ± 10	3990 ± 150	170 ± 10	95 ± 5	-7.8 ± 0.5
DES-3	303.15	1:1	3680 ± 90	380 ± 10	3670 ± 90	460 ± 20	88 ± 4	-6.5 ± 0.4
DES-3	303.15	2:1	3420 ± 30	270 ± 10	4120 ± 140	270 ± 10	93 ± 4	-6.0 ± 0.4
DES-3	333.15	1:1	4970 ± 40	140 ± 10	4970 ± 40	110 ± 10	97 ± 6	-11.5 ± 0.5
DES-3	333.15	2:1	4970 ± 40	30 ± 2	4970 ± 40	24 ± 2	99 ± 6	-14.0 ± 0.5
DES-4	303.15	1:1	4160 ± 60	550 ± 10	4160 ± 60	480 ± 20	88 ± 3	-6.2 ± 0.3
DES-4	303.15	2:1	4160 ± 60	460 ± 20	4120 ± 140	220 ± 10	92 ± 6	-5.8 ± 1.4
DES-4	333.15	1:1	3710 ± 110	400 ± 10	3710 ± 110	450 ± 10	88 ± 3	-7.1 ± 0.3
DES-4	333.15	2:1	3710 ± 110	490 ± 20	3710 ± 110	490 ± 20	87 ± 4	-4.7 ± 0.2

---

## 4 THE SOLUBILITY OF CO<sub>2</sub> IN TETRAHEXYLAMMONIUM-BASED DEEP EUTECTIC SOLVENTS

*The results presented in this chapter will be submitted to the Journal of Chemical Engineering Data*

*Global warming and climate change threads have provoked global research efforts to reduce the concentration of atmospheric carbon dioxide (CO<sub>2</sub>). CO<sub>2</sub> capture is considered a crucial strategy for meeting CO<sub>2</sub> emission mitigation targets. In this work, two deep eutectic solvents (DESs) constituted of tetrahexylammonium bromide as a hydrogen bond acceptor (HBA) and either ethylene glycol or glycerol as a hydrogen bond donor (HBD) with molar ratios of HBA:HBD equal to 1:2, were investigated as novel sustainable absorbents for CO<sub>2</sub> capture. The phase behavior of CO<sub>2</sub> with the DESs was measured using a gravimetric magnetic suspension balance operating in the static mode at 293.2 K and 298.2 K and pressures up to 2 MPa. The Henry's law coefficient and the enthalpy of absorption were calculated from the solubility data for the purpose of comparing their performance to existing state-of-the-art physical solvents for CO<sub>2</sub> capture. It was observed that the CO<sub>2</sub> solubility increased with pressure and decreased with temperature. The CO<sub>2</sub> solubilities in the studied DES were found to be lower than those of conventional physical solvents. Nevertheless, DESs are a promising class of absorbents because of their low cost starting materials and preparation methods, their environmentally friendly character, and their tunability, which allows further optimization for CO<sub>2</sub> capture.*

## 4.1 Introduction

Carbon dioxide (CO<sub>2</sub>) is a primary anthropogenic greenhouse gas (GHG) that contributes significantly to global warming and climate change. In the past decades, the world has witnessed a continuous increase of CO<sub>2</sub> emissions reaching 400 ppm in 2014 according to the Keeling Curve measurements of CO<sub>2</sub> at Mauna Loa Observatory.<sup>1</sup> It is known that the combustion of fossil fuels has been historically the dominant source of CO<sub>2</sub> emissions. The increasing global demand for energy since the industrial revolution as a result of population growth, economic growth and other factors has led to a high dependence on fossil fuels with the associated increased CO<sub>2</sub> emissions. The rising CO<sub>2</sub> levels in the atmosphere ringed a warning bell of an urgent need for innovative control approaches. And, in spite of the tremendous research efforts towards the production of green, low-carbon and renewable energy, fossil fuels-based power plants are still the most effective solution ‘so far’ for energy production. Thus, developing efficient CO<sub>2</sub> capturing techniques would be a better option for mitigating emissions.

In this regards, CO<sub>2</sub> has been conventionally captured via either *pre*-combustion, *post*-combustion or oxyfuel approaches.<sup>2</sup> Each approach has its advantages and disadvantages. However, *post*-combustion using aqueous solutions of amines has been widely applied on commercial scale in contrast to the other two approaches.<sup>3</sup> In this technology, the CO<sub>2</sub> containing flue gas and a 20–30 wt % monoethanol amine (MEA) solution are introduced concurrently to an absorption column. The CO<sub>2</sub> in the flue gas is then chemically absorbed by the primary amine (MEA) to form carbamates. The MEA is then regenerated at temperatures typically at 100–140 °C and atmospheric pressure, whereby the MEA is recycled and the concentrated CO<sub>2</sub> is pressurized and sent to storage.<sup>2</sup> As a consequence of the high chemical reactivity of the MEA with the CO<sub>2</sub>, the solvent regeneration results in a high energy consumption. Besides the considerable energy consumption, amines are also volatile, corrosive and suffer from degradation in the presence of oxygen leading to solvent losses, making them unattractive alternatives for CO<sub>2</sub> capture.<sup>3</sup> The environmental and economic concerns associated with amine-based processes, triggered researchers to look for alternatives that can be environmentally more benign, thermally and chemically stable and with a lower energy penalty for solvent regeneration. In the past few decades, ionic liquids (ILs), have been proposed to overcome the drawbacks of conventional amine solvents. This is due to the attractive properties of the ILs including negligible volatility, high chemical/thermal stability, and tunability.<sup>4,5</sup> They have been widely studied for CO<sub>2</sub> capture applications.<sup>3</sup> The absorption capacity of ILs was comparable to conventional physical solvents. However, ILs are costly to prepare, often toxic and none biodegradable.

As highlighted in *Chapter 2*, DESs share many attractive properties with ILs including negligible vapor pressure, low flammability, thermal and chemical stability, good solvation properties and tunability. However, in comparison with ILs, DESs offer other advantages, such as simple preparation with 100% atom economy without purification required. Moreover, the DES constituents HBA (hydrogen bond acceptor) and HBD (hydrogen bond donor) are mostly low-cost, non-toxic and

often biodegradable. Due to the environment-friendly characteristics and good economic prospects of the DESs, they have been investigated as alternatives to amines and ILs for CO<sub>2</sub> capture in many recent studies.<sup>6-9</sup> Considering the solubility data available in the literature, it can be deduced that the CO<sub>2</sub> solubility increases with increasing pressure and decreasing temperature. The type of the HBA and HBD, and their molar ratios strongly affect the CO<sub>2</sub> absorption capacity. Ammonium based-DESs, particularly, choline chloride (ChCl) based-DESs were the most investigated DESs for CO<sub>2</sub> capture. To date, the ChCl:Glycerol (1:2) is found to have the best performance (3.692 mol·kg<sup>-1</sup>) at 303.2 K and 5.863 MPa.<sup>10</sup> The DES constituted of ChCl:Ethylene Glycol (1:2) is found to have a slightly lower CO<sub>2</sub> solubility (3.1265 mol·kg<sup>-1</sup>) at the same conditions.<sup>10</sup> Zubeir *et al.*<sup>11,12</sup> studied the effect of the alkyl chain length in DESs constituted of tetraalkylammonium chloride:lactic acid (1:2) and it was found that the CO<sub>2</sub> solubility increased with increasing alkyl chain length of the ammonium salt, where tetrabutylammonium chloride:lactic acid exhibited the highest solubility.

Building on these literature findings, it can be anticipated that ammonium based-DESs with a long alkyl chain length and polyols might be good alternatives for CO<sub>2</sub> capture. Therefore, in this work, two DESs constituted of tetrahexylammonium bromide (HBA) and either ethylene glycol or glycerol (HBDs) with molar ratios of the HBA:HBD equal to 1:2, were studied for CO<sub>2</sub> capture. A gravimetric magnetic suspension balance operating in the static mode at 293.2 and 298.2 K and pressures up to 2 MPa, has been used to measure the phase behavior of CO<sub>2</sub> in these DESs. Then, the Henry's law coefficient and the enthalpy of absorption were calculated from the solubility data in order to compare the performance of the DESs to existing state-of-the-art physical solvents for CO<sub>2</sub> capture.

## 4.2 Experimental procedures

### 4.2.1 Chemicals

The source and purity (as stated by the suppliers) of all the chemicals used in this work are presented in Table 1. All the chemicals were used without further purification.

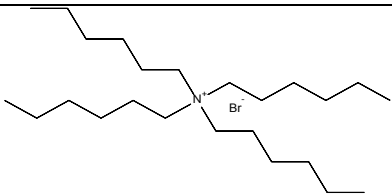
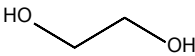
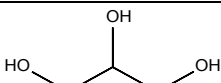
**Table 1:** Source, purity (as stated by the suppliers) and CAS number of the chemicals used in this work.

Chemical	Source	Purity (wt %)	CAS number
Carbon dioxide	Air Products	≥ 99	124-38-9
Tetrahexylammonium bromide	Sigma-Aldrich	≥ 99	4328-13-6
Glycerol	Merck KGaA	≥ 99	56-81-5
Ethylene glycol	Sigma-Aldrich	≥ 99	107-21-1

## 4.2.2 DES Preparation

The DESs used in this work were prepared according to the heating method. The heating method requires that the precisely weighted amounts of HBD and HBA are heated together at a certain temperature while stirring in a sealed flask until a clear liquid is formed. The weighing of both the HBD and the HBA was done using a balance Mettler AX205 with an uncertainty in the measurement of  $\pm 0.2$  mg. The mixture was heated at 333.2 K in a thermostatic bath (IKA RCT basic) with a temperature controller (IKA ETS-D5) with an uncertainty in the measurement of  $\pm 0.1$  K. The DESs prepared were: (i) tetrahexylammonium bromide:ethylene glycol with molar ratio = 1:2 (THABr:EG) and (ii) tetrahexylammonium bromide:glycerol with molar ratio = 1:2 (THABr:Gly). The molecular structures of THABr:EG and THABr:Gly are shown in Table 2. The structure of the DESs was verified by 400 Bruker nuclear magnetic resonance (NMR) spectrometer for  $^1\text{H-NMR}$  (Appendix of Chapter 5, Figure 11 and 12). The density and viscosity of the prepared DESs can be found elsewhere<sup>13</sup>.

**Table 2:** The molecular structures of the DESs, THABr:EG and THABr:Gly.

DES	HBA	Molar ratio	HBD
THABr:EG		1:2	
THABr:Gly			

4.2.3 CO<sub>2</sub> Absorption

A magnetically suspended balance (MBS) from Rubotherm was used to accurately weigh a sample over a range of temperature and pressure conditions. The current facility features highly accurate weight measurements in a closed environment. In the MBS, the sample is linked to a so-called suspension magnet which consists of a permanent magnet, a sensor core and a device for decoupling the measuring load (the sample). An electromagnet, which is attached to the underfloor weighing hook of a balance, maintains a freely suspended state of the suspension magnet via an electronic control unit. Using this magnetic suspension coupling the measuring force is transmitted contactlessly from the measuring chamber to the microbalance, which is located outside the chamber under ambient atmospheric conditions.

Prior to the solubility measurement, the DES was dried and degassed for 6 h under vacuum. During the course of experiments, the MBS measures the weight change, pressure and temperature as a function of time. CO<sub>2</sub> sorption in DES causes an increase of the sample weight container and the weight

change of the sample is continuously recorded along with the pressure and the gas density until equilibrium is reached. The mass of CO<sub>2</sub> absorbed in DES is calculated by the following equation:

$$m_{CO_2} = m_{bal} - m_s - m_{sc} + (V_{sc} + V_s + V_A) * \rho(P, T) \quad (1)$$

$m_{bal}$	Balance recorded weight
$m_s$	Mass of the sample
$m_{sc}$	Mass of the sample container
$V_{sc}$	Volume of the sample container
$V_s$	Volume of the sample
$V_A$	Volume of CO <sub>2</sub> absorbed
$\rho(P, T)$	Density of the gas CO <sub>2</sub>

The mass and volume of the sample container is measured by using blank measurements at 308.2 K, the intercept and the slope of the measurement gives the mass and volume of the sample container respectively, as shown in Appendix, Figure 2. Moreover, the mass and volume of the sample are measured using buoyancy measurements for THABr:EG and THABr:Gly. The buoyancy measurement of THABr:EG and THABr:Gly can be found in the Appendix Figures 3 and 4, respectively. Detailed experimental procedures of the MBS can be found elsewhere.<sup>11</sup>

### 4.3 Results and discussion

#### 4.3.1 CO<sub>2</sub> Absorption data

The CO<sub>2</sub> solubilities in THABr:EG and THABr:Gly were measured at temperatures of 293.2 K and 298.2 K, and pressures up to 2 MPa. The CO<sub>2</sub> uptake was determined by measuring the bubble-point pressures at various compositions of CO<sub>2</sub> in the DES using the MBS. The results are shown in Table 3 and are graphically presented in Figure 1. From Figure 1 it can be observed that: (i) the CO<sub>2</sub> solubility increases with a pressure increase, and (ii) the CO<sub>2</sub> solubility decreases upon a temperature increase. The observed trends are typical for the solubility of CO<sub>2</sub> in DESs.<sup>10–12,14–18</sup>

**Table 4:** CO<sub>2</sub> uptake in DESs using the Magnetic Suspension Balance\*

THABr:EG			
$T (K) = 293.2$		$T (K) = 298.2$	
P(MPa)	Uptake (mol/kg)	P(MPa)	Uptake (mol/kg)
0.000	0.000	0.000	0.000
0.191	0.019	0.191	0.060
0.391	0.119	0.391	0.163
0.592	0.245	0.589	0.262
0.791	0.364	0.793	0.403
0.993	0.494	0.994	0.479
1.190	0.656	1.187	0.652
1.393	0.791	1.392	0.760
1.596	0.925	1.591	0.891
		1.793	1.023
		1.986	1.136
THABr:Gly			
$T (K) = 293.2$		$T (K) = 298.2$	
0.000	0.000	0.000	0.000
0.191	0.026	0.191	0.005
0.391	0.073	0.391	0.056
0.590	0.132	0.592	0.111
0.792	0.199	0.790	0.180
0.992	0.272	0.991	0.240
1.190	0.345	1.191	0.303
1.391	0.417	1.391	0.358
1.591	0.492	1.593	0.429
1.792	0.567	1.791	0.473
1.991	0.642	1.993	0.558

\* The standard uncertainties in the measurements are  $u(p) = 0.001$  MPa,  $u(T) = 0.021$  K, and standard uncertainties in weight  $u(m) = 0.0071$  mg

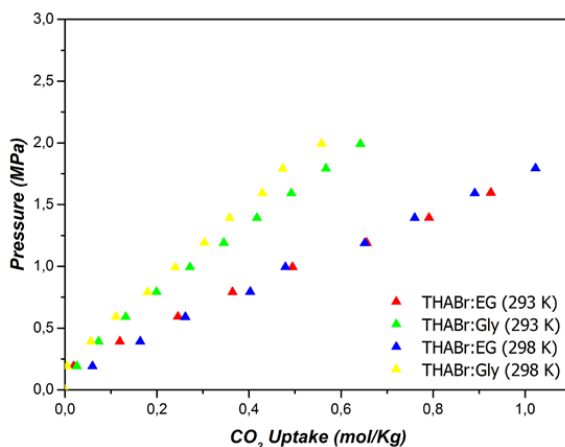


**Figure 4:** Isotherms of CO<sub>2</sub> uptake (mol of CO<sub>2</sub>/kg of DES) in the prepared DESs as function of pressure

Comparing the performance of the studied DESs, the glycerol-based DES (THABr:Gly) showed lower CO<sub>2</sub> uptake than the ethylene glycol-based DES (THABr:EG). This could be ascribed to the polarity difference between the two DESs. THABr:Gly has three hydroxyl groups (-OH) and is presumably more polar than THABr:EG with two -OH groups for the same molar ratio (1:2). This might contribute to lowering the solubility of non-polar molecules like CO<sub>2</sub> in THABr:Gly. Another factor is that, the viscosity of THABr:Gly is much higher than THABr:EG,<sup>13</sup> which implies stronger intermolecular interactions between the DES “THABr:Gly” constituents. And therefore, increased steric hindrance that leads to lowering the CO<sub>2</sub> solubility.

This observation is opposite to the finding reported in the literature by Leron *et. al.*<sup>19,20</sup>, who found that the solubility of CO<sub>2</sub> in a glycerol-based DES (choline chloride:glycerol (1:2))<sup>19</sup> is slightly higher than in the ethylene glycol-based DES (choline chloride:ethylene glycol (1:2))<sup>20</sup>. Some other studies<sup>11,12</sup> suggested that the salt (HBA) of the DES is dominating the CO<sub>2</sub> absorption capacity due to its large free volume. The longer the alkyl chain length of the cation of the salt, the higher the solubility. However, the mechanism of CO<sub>2</sub> capture, whether it depends on the free volume or on the molecular interaction of the CO<sub>2</sub> and the DES, is still a debate and further research is highly desired.

#### 4.3.2 Henry's law constant

Henry's law states that at equilibrium, the amount of the gas dissolved in a liquid is proportional to its partial pressure in the gas phase at infinite dilution. It should be noted that, Henry's law is only applicable under low pressures and low solubilities. The proportionality constant is Henry's law constant:



$$H_{2,1}(T, P) [\text{MPa}] = \lim_{x_2 \rightarrow 0} \frac{f_2(T, P, x_2)}{x_2} \approx \frac{P_2}{x_2} \quad (2)$$

$$H_{2,1}^*(T, P) [\text{MPa} \cdot \text{kg/mol}] \approx \frac{P_2}{m_2} \quad (3)$$

where  $H_{2,1}(T, P)$  is the Henry's constant,  $x_2$  is the mole fraction of  $\text{CO}_2$  dissolved in the DES,  $f_2$  fugacity of  $\text{CO}_2$  in the gas phase, and  $P_2$  is the partial pressure of  $\text{CO}_2$  at phase equilibrium. At the experimental conditions investigated, the DESs have essentially negligible vapor pressure. This implies that the fugacity of the gas phase can fairly be assumed to equal that of pure  $\text{CO}_2$ . Henry's law constant can be determined from the slope of the solubility data ( $P_2$  vs  $x_2$ ) (see eq. (2)). It can also be quantified on a mass basis by determining the slope of the  $\text{CO}_2$  uptake data (mol  $\text{CO}_2$  / kg DES) ( $P_2$  vs  $m_2$ ) (see eq. (3)). The larger the  $H_{2,1}^*$  the lower the solubility. Henry's law constant is frequently used in the literature as a comparison parameter for gas solubility at low pressures. In this work  $H_{2,1}$  were determined for the investigated DESs and compared to the state-of-art solvent for  $\text{CO}_2$  capture Selexol,<sup>21</sup> the hydrophobic DES that are known to exhibit the highest  $\text{CO}_2$  capacity among DESs, reported by Zubier *et al.*,<sup>22</sup> and two fluorinated ionic liquids ( $[\text{C}_4\text{mim}][\text{BF}_4]$ <sup>23</sup> and  $[\text{C}_4\text{mim}][\text{Tf}_2\text{N}]$ <sup>23</sup>) that are known by their high absorption capacity, reported by Anthony *et al.* It should be mentioned that the comparisons were done on a mass basis due to the differences in the molar masses of the solvents. The mass basis comparisons are more realistic and practical for large scale/industrial solvent selection.

From Table 4 it can be noticed that THABr:Gly showed the lowest solubility (highest  $H_{2,1}^*$ ) among all other solvents. While the  $H_{2,1}^*$  of THABr:EG was found to be comparable to the hydrophobic DESs "N<sub>8881</sub>-Cl:DecA, N<sub>8888</sub>-Cl:DecA, and N<sub>8888</sub>-Br:DecA" but higher than Selexol, N<sub>8881</sub>-Br:DecA, and the fluorinated ILs. Although the  $\text{CO}_2$  solubilities in the studied DESs were found to be lower than some of the best solvents for  $\text{CO}_2$  capture, the physiochemical properties of the DESs, including the  $\text{CO}_2$  absorption capacity, are tunable depending on the starting HBA and HBD, allowing further optimization for  $\text{CO}_2$  capture.

**Table 4:** Henry's law constants  $H_{2,1}^*$  of  $\text{CO}_2$  in the prepared DESs and in DESs and ILs reported in literature at 298.2 K

<i>Solvent</i>	$H_{2,1}^* (\text{MPa Kg mol}^{-1})$
N <sub>8881</sub> -Br:DecA <sup>22</sup>	0.04
N <sub>8881</sub> -Cl:DecA <sup>22</sup>	1.79
N <sub>4444</sub> -Cl:DecA <sup>22</sup>	1.57
N <sub>8888</sub> -Cl:DecA <sup>22</sup>	1.87
N <sub>8888</sub> -Br:DecA <sup>22</sup>	1.86
THABr:EG	1.81
THABr:Gly	3.80
Selexol <sup>21</sup>	0.97

$[\text{C}_4\text{mim}][\text{BF}_4]^{23}$	1.33
$[\text{C}_4\text{mim}][\text{Tf}_2\text{N}]^{23}$	1.38

### 4.3.3 Enthalpy of Absorption

The partial molar enthalpy of the dissolution of  $\text{CO}_2$  in the DESs can be calculated using the Clausius-Clapeyron equation, as follows:

$$\Delta_{abs}h = R \left( \frac{\partial \ln P_2}{\partial \frac{1}{T}} \right)_{x_2}$$

where  $R$  is the universal gas constant,  $T$  is the absolute temperature,  $P$  is the  $\text{CO}_2$  partial pressure at equilibrium and  $P_2$  is the partial pressure of  $\text{CO}_2$  in the DES at equilibrium.

**Table 5:** Molar enthalpy ( $\Delta_{abs}H$ ) of dissolution of  $\text{CO}_2$  in the DESs and the fluorinated IL at fixed composition ( $x_{\text{CO}_2} = 0.1$ )

Solvent	$\Delta_{abs}H/\text{kJ}\cdot\text{mol}^{-1}$
$\text{N}_{8888}\text{-Cl:DecA}^{22}$	-10.5
$\text{N}_{4444}\text{-Cl:DecA}^{22}$	-11.6
$\text{N}_{8888}\text{-Br:DecA}^{22}$	-10.5
$[\text{C}_4\text{mim}][\text{Tf}_2\text{N}]^{23}$	-12.5
Selexol <sup>3</sup>	-14.3
Fluor Solvent <sup>3</sup>	-15.9
Purisol <sup>3</sup>	-16.4
Rectisol <sup>3</sup>	-13.0
THABr:EG	-25.9
THABr:Gly	-17.2

It is well known that the molar enthalpy of dissolution  $\Delta_{sol}H$  is an indication of the strength of the bond between the solvent and the solute. The higher the  $\Delta_{sol}H$ , the stronger the molecular interaction between the solute and the solvent. The negative sign is an indication of exothermic absorption. From Table 5 it can be seen that the  $\Delta_{sol}H$  of THABr:Gly is quite similar to the hydrophobic DESs and  $[\text{C}_4\text{mim}][\text{Tf}_2\text{N}]$ , and the existing state-of-art physical solvents (e.g. Selexol, Fluor Solvent, Purisol, and Rectisol) reported in the literature. While, THABr:EG was almost twice as high as the physical solvents listed in Table 5. However, it is much lower than the chemical solvents ( $< -80 \text{ kJ}\cdot\text{mol}^{-1}$ ).<sup>24</sup>

In the physical solvents, as well as the fluorinated ILs, the molecular interactions are mainly electrostatic. Therefore, it could be deduced that the THABr:EG and THABr:Gly act as physical solvents for  $\text{CO}_2$  capture. This an advantage as the physical solvents usually require less energy for regeneration. However, further studies are necessary to investigate the nature of interactions within the DESs and their interactions with  $\text{CO}_2$ .

#### 4.4 Conclusions

In this chapter two DESs were investigated as absorbents for CO<sub>2</sub>. The DESs constituted of tetrahexylammonium bromide as a hydrogen bond acceptor (HBA) and either ethylene glycol or glycerol as a hydrogen bond donors (HBDs) with molar ratios of HBA:HBD equal to 1:2. The CO<sub>2</sub> uptakes in the DESs were measured using a magnetic suspension balance at 293.2 K and 298.2 K and pressures up to 2 MPa. It was observed that the CO<sub>2</sub> solubility increased with pressure and decreased with temperature, as expected. The Henry's law constants and the enthalpy of absorption were calculated for the investigated DESs and compared to the relevant literature. THABr:Gly showed the highest Henry's law constant among all other solvents, and therefore the lowest solubility, while the Henry's law constant of THABr:EG was found to be comparable to the hydrophobic DESs. Further, the enthalpy of absorption was found to be comparable to those of physical solvents. In spite of the relatively low CO<sub>2</sub> solubilities observed in the studied DESs compared to other physical solvents, the results are promising, especially in view of the tunability of the DESs that allow further optimization for CO<sub>2</sub> capture.

#### 4.5 References

- (1) Oceanography, S. I. of. The Keeling Curve <https://scripps.ucsd.edu/programs/keelingcurve/>.
- (2) A. J. Kidnay, W. R. Parrish, D. G. M. *Fundamental of Natural Gas Processing*, Second edi.; CRC PressINC, 2011.
- (3) Ramdin, M.; De Loos, T. W.; Vlugt, T. J. H. State-of-the-Art of CO<sub>2</sub> Capture with Ionic Liquids. *Ind. Eng. Chem. Res.* **2012**, *51* (24), 8149–8177.
- (4) Welton, T. Ionic Liquids in Catalysis. *Coord. Chem. Rev.* **2004**, *248* (21–24), 2459–2477.
- (5) Gordon, C. M. New Developments in Catalysis Using Ionic Liquids. *Appl. Catal. A Gen.* **2001**, *222* (1–2), 101–117.
- (6) Smith, E. L.; Abbott, A. P.; Ryder, K. S. Deep Eutectic Solvents (DESs) and Their Applications. *Chem. Rev.* **2014**, *114* (21), 11060–11082.
- (7) Garcia, G.; Aparicio, S.; Ullah, R.; Atilhan, M. Deep Eutectic Solvents: Physicochemical Properties and Gas Separation Applications. *Energy & Fuels* **2015**, *29*, 2616–2644.
- (8) Pena-Pereira, F.; Namieśnik, J. Ionic Liquids and Deep Eutectic Mixtures: Sustainable Solvents for Extraction Processes. *ChemSusChem* **2014**, *7* (7), 1784–1800.
- (9) Zhang, Q.; De Oliveira Vigier, K.; Royer, S.; Jérôme, F. Deep Eutectic Solvents: Syntheses, Properties and Applications. *Chem. Soc. Rev.* **2012**, *41* (21), 7108–7146.
- (10) Sarmad, S.; Mikkola, J.-P.; Ji, X. Carbon Dioxide Capture with Ionic Liquids and Deep Eutectic Solvents: A New Generation of Sorbents. *ChemSusChem* **2017**, *10* (2), 324–352.
- (11) Zubeir, L. F.; Lacroix, M. H. M.; Kroon, M. C. Low Transition Temperature Mixtures as Innovative and Sustainable CO<sub>2</sub> Capture Solvents. *J. Phys. Chem. B* **2014**, *118* (49), 14429–14441.
- (12) Zubeir, L. F.; Held, C.; Sadowski, G.; Kroon, M. C. PC-SAFT Modeling of CO<sub>2</sub> Solubilities in Deep Eutectic Solvents. *J. Phys. Chem. B* **2016**, *120* (9), 2300–2310.
- (13) Rodriguez, N. R.; Requejo, P. F.; Kroon, M. C. Aliphatic–Aromatic Separation Using Deep Eutectic Solvents as Extracting Agents. *Ind. Eng. Chem. Res.* **2015**, *54* (45), 11404–11412.
- (14) Garcia, G.; Aparicio, S.; Ullah, R.; Atilhan, M. Deep Eutectic Solvents: Physicochemical Properties and Gas Separation Applications. *Energy & Fuels* **2015**, *29* (4), 2616–2644.
- (15) Trivedi, T. J.; Lee, J. H.; Lee, H. J.; Jeong, Y. K.; Choi, J. W. Deep Eutectic Solvents as Attractive Media for CO<sub>2</sub> Capture. *Green Chem.* **2016**, *18* (9), 2834–2842.

- 
- (16) Ali, E.; Hadj-Kali, M. K.; Mulyono, S.; Alnashef, I.; Fakeeha, A.; Mjalli, F.; Hayyan, A. Solubility of CO<sub>2</sub> in Deep Eutectic Solvents: Experiments and Modelling Using the Peng-Robinson Equation of State. *Chem. Eng. Res. Des.* **2014**, *92* (10), 1898–1906.
- (17) Francisco, M.; van den Bruinhorst, A.; Zubeir, L. F.; Peters, C. J.; Kroon, M. C. A New Low Transition Temperature Mixture (LTTM) Formed by Choline Chloride+lactic Acid: Characterization as Solvent for CO<sub>2</sub> Capture. *Fluid Phase Equilib.* **2013**, *340*, 77–84.
- (18) Lu, M.; Han, G.; Jiang, Y.; Zhang, X.; Deng, D.; Ai, N. Solubilities of Carbon Dioxide in the Eutectic Mixture of Levulinic Acid (or Furfuryl Alcohol) and Choline Chloride. *J. Chem. Thermodyn.* **2015**, *88*, 72–77.
- (19) Leron, R. B.; Li, M.-H. Solubility of Carbon Dioxide in a Eutectic Mixture of Choline Chloride and Glycerol at Moderate Pressures. *J. Chem. Thermodyn.* **2013**, *57*, 131–136.
- (20) Leron, R. B.; Li, M.-H. Solubility of Carbon Dioxide in a Choline Chloride–ethylene Glycol Based Deep Eutectic Solvent. *Thermochim. Acta* **2013**, *551*, 14–19.
- (21) Xu, Y.; Schutte, R. P.; Hepler, L. G. Solubilities of Carbon Dioxide, Hydrogen Sulfide and Sulfur Dioxide in Physical Solvents. *Can. J. Chem. Eng.* **1992**, *70* (3), 569–573.
- (22) Zubeir, L. F.; van Osch, D. J. G. P.; Rocha, M. A. A.; Banat, F.; Kroon, M. C. Carbon Dioxide Solubilities in Decanoic Acid-Based Hydrophobic Deep Eutectic Solvents. *J. Chem. Eng. Data* **2018**, acs.jced.7b00534.
- (23) Anthony, J. L.; Anderson, J. L.; Maginn, E. J.; Brennecke, J. F. Anion Effects on Gas Solubility in Ionic Liquids. *J. Phys. Chem. B* **2005**, *109* (13), 6366–6374.
- (24) Carson, J. K.; Marsh, K. N.; Mather, A. E. Enthalpy of Solution of Carbon Dioxide in (Water + Monoethanolamine, or Diethanolamine, or N-Methyldiethanolamine) and (Water + Monoethanolamine + N-Methyldiethanolamine) at T = 298.15 K. *J. Chem. Thermodyn.* **2000**, *32* (9), 1285–1296.

## 4.6 Appendix chapter 4

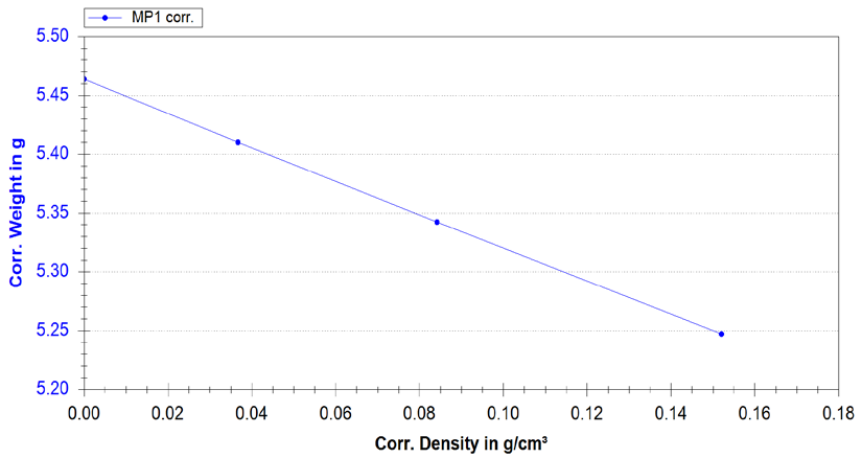


Figure 2: Blank measurement for mass and volume of the sample container

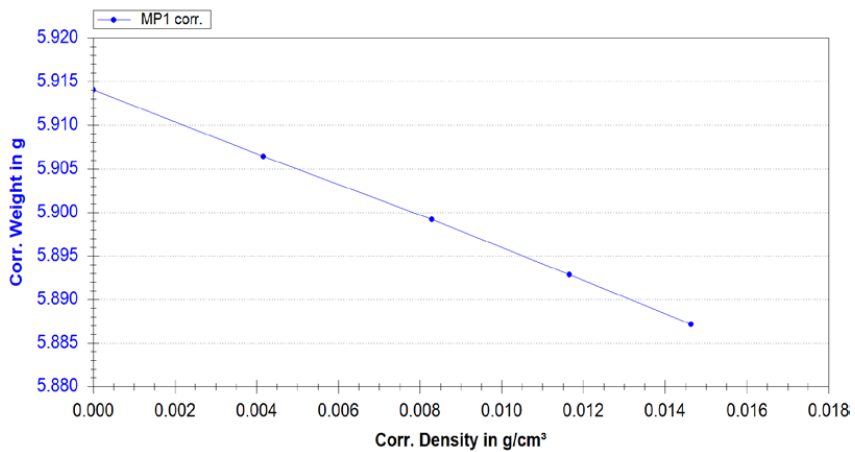
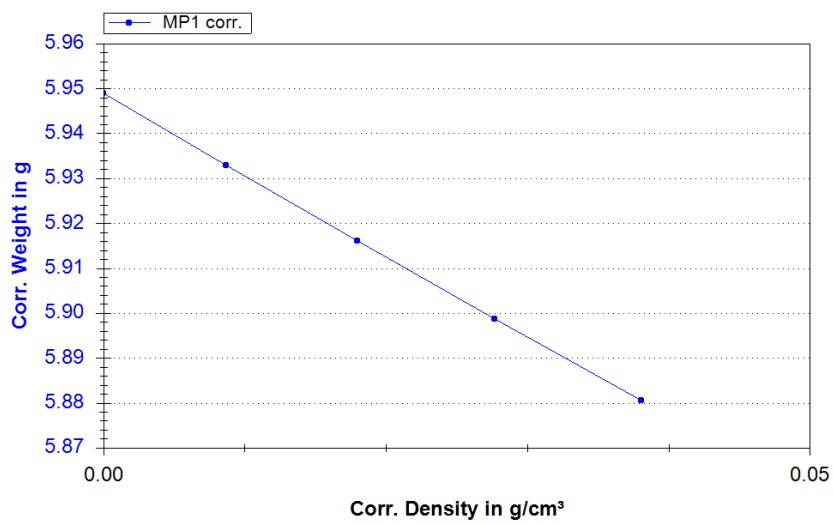


Figure 4: Buoyancy measurement for mass and volume of the THABr:EG



**Figure 4:** Buoyancy measurement for mass and volume of the THABr:Gly

## 5 OIL DESULFURIZATION USING DEEP EUTECTIC SOLVENT AS EXTRACTANT VIA LIQUID-LIQUID EXTRICATION

Parts of this chapter have been published in: **S. E. E Warrag**, N. R. Rodriguez, I. M. Nashef, M. van Sint Annaland, M. C. Kroon, C. J. Peters, "Separation of Thiophene from Aliphatic Hydrocarbons Using Tetrahexylammonium-Based Deep Eutectic Solvents as Extracting Agents" *Journal of Chemical & Engineering Data*, **2017**, 62, 2911–2919.

Parts of this chapter have been published in: **S. E. E Warrag**, C. Pototzki, N. R. Rodriguez, M. van Sint Annaland, M. C. Kroon, C. Held, G. Sadowski, C. J. Peters, "Oil Desulfurization Using Deep Eutectic Solvents as Sustainable and Economical Extractants via Liquid-Liquid Extraction: Experimental and PC-SAFT Predictions" *Fluid Phase Equilibria*, **2018**, 467, 33-44

Parts of this chapter have been published in: **S. E. E Warrag**, I. Adeyemi, N. R. Rodriguez, I. M. Nashef, M. van Sint Annaland, M. C. Kroon, C. J. Peters, "Effect of the Type of Ammonium Salt on the Extractive Desulfurization of Fuels using Deep Eutectic Solvents" *Journal of Chemical & Engineering Data*, **2018**, 63, 1088–1095

In this chapter, the extraction of sulfur compounds from {*n*-alkane + thiophene} mixtures using DESs as extracting agents is studied. The LLE data of the binary and ternary systems {*n*-hexane + DES}, {*n*-octane + DES}, {thiophene + DES}, {*n*-hexane + thiophene + DES}, {*n*-octane + thiophene + DES} were measured at 298.2 K and atmospheric pressure. The distribution ratio of thiophene aromatic and the selectivities were calculated and compared with the available literature. The effect on the extraction efficiency on: (ii) the type/length of the *n*-alkane, (iii) the characteristics of the HBAs, i.e. different chain length of the alkyl group and the functional group on the ammonium cation, (iv) the HBDs type of the polyol. The extraction mechanism of the thiophene was explained using Conductor-like Screening Model for Real Solvents (COSMO-RS). Finally, the DESs were successfully regenerated by means of vacuum evaporation.



## 5.1 Introduction

The sulfur concentration in crude oil can reach up to 2 wt% or greater depending on the geological location of the oil reservoir.<sup>1</sup> The crude oil contains a large variety of organosulfur compounds, including thiols (R-S), sulfides (R-S-R), and sulfur-containing aromatics: “thiophene’s family”.<sup>2</sup> The combustion of sulfur-containing fuel leads to undesirable SO<sub>x</sub> emissions. Therefore, governmental regulations such as EPA’s Acid Rain Program established under title IV of the 1990 Clean Air Act (CAA) amendments regarding the sulfur content of fuels continue to be enacted worldwide.<sup>3</sup> Furthermore, sulfur derivatives are major causes of coking, sintering, and corrosion of metal-based catalysts in oil refining processes.<sup>4</sup> Thus, the desulfurization of crude oil is an important step in the fuel production industry. Throughout the years, the catalytic hydrodesulfurization (HDS) has been conventionally utilized for the removal of sulfur and sulfur derivatives from crude oil.<sup>5,6</sup> In this process, the sulfur compounds are converted into hydrogen sulfide H<sub>2</sub>S. The HDS reaction takes place in a fixed-bed reactor at a temperature range of 573 – 673 K and a pressure range of 3.5-7.0 MPa, in the presence of an alumina-based catalyst that is impregnated with cobalt and molybdenum, and usually called ‘a CoMo catalyst’.<sup>7</sup> The elevated operating conditions (pressure and temperature) result in costly and energy-intensive process. Moreover, the presence of thiophenes (i.e.: thiophene, methyl thiophene, benzothiophene, dibenzothiophene, etc.) in the oil streams poses operating challenges, as thiophenes exhibit steric hindrance with respect to the active sites of the catalyst, increasing their resistance towards desulfurization.<sup>8</sup> Thus, exploring an energy-efficient, effective and economical alternative for desulfurization is an important assignment for researchers. A number of methods have been proposed such as extractive desulfurization<sup>9,10</sup>, oxidation<sup>11</sup>, adsorption<sup>12</sup>, and bio-desulfurization<sup>13</sup>. Among the mentioned alternatives, the extractive desulfurization has arisen to be the most promising because: (i) it can usually be operated at mild conditions (i.e. room temperature and atmospheric pressure), (ii) the chemical structure of the sulfur compound in the oil fuel does not change, and therefore, the sulfur compound can be used as a starting material in many agrochemicals and pharmaceuticals industries. In the extractive desulfurization process, the choice of the solvent is the most crucial factor that determines the efficiency of the process. Several volatile organic compounds (VOCs) were successfully applied for desulfurization.<sup>9</sup> However, the loss of solvent via evaporation and the difficulty of regeneration were major drawbacks. In the last decades, many research groups studied the application of ionic liquids (ILs) for the desulfurization of fuels.<sup>14-16</sup> ILs were proposed to efficiently replace the VOCs due to their negligible vapor pressure that significantly reduces the solvent losses; further, the solvent regeneration can be simply performed using flash distillation. Remarkable desulfurization efficiency (> 95% in multiple extraction cycles) can be attained using ILs<sup>17</sup>; nevertheless, their high synthesis cost and toxicity hindered their utilization on an industrial scale.

One promising alternative to this technology is the extraction of the organosulfur using deep eutectic solvents (DESs). As highlighted in *Chapter 2*, the non-volatility character has inspired scientists to investigate the feasibility of utilizing DESs in many separation applications related to the fuel

production industry<sup>18</sup>, such as the aromatics extraction from fuels<sup>19-21</sup> and the removal of excess glycerol from biofuels.<sup>22,23</sup> DESs were also successfully applied for desulfurization.<sup>24-28</sup> The results have been encouraging enough to merit further investigation. Interestingly, extraction efficiencies (up to 98% after 3-5 extraction cycles) at mild operating conditions of 298 K and atmospheric pressures were reported in the literature<sup>24,25</sup>. Although the efficiency of DESs for desulfurization and the effect of temperature and DES:oil ratio have been reported in some works,<sup>24,25</sup> the type/length of hydrocarbon, the influences and/or characteristics of the HBDs and HBAs on the extractive desulfurization have rarely been studied so far. Moreover, there is a lack of fundamental studies on the liquid-liquid equilibrium (LLE) of the {*n*-alkane + thiophene/thiophene derivative + DES} systems. To present, only one LLE study for the system {*n*-heptane + thiophene + DES} has been reported by Hadj-Kali *et al.*<sup>28</sup>. Knowledge of LLE is vital for the design and optimization of efficient deep desulfurization processes.

In this chapter, DESs were evaluated as extracting agents for the separation of thiophene from {*n*-alkane + thiophene} mixtures via liquid-liquid extraction. The mixtures {thiophene + *n*-hexane} and {thiophene + *n*-octane} were selected as oil models. It has been reported in the literature that, the DESs constituted of salts and polyols are good candidates for the extraction of aromatics from {*n*-alkanes + aromatic} mixtures.<sup>21,29</sup> As described in the cited works,<sup>21,29</sup> the  $\pi$ -electrons in the aromatic ring induce the interaction with the DES leading to an efficient extraction of the aromatic compound.  $\pi$ -electrons are also available in thiophene and in addition, the existence of sulfur increases its electronegativity; thus, the workability of these DESs was expected. Therefore, six DESs were prepared, the HBAs were tetraethylammonium chloride (TEACl), tetrahexylammonium bromide (THABr) and methyltriphenylphosphonium bromide (MTPPBr), and the HBDs were ethylene glycol (EG) and glycerol (Gly). And so, to confirm the suitability of these DESs for the systems {*n*-alkane + thiophene + DES}, the solubility of thiophene/DES and *n*-alkane/DES was tested at 298.2 K and atmospheric pressure. Then, LLE data of 12 ternary systems {*n*-hexane + thiophene + DESs} and {*n*-octane + thiophene + DESs} were determined at 298.2 K and atmospheric pressure. The objective of this study is to provide insights on: (i) the LLE {*n*-alkane + thiophene + DESs} systems, (ii) the effect of type/length of the *n*-alkane, (iii) the influences and/or characteristics of the HBAs, i.e. different chain length of the alkyl group and the functional group on the ammonium cation, (iv) and HBDs type of the polyol and on the extraction of thiophene from a {*n*-alkane + thiophene} mixture. To evaluate the separation capability of the studied DESs, the solute distribution ratio and the selectivity were calculated from the experimental LLE data and compared to relevant literature data. Moreover, to better understand the extraction mechanism of the thiophene, the sigma profiles of the *n*-hexane, *n*-octane, thiophene and DESs were obtained using Conductor-like Screening Model for Real Solvents (COSMO-RS). Finally, the DESs were successfully regenerated by means of vacuum evaporation.

## 5.2 Experimental and modeling procedures

### 5.2.1 Chemicals

The source and purity (as stated by the suppliers) of all the chemicals used in this work are presented in Table 1. All the chemicals were used without further purification.

**Table 1:** Source and purity (as stated by the suppliers) of the chemicals used in this work.

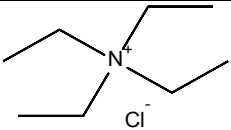
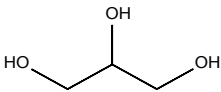
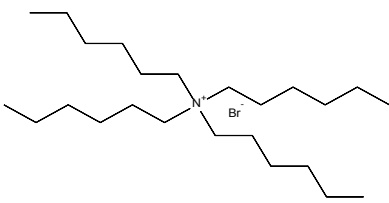
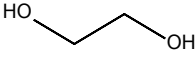
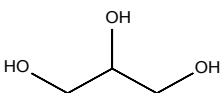
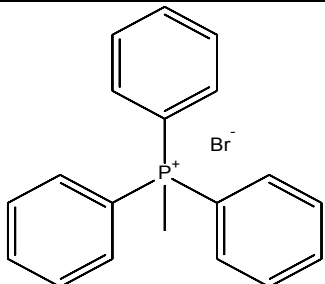
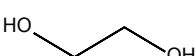
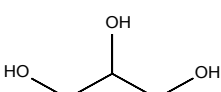
Chemical	Source	Purity (wt %)
Thiophene	Sigma-Aldrich	≥ 99
Hexane	Sigma-Aldrich	≥ 95
Octane	Sigma-Aldrich	≥ 99
Tetrahexylammonium bromide	Sigma-Aldrich	≥ 99
Methyltriphenylphosphonium bromide	Merck KGaA	≥ 99
Tetraethylammonium chloride	Merck KGaA	≥ 99
Glycerol	Merck KGaA	≥ 99
Ethylene glycol	Sigma-Aldrich	≥ 99
Ethanol	TechniSolv	≥ 99.5

### 5.2.2 Preparation of the DESs

The DESs used in this work were prepared according to the heating method.<sup>30</sup> The heating method requires that the precisely weighted amounts of HBD and HBA are heated together at a certain temperature while stirring in a sealed flask until a clear liquid is formed. The weighing of both the HBD and the HBA was done using a balance Mettler AX205 with an uncertainty in the measurement of  $\pm 0.2 \cdot 10^{-4}$  g. The mixture was heated at 333 K in a thermostatic bath (IKA RCT basic) with a temperature controller (IKA ETS-D5) with an uncertainty in the measurement of  $\pm 0.1$  K. The DESs prepared were: (i) tetraethylammonium chloride:ethylene glycol (TEACl:EG) with molar ratio of 1:2, (ii) tetraethylammonium chloride:glycerol (TEACl:Gly) with molar ratio of 1:2, (iii) tetrahexylammonium bromide:ethylene glycol (THABr:EG) with molar ratio of 1:2 and (iv) tetrahexylammonium bromide:glycerol (THABr:Gly) with molar ratio of 1:2, (v) methyltriphenylphosphonium bromide:ethylene glycol (MTPPBr:EG) with molar ratio of 1:3 and (vi) methyltriphenylphosphonium bromide:glycerol (MTPPBr:Gly) with molar ratio of 1:3. The molecular structures of the DESs are shown in Table 2. The structure of the DES was verified by 400 Bruker nuclear magnetic resonance (NMR) spectrometer for <sup>1</sup>H-NMR (Appendix, Figures 9 to 14).

**Table 2:** The molecular structures of the DESs under investigation in this work

DES	HBA	Molar ratio	HBD
TEACl:EG		1:2	

TEACl:Gly			
THABr:EG		1:2	
THABr:Gly			
MTPPBr:EG		1:3	
MTPPBr:Gly			

### 5.2.3 Experimental determination of the LLE data

The solubility of thiophene/DES and *n*-alkane/DES and the LLE data for the ternary mixtures {*n*-hexane + thiophene + DES}, and {*n*-octane + thiophene + DES} were experimentally determined using the equilibrium cell method at 298.2 K and atmospheric pressure. On the contrary, the solubility of thiophene in THABr:EG and THABr:Gly was experimentally determined using the cloud point method. The reason for using the cloud point method instead of the equilibrium cell method is the high/full solubility of thiophene in those DESs. This means that the obtained phase would be too small for a proper sampling. It is important to remark that the cloud point method is a qualitative method, highly dependent on the experimentalist observation; therefore, the obtained results should be considered with caution.

For the equilibrium cell method, different amounts of DES, thiophene and/or the *n*-alkane compound were added to 20 mL headspace vials. The quantity of added components was measured with a balance Mettler AX205 with an uncertainty in the measurement of  $\pm 0.2 \cdot 10^{-4}$  g. The vials were stirred for 2 h at 500 rpm in a temperature controlled incubated shaker (IKA KS 4000) i-control with temperature stability of  $\pm 0.1$  K kept at 298.2 K. Then, the mixtures were left to settle overnight in a heating block to reach thermodynamic equilibrium. The heating block was kept at 298.2 K on a hot plate (IKA RCT basic) with a temperature controller (IKA ETS-D5). Thereafter, both phases were sampled using needled syringes.

The composition of both phases was determined via gas chromatography (Varian 430 equipped with flame ionization detector). The column and the GC method used for the analysis is described in Table 3. In all the measurements ethanol was used as dilution agent. Since the DES cannot be quantified via gas chromatography, its concentration was determined via mass balance calculation. The GC method was validated with samples of known composition and the obtained root mean square deviation (RMSD) was equal to 0.05 for all the samples. During the experiments, all samples were measured 5 times and the statistical uncertainty in the measurement was found to be less than 0.005.

**Table 3:** Column type and analysis conditions of the GC method used for the determination of the compositions.

Column	Varian CP-SIL 5CB (25 m · 0.25 mm · 1.25 $\mu$ m)
Injector temperature	548 K
Oven temperature profile	313.2 – 353.2 K at 12.5 K/min
Detector temperature	473.2 K
Carrier gas	Helium
Flow rate	3 mL/min
Split ratio	200
Injection volume	1 $\mu$ L

As previously mentioned, the cloud point method was used for the determination of the thiophene solubility in THABr:EG and THABr:Gly. For this method, a certain amount of DES was placed in a 20 mL headspace vial and thiophene was added drop-wise until turbidity was visually observed. Then, the composition of the samples was gravimetrically determined using a Mettler AX205 balance with an uncertainty in the measurement of  $\pm 0.2 \cdot 10^{-4}$  g. The temperature of the vial as controlled using a thermostatic bath with a temperature controller (IKA ETS-D5) with a precision of  $\pm 0.1$  K.

#### 5.2.4 COSMO-RS

The COSMO-RS model is a quantum chemistry based method with the purpose of predicting chemical potentials ( $\mu$ ) in liquids. In COSMO-RS, the molecules are placed in a conductor as the reference state, then the screening charge density ( $\sigma$ ) on the surface of each molecule is calculated and stored in a *.cosmo file*. The electrostatic misfit energy ( $E_{\text{misfit}}$ ), hydrogen bond interaction ( $E_{\text{hb}}$ ), and van der Waals interaction ( $E_{\text{vdw}}$ ) represent the molecular interactions in COSMO-RS.<sup>31–33</sup> The surface of the molecules in the liquid is divided into segments each with a certain surface charge density. Then, a probability function ( $\sigma$ -profile) can be obtained by applying a local averaging algorithm on the surface charge densities over effective contact segments. The  $\sigma$ -profile can help to understand the properties and the solvation of the compounds and their mixtures in terms of charge interactions.<sup>31–33</sup>

All compounds were generated with the TMoleX tool.<sup>34</sup> The geometry was optimized with Hartree-Fock method for higher accuracy and using the 6-31 G basis set to allow for polarization effects of the species in the complexes.<sup>35</sup> After the optimization, a single point estimation was conducted and the *.cosmo file* was generated for use in the analysis. Each DES was represented by three different species, e.g. HBD, HBA cation and HBA anion, whereby the electro-neutrality between HBA cation

and anion was guaranteed.<sup>36</sup> The TMoleX tool also provided the *COSMOTermX file*,<sup>34</sup> which was used for analysis of the extraction capacity for thiophene and *n*-hexane of each DES.

### 5.3 Results and discussion

#### 5.3.1 Solubility test

The liquid-liquid equilibrium compositions of the systems {*n*-alkane + DES} or {thiophene + DES} were experimentally determined at 298 K and atmospheric pressure as described in section 4.2.3. The obtained values are listed in Table 4. Please note that the solubility of thiophene in the DESs, THABr:EG and THABr:Gly were determined by the cloud point methods.

**Table 4:** Equilibrium compositions (weight fraction) of the DES-rich phase for the mixtures {*n*-alkane or thiophene + DES}\*

DES	{ <i>n</i> -octane+DES}	{ <i>n</i> -hexane+DES}	{thiophene +DES}
	<i>w</i> <sub>octane</sub>	<i>w</i> <sub>hexane</sub>	<i>w</i> <sub>thiophene</sub>
TEACl:EG	0.0006	0.0036	0.3253
TEACl:Gly	0.0003	0.0008	0.1527
THABr:EG	0.073	0.103	Fully soluble
THABr:Gly	0.039	0.049	0.821
MTPPBr:EG	0.0010	0.0034	0.4968
MTPPBr:Gly	0.0002	0.0091	0.1165

\*Standard uncertainty in temperature  $u(T) = 0.1$  K and  $u(w) = 0.0005$

As it can be observed from Table 4, the solubilities of thiophene in all the DESs are greater compared to those of the *n*-alkanes in the DESs. This difference can be presumably related to the electrostatic interactions between the  $\pi$ -electrons present in the thiophene and the cations of the DES. Moreover, the interactions between the sulfur, due to its electron density and the components of the DES, might also play a role<sup>37</sup>. It worth mentioning that the solubility of thiophene in the six DESs is significantly greater than its solubility in pure ethylene glycol and glycerol presented in Table 5. Therefore, the addition of the salt TEACl, THABr and MTPPBr to form a DES has remarkably increased the solubility of thiophene. This proves the aforementioned speculation that the thiophene  $\pi$ -electrons interact with the DES cations. Another factor is that, the anion [Br or Cl<sup>-</sup>] of the salt could also play a role of disrupting the hydrogen-bond network for ethylene glycol and glycerol. This disruption could also allow for improved interactions and additional void space to accommodate thiophene.

**Table 5:** Solubility of thiophene in pure ethylene glycol and glycerol expressed in mass fractions. The measurements were done following the cloud point method at 298.2 K and atmospheric pressure

System	<i>w</i> <sub>thiophene</sub>
{thiophene + ethylene glycol}	0.05
{thiophene + glycerol}	0.04

Thiophene was found to be more soluble in DESs containing ethylene glycol as HBD than the glycerol-based DESs for the same HBA. At the same molar ratios (HBA:HBD) of the DESs (1:2 and 1:3), the glycerol-based DESs are presumably more polar due to the presence of more hydroxyl groups. This causes lower solubility of nonpolar and/or weakly polar compounds (i.e., thiophene and *n*-alkane) in glycerol-based DESs compared to ethylene glycol-based DESs. The role of HBAs salts can also be observed from solubility differences of thiophene in TEACl-based DESs and THABr-based DESs. It was found that, the longer the cation alkyl chain length, the higher the solubility. This can be attributed to the increase in the non-polar domain of the DESs. Moreover, addition of the MTPPBr salt to the ethylene glycols and glycerol also increases the thiophene solubility. The presence of a phenyl ring in the MTPPBr:EG provided a preferred environment for thiophene through  $\pi$ - $\pi$  interactions.

As for the *n*-alkane, the solubility of the *n*-hexane in all the six DESs was found to be slightly higher than that of the *n*-octane, except for MTPPBr:Gly. This might be due to the fact that alkanes with longer alkyl chains have a lower solubility in more polar solvents like the DESs applied in this work. The large differences in the solubilities of the {*n*-alkane + DES} and {thiophene + DES} systems, implies that the selected DESs are potential extractants for the separation of *n*-alkane/thiophene mixtures.

### 5.3.2 Ternary LLE experiments

The LLE data of the 12 ternary systems {*n*-hexane + thiophene + DESs} and {*n*-octane + thiophene + DESs} were experimentally determined at 298 K and atmospheric pressure. The obtained results are depicted in Figure 1 by means of triangular diagrams and the numerical equilibrium compositions of the measured systems are listed in the Appendix, Table 6.

According to the Sørensen *et al.* classification<sup>38</sup>, the two ternary systems {*n*-hexane/*n*-octane + thiophene + THABr:EG} showed a type I ternary behavior, in which two of the pairs of compounds exhibit complete miscibility ({aliphatic + thiophene} and {thiophene + THABr:EG}). While, all the other ternary systems {*n*-hexane/*n*-octane + thiophene + DES} showed a type II ternary behavior. This is: one completely miscible pair {aliphatic + thiophene} and two partially miscible ones {aliphatic + DES} and {thiophene + DES} with only one immiscibility region (see Figure 1). It can be observed from Figure 1 that the *n*-alkane-rich phase was found to be DES-free, and this was verified via <sup>1</sup>H-NMR. The obtained spectra are presented in the Appendix (Figures 15-16). As it can be seen from the spectra, within the detection limits of the equipment, only *n*-hexane or *n*-octane and thiophene were detected in the top phase samples. This behavior was also observed in systems of {*n*-alkanes + thiophene + ILs}<sup>39-43</sup>. The absence of the DES can prevent solvent losses during extraction and this is an added value from an economical point of view. It means that no solvent recovery column is needed for the *n*-alkane-rich stream. This will contribute to reducing the operational costs of the process. Furthermore, it can be observed that the miscibility region slightly decreases with the increase of the *n*-alkane carbon number.

The performance of the studied DESs on the extraction of thiophene can be evaluated using the distribution coefficient and the selectivity.

The solute “thiophene” distribution coefficient ( $\beta$ ) measures the concentration of the solute in the extract phase (DES-rich phase) with respect to its concentration in the raffinate phase ( $n$ -alkane rich phase). It can be calculated from the experimental data as follows<sup>44</sup>:

$$\beta_2 = \frac{w_{2,E}}{w_{2,R}} \quad (1)$$

where  $w_{2,E}$  is the weight fraction of thiophene in the DES-rich phase and  $w_{2,R}$  is the weight fraction of thiophene in the  $n$ -alkane-rich phase. The values of the distribution coefficient are presented in the Appendix of *chapter 5*, Table 6 and graphically shown in Figure 2. The higher the  $\beta$ , the better the quality of the raffinate and consequently more thiophene is extracted. This implies that less solvent is needed to achieve the desired efficiency.

For all the measured systems, the thiophene distribution coefficients were found to be less than unity, shown in Figure 2. Also, the obtained distribution coefficients slightly decreased with an increase in the thiophene concentration. This means that the thiophene concentration in the system does not significantly affect the extraction efficiency of all the considered DESs. It can also be observed that for both alkanes,  $n$ -hexane and  $n$ -octane, the distribution coefficients are approximately similar. Moreover, the THABr-based DESs exhibited the highest distribution coefficients. Comparing the results obtained for the TEACl-based DESs and THABr-based DESs, it can be deduced that the longer the alkyl chain length on the HBA, the higher the thiophene distribution coefficient. This behavior of  $\beta_2$  has also been observed for THABr-based vs. TEACl-based DESs in the separation of aromatic compounds from alkanes using the same DES. Furthermore, in all cases ethylene glycol-based DESs are better extracting agents (higher  $\beta_2$ ) than glycerol based DESs.

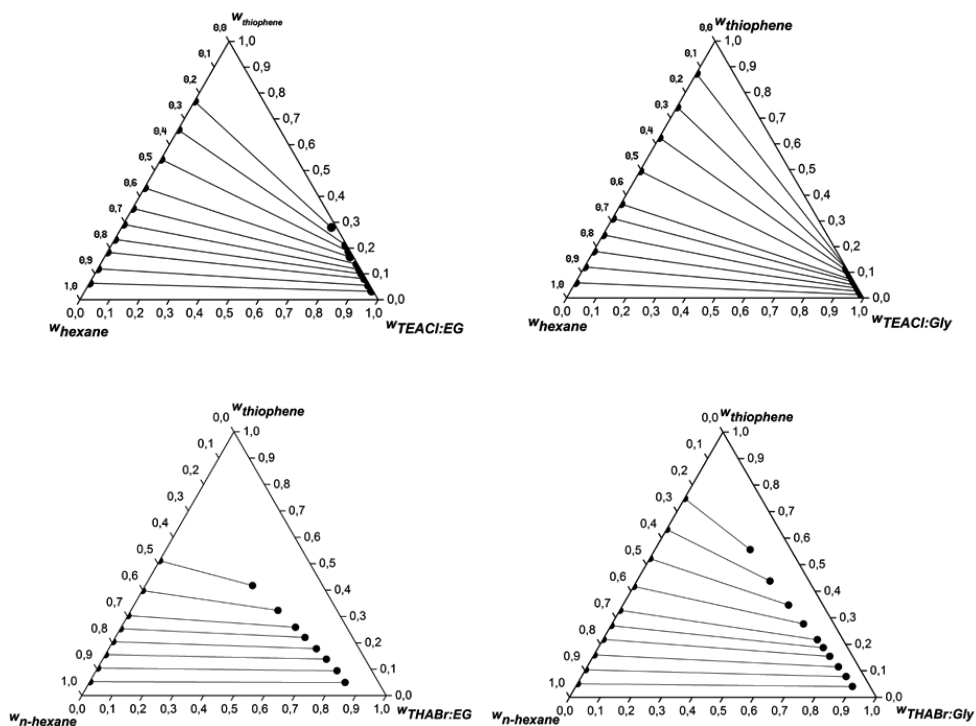
The selectivity of the thiophene over the aliphatic compound can be measured by the separation factor, which is more often simply called selectivity ( $S$ ), and is defined as<sup>44</sup>:

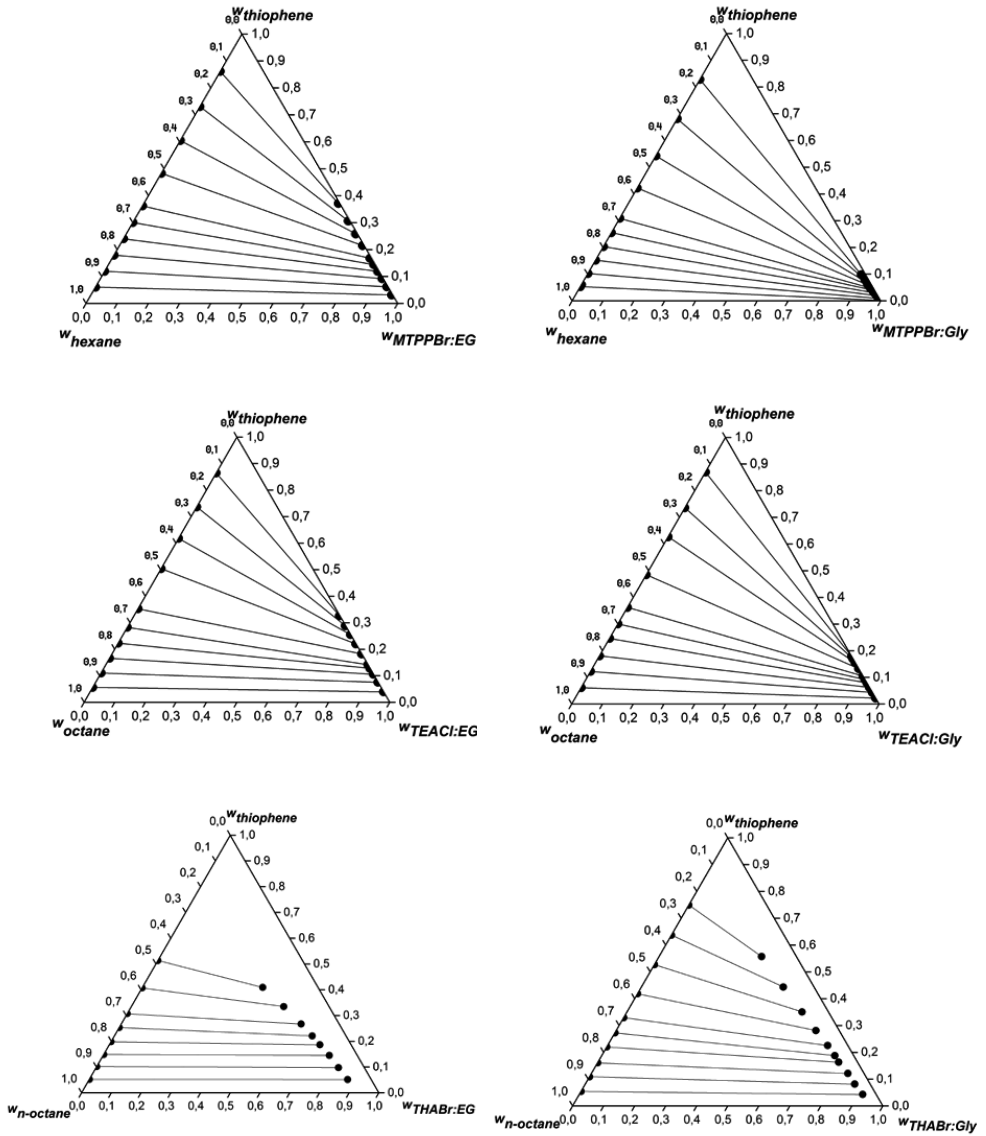
$$S = \frac{\beta_2}{\beta_1} \quad (2)$$

where  $\beta_1$  and  $\beta_2$  refer to the distribution coefficients of the aliphatic compound and thiophene, respectively. The calculated selectivity values are presented in the Appendix of *chapter 5*, Table 6, and depicted in Figure 3. As shown in Figure 3, the selectivity decreases with an increase in the thiophene concentration. In all the studied systems the selectivity was found to be greater than unity. This implies that the extraction of thiophene using DESs is feasible. Opposite to the distribution coefficients, the longer the alkyl chain length on the HBA, the lower the selectivity. And the glycerol based-DESs showed higher selectivities. Also, higher selectivities are obtained for the  $\{n$ -octane + thiophene + DES $\}$  in comparison to the  $\{n$ -hexane + thiophene + DES $\}$ .



All the observations outlined above can also be explained on basis of the solubilities of thiophene, *n*-hexane and *n*-octane presented in the previous section. On the basis of the obtained LLE results, it can be concluded that all the considered DESs are potential candidates for the desulfurization of fuels. The high selectivity values imply that smaller equipment is needed, which results in a lower initial investment of capital cost. The smaller initial capital investment and the ease of solvent recovery, coupled with the cheap price of the DESs are all added values that could compensate the slightly higher amount of solvent needed due to the lower distribution coefficient.





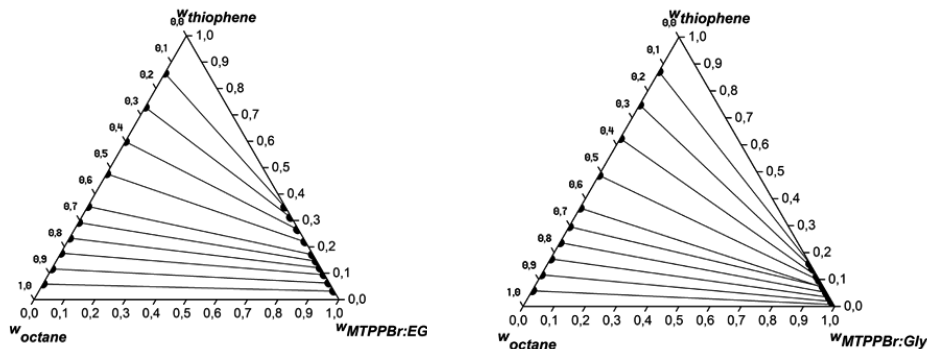


**Figure 1:** Experimental tie lines (●, solid line) in weight fractions for the ternary systems {*n*-alkane + thiophene + DES} at 298.2 K and atmospheric pressure.

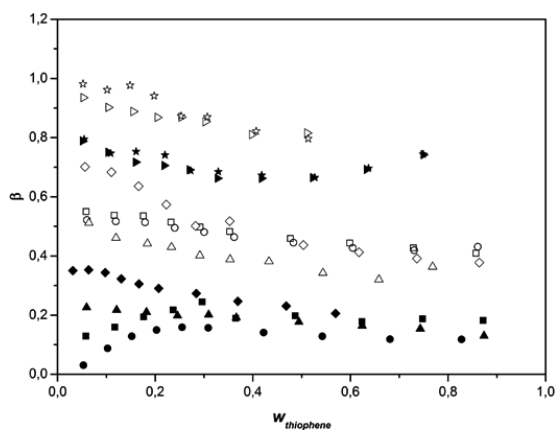


**Figure 2:** Solute distribution coefficient as a function of the weight fraction of thiophene in the *n*-alkane-rich phase. (○) {*n*-hexane + thiophene + MTPPBr:EG}, (●) {*n*-hexane + thiophene + MTPPBr:Gly}, (□) {*n*-octane + thiophene + MTPPBr:EG}, (■) {*n*-octane + thiophene + MTPPBr:Gly}, (Δ) {*n*-hexane + thiophene TEACl:EG}, (▲) {*n*-hexane + thiophene TEACl:Gly}, (◇) {*n*-octane + thiophene TEACl:EG}, (◆) {*n*-octane + thiophene TEACl:Gly}, (▷) {*n*-hexane + thiophene THABr:EG}, (▸) {*n*-hexane + thiophene THABr:Gly}, (☆) {*n*-octane + thiophene THABr:EG}, and (★) {*n*-octane + thiophene THABr:Gly} determined at 298.2 K and atmospheric pressure

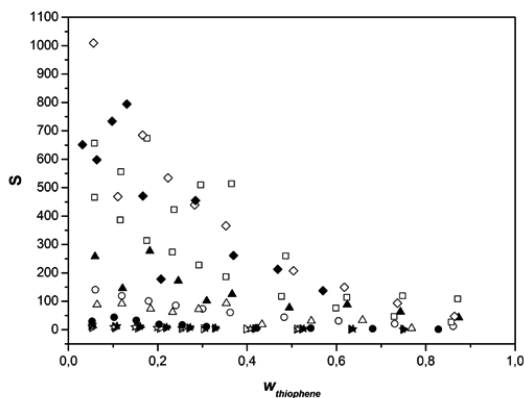


**Figure 3:** Selectivity as a function of the weight fraction of thiophene in the *n*-alkane-rich phase. (○) {*n*-hexane + thiophene +MTPPB:EG}, (●) {*n*-hexane + thiophene + MTPPB:Gly}, (□) {*n*-octane + thiophene +MTPPB:EG}, (■) {*n*-octane + thiophene +MTPPB:Gly}, (Δ) {*n*-hexane + thiophene TEACl:EG}, (▲) {*n*-hexane + thiophene TEACl:Gly}, (◇) {*n*-octane + thiophene TEACl:EG}, (◆) {*n*-octane + thiophene TEACl:Gly}, (▷) {*n*-hexane + thiophene THABr:EG}, (►) {*n*-hexane + thiophene THABr:Gly}, (★) {*n*-octane + thiophene THABr:EG}, and (♠) {*n*-octane + thiophene THABr:EG} determined at 298.2 K and atmospheric pressure.

### 5.3.3 Literature comparisons

The performance of the DESs has been compared to the performance of systems using ILs as extracting agents. The comparison factors were the distribution coefficient and the selectivity, calculated at 298.2 K and atmospheric pressure. It should be mentioned that the comparisons were done on a mass basis due to the differences in the molar masses of the solvents. The mass basis comparisons are more realistic and practical for large scale/industrial solvent selection. The distribution coefficients for the systems {*n*-hexane + thiophene + DES/IL} and {*n*-octane + thiophene + DES/IL} can be found in Figure 4 and Figure 5, respectively. The selectivities for the systems {*n*-hexane + thiophene + DES/IL} and {*n*-octane + thiophene + DES/IL} can be found in Figure 6 and Figure 7, respectively. From Figure 4 it can be observed that the distribution coefficients of the DESs in the systems {*n*-hexane + thiophene + DES/IL} were lower than those of the ILs except for the THABr:EG and THABr:Gly DESs. The distribution coefficients of THABr-based DESs were found to be similar to those of the ILs and in some cases the DES shows higher distribution coefficients, except for [C<sub>8</sub>mim][NO<sub>3</sub>] and [C<sub>4</sub>mim][NO<sub>3</sub>]<sup>45</sup>. As shown in Figure 6, the selectivities of the DESs were found to be only slightly higher or similar to those of the previously studied ILs. Remarkably, the selectivity of the TEACl:Gly, studied in this work, was found to be the highest among all the ILs and DESs.

For the systems {*n*-octane + thiophene + DES/IL}, the distribution coefficients of the DESs were somewhat lower than those of all the studied ILs (see Figure 5). While the selectivities of the DESs

were higher than those of the ILs in the case of TEACl:EG, TEACl:Gly, MTPPB:EG and MTPPB:Gly and comparable in the case of THABr:EG and THABr:Gly (see Figure 7).

As outlined in the previous section (sec. 4.3.2), the longer the alkyl-chain length on the HBA “the cation of the DES”, the higher the thiophene distribution coefficient. Similar behavior can also be observed when comparing the thiophene distribution coefficients of  $[C_8mim][NO_3]$  and  $[C_4mim][NO_3]$  (see Figure 4 and 5).

The distribution coefficient is an important factor for the design of an economical process. The higher the distribution factor, the smaller the amount of the solvent needed. This is beneficial because it reduces the operational cost for solvent recovery. The selectivity affects the extractor size. High selectivity values (as obtained here for TEACl:Gly) imply that smaller equipment is needed, which results in a lower initial investment of capital cost. DESs are easier to be prepared compared to ILs (no synthesis required, just mixing is enough). As mentioned previously, DESs can be prepared from cheap starting materials (e.g., ammonium and phosphonium salts, ethylene glycol, and glycerol). Further studies should contemplate if the lower price of the solvent compensates the slightly higher amount of solvent needed.

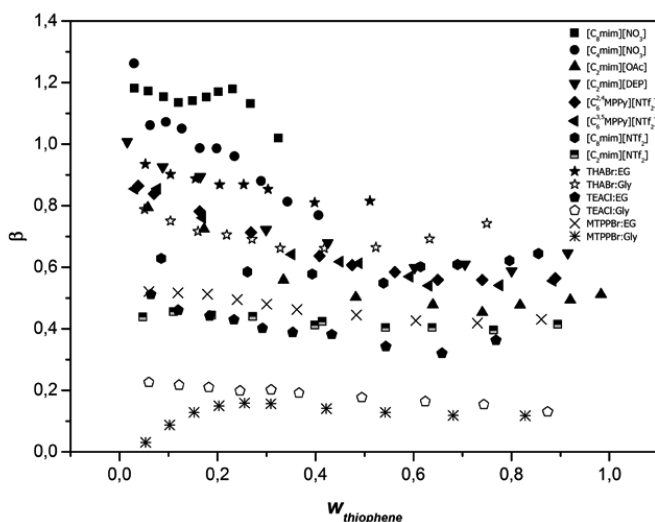


**Figure 4:** Solute distribution coefficient as a function of the weight fraction of thiophene in the *n*-alkane-rich phase for the system  $\{n\text{-hexane} + \text{thiophene} + \text{IL or DES}\}$  calculated at 298 K and atmospheric pressure<sup>39-42,45,46</sup>

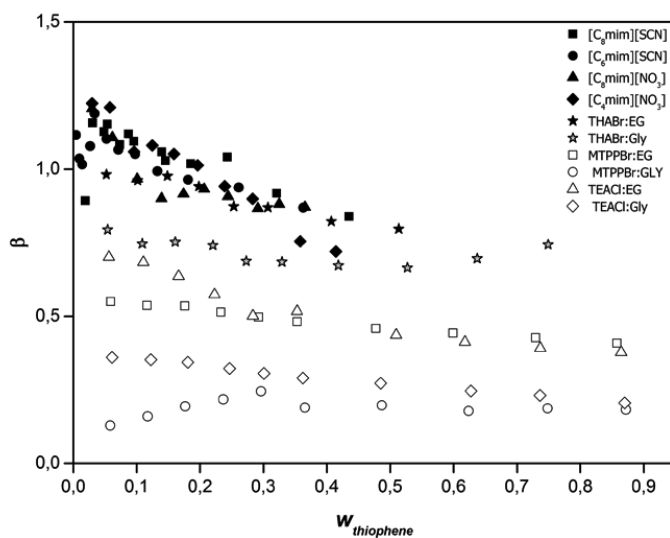


**Figure 5:** Solute distribution coefficient as a function of the weight fraction of thiophene in the *n*-alkane-rich phase for the system {*n*-octane+ thiophene + IL or DES} calculated at 298.2 K and atmospheric pressure<sup>43,45</sup>

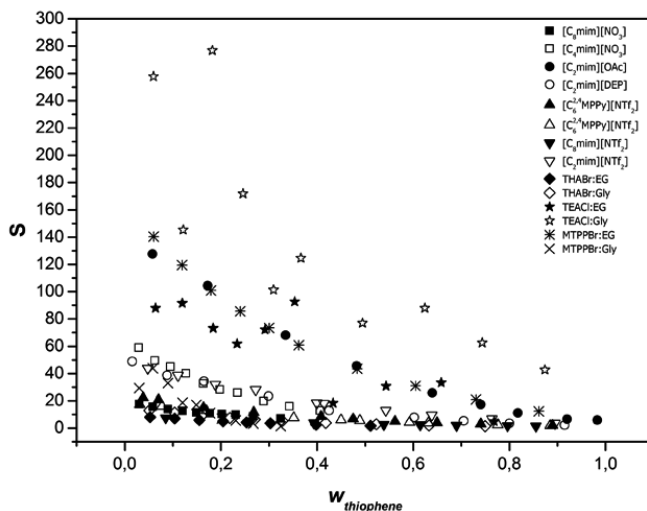


**Figure 6:** Selectivity as a function of the weight fraction of thiophene in the *n*-alkane-rich phase for the system {*n*-hexane+ thiophene + IL or DES} calculated at 298 K and atmospheric pressure<sup>39-42,45,46</sup>

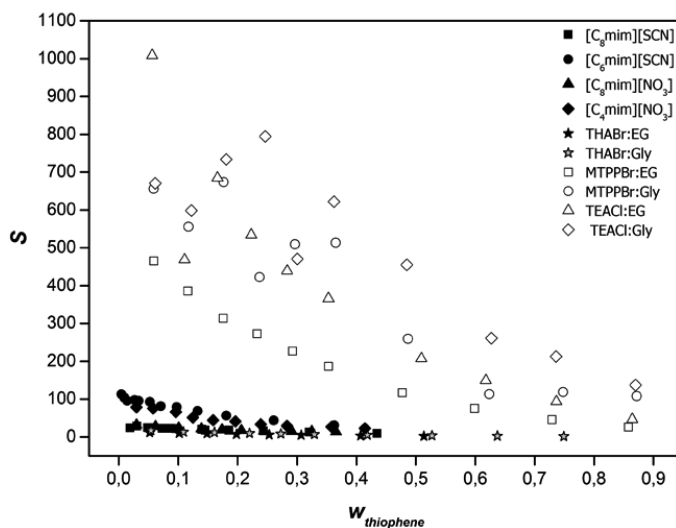


**Figure 7:** Selectivity as a function of the weight fraction of thiophene in the *n*-alkane-rich phase for the system {*n*-octane+ thiophene + IL or DES} calculated at 298 K and atmospheric pressure<sup>43,45</sup>

#### 5.3.4 Extraction mechanism

The analysis of the sigma profiles obtained with COSMO-RS can provide an in-depth understanding of the interactions between the DESs and thiophene. The threshold value for the hydrogen bonding interactions applied was:  $\sigma_{\text{hb}} = \pm 0.0084 \text{ eA}^{-2}$ . From Figure 4, it can be clearly seen that the four DESs have peaks on both sides beyond the threshold value, which confirms the formation of hydrogen bonding within the DES. It can also be deduced that thiophene is a non-basic compound due to its location that is barely exceeding the lower limit of  $\sigma_{\text{hb}} = -0.0084 \text{ eA}^{-2}$ .<sup>36</sup> This means that the thiophene is a weak HBD. Instead, it is showing a very small peak above the upper limit (at  $\sigma > +\sigma_{\text{hb}}$ ) indicating the ability to be a HBA. However, based on the  $\sigma$ -profiles, the pronounced interaction between thiophene and DESs is the electrostatic interaction, with negligible and/or absent hydrogen bonding interaction. Thus, thiophene is extracted by the DESs mainly on basis of electrostatic interactions, which confirms our observations for thiophene solubilities in the DESs presented in Table 4.

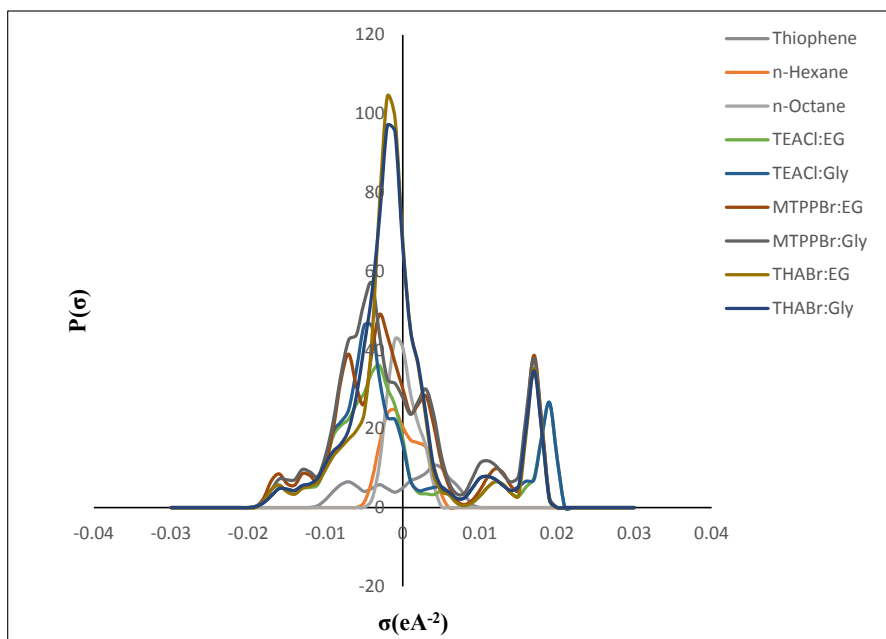


**Figure 8:** Sigma profile of thiophene, *n*-hexane, *n*-octane and the six DESs studied

### 5.3.5 DES regeneration

In terms of designing an economical desulfurization process, the regeneration of the DES is an important step. The regeneration of THABr:EG was performed under vacuum using a rotary evaporator at 303 K and a pressure of < 100 mbar. A sample of a DES-rich phase for the system {*n*-hexane (1) + thiophene (2) + THABr:EG (3)} with the composition ( $w_1 = 0.110$ ;  $w_2 = 0.049$  and  $w_3 = 0.840$ ) was placed in the rotary evaporator for 12 h. Thereafter, the regenerated DES was analyzed via  $^1\text{H-NMR}$ . From the obtained NMR spectra (shown in Appendix, Figure 17), the fresh DES and the regenerated DES structures are identical, and no traces of *n*-hexane and thiophene were detected.

## 5.4 Conclusions

In this work, two deep eutectic solvents (DESs) were evaluated for their extraction properties of thiophene from two aliphatic hydrocarbons via liquid–liquid extraction. The aliphatic hydrocarbons were *n*-hexane and *n*-octane. The selected DESs were: (i) tetraethylammonium chloride:ethylene glycol (TEACl:EG) with molar ratio of 1:2, (ii) tetraethylammonium chloride:glycerol (TEACl:Gly) with molar ratio of 1:2, (iii) tetrahexylammonium bromide:ethylene glycol (THABr:EG) with molar ratio of 1:2 and (iv) tetrahexylammonium bromide:glycerol (THABr:Gly) with molar ratio of 1:2, (v) methyltriphenylphosphonium bromide:ethylene glycol (MTPPBr:EG) with molar ratio of 1:3 and (vi) methyltriphenylphosphonium bromide:glycerol (MTPPBr:Gly) with molar ratio of 1:3. The first step was to determine the solubility of the thiophene, *n*-hexane and *n*-octane in the DESs at 298 K and



atmospheric pressure. Then, the liquid–liquid equilibrium (LLE) data of the ternary systems {*n*-hexane + thiophene + DESs} and {*n*-octane + thiophene + DESs} were determined at 298 K and atmospheric pressure. Also, the solute distribution ratios and the selectivities were calculated from the experimental LLE data. The solute distribution coefficients obtained for the ethylene glycol-based DESs are always higher than those of glycerol based-DESs. Also, the longer the alkyl chain length on the HBA, the higher the thiophene distribution coefficient. Moreover, it was found that, for the same DES, roughly similar distribution coefficients and lower selectivities were obtained for the {*n*-hexane + thiophene + DES} system than for the {*n*-octane + thiophene + DES} system.

Conductor-like Screening Model for Real Solvents (COSMO-RS) was used to better understand the extraction mechanism of thiophene. Based on the  $\sigma$ -profiles, it was observed that the pronounced interaction between thiophene and DESs is the electrostatic interaction, with negligible and/or absent hydrogen bonding interaction. Regeneration of the DESs has been successfully achieved by means of vacuum evaporation. On the basis of the obtained distribution coefficients and selectivities, DESs were found to be competitors for the desulfurization of fuels to ILs with almost similar performance but lower price.

## 5.5 References

- (1) Babich, I. V.; Moulijn, J. A. Science and Technology of Novel Processes for Deep Desulfurization of Oil Refinery Streams : A Review Q. **2003**, *82*, 607–631.
- (2) Kelemen, S. R.; George, G. N.; Gorbaty, M. L. Direct Determination and Quantification of Sulphur Forms in Heavy Petroleum and Coals, 1. The X-Ray Photoelectron Spectroscopy (XPS) Approach. **1990**, *69* (6), 939–944.
- (3) Portney, P. R. Economics and the Clean Air Act. *J. Econ. Perspect. Fall* **1990**, *4* (4), 173–181.
- (4) Rodriguez, J. A.; Hrbek, J. Interaction of Sulfur with Well-Defined Metal and Oxide Surfaces: Unraveling the Mysteries behind Catalyst Poisoning and Desulfurization. *Acc. Chem. Res.* **1999**, *32* (9), 719–728.
- (5) Brunet, S.; Mey, D.; Perot, G.; Bouchy, C.; Diehl, F. On the Hydrodesulfurization of FCC Gasoline: A Review. *Appl. Catal. A Gen.* **2005**, *278* (2), 143–172.
- (6) Shafi, R.; Hutchings, G. J. Hydrodesulfurization of Hindered Dibenzothiophenes: An Overview. *Catal. Today* **2000**, *59* (3), 423–442.
- (7) Debajyoti, B. Design Parameters for a Hydro Desulfurization (HDS) Unit for Petroleum Naphtha at 3500 Barrels per Day. *World Sci. News* **2015**, *3*, 99–111.
- (8) Song, C. An Overview of New Approaches to Deep Desulfurization for Ultra-Clean Gasoline , Diesel Fuel and Jet Fuel. **2003**, *86*, 211–263.
- (9) Ali, S. H.; Hamad, D. M.; Albusairi, B. H.; Fahim, M. A. Removal of Dibenzothiophenes from Fuels by Oxy-Desulfurization. *Energy and Fuels* **2009**, *23* (12), 5986–5994.
- (10) Kianpour, E.; Azizian, S. Polyethylene Glycol as a Green Solvent for Effective Extractive Desulfurization of Liquid Fuel at Ambient Conditions. *Fuel* **2014**, *137*, 36–40.
- (11) Gatan, R.; Barger, P.; Gembicki, V.; Cavanna, A.; Molinari, D. Oxidative Desulfurization: A New Technology for ULSD. *ACS Div. Fuel Chem. Prepr.* **2004**, *49* (2), 577–579.
- (12) Muzic, M.; Sertic-Bionda, K.; Gomzi, Z.; Podolski, S.; Telen, S. Study of Diesel Fuel Desulfurization by Adsorption. *Chem. Eng. Res. Des.* **2010**, *88* (4), 487–495.
- (13) Song, C.; Ma, X. New Design Approaches to Ultra-Clean Diesel Fuels by Deep Desulfurization and Deep Dearomatization. *Appl. Catal. B Environ.* **2003**, *41* (1–2), 207–238.
- (14) Kulkarni, P. S.; Afonso, C. A. M. Deep Desulfurization of Diesel Fuel Using Ionic Liquids: Current Status and Future Challenges. *Green Chem.* **2010**, *12* (7), 1139.
- (15) Abro, R.; Abdeltawab, A. A.; Al-Deyab, S. S.; Yu, G.; Qazi, A. B.; Gao, S.; Chen, X. A Review

- of Extractive Desulfurization of Fuel Oils Using Ionic Liquids. *RSC Adv.* **2014**, *4* (67), 35302.
- (16) Ibrahim, M. H.; Hayyan, M.; Hashim, M. A.; Hayyan, A. The Role of Ionic Liquids in Desulfurization of Fuels: A Review. *Renew. Sustain. Energy Rev.* **2015**, *76* (November 2016), 1534–1549.
- (17) Chen, X.; Liu, G.; Yuan, S.; Asumana, C.; Wang, W.; Yu, G. Extractive Desulfurization of Fuel Oils with Thiazolium-Based Ionic Liquids. *Sep. Sci. Technol.* **2012**, *47* (6), 819–826.
- (18) Warrag, S. E. E.; Peters, C. J.; Kroon, M. C. Deep Eutectic Solvents for Highly Efficient Separations in Oil and Gas Industries. *Curr. Opin. Green Sustain. Chem.* **2017**, *5*, 55–60.
- (19) Gonzalez, A. S. B.; Francisco, M.; Jimeno, G.; De Dios, S. L. G.; Kroon, M. C. Liquid-Liquid Equilibrium Data for the Systems {LTTM+benzene+hexane} and {LTTM+ethyl Acetate+hexane} at Different Temperatures and Atmospheric Pressure. *Fluid Phase Equilib.* **2013**, *360*, 54–62.
- (20) Kareem, M. A.; Mjalli, F. S.; Hashim, M. A.; AlNashef, I. M. Liquid-Liquid Equilibria for the Ternary System (Phosphonium Based Deep Eutectic Solvent-Benzene-Hexane) at Different Temperatures: A New Solvent Introduced. *Fluid Phase Equilib.* **2012**, *314*, 52–59.
- (21) Rodriguez, N. R.; Requejo, P. F.; Kroon, M. C. Aliphatic–Aromatic Separation Using Deep Eutectic Solvents as Extracting Agents. *Ind. Eng. Chem. Res.* **2015**, *54* (45), 11404–11412.
- (22) Abbott, A. P.; Cullis, P. M.; Gibson, M. J.; Harris, R. C.; Raven, E. Extraction of Glycerol from Biodiesel into a Eutectic Based Ionic Liquid. *Green Chem.* **2007**, *9* (8), 868.
- (23) Shahbaz, K.; Mjalli, F. S.; Hashim, M. A.; AlNashef, I. M. Elimination of All Free Glycerol and Reduction of Total Glycerol from Palm Oil-Based Biodiesel Using Non-Glycerol Based Deep Eutectic Solvents. *Sep. Sci. Technol.* **2013**, *48* (8), 1184–1193.
- (24) Li, C.; Li, D.; Zou, S.; Li, Z.; Yin, J.; Wang, A.; Cui, Y.; Yao, Z.; Zhao, Q. Extraction Desulfurization Process of Fuels with Ammonium-Based Deep Eutectic Solvents. *Green Chem.* **2013**, *15* (10), 2793–2799.
- (25) Li, J. J.; Xiao, H.; Tang, X. D.; Zhou, M. Green Carboxylic Acid-Based Deep Eutectic Solvents as Solvents for Extractive Desulfurization. *Energy and Fuels* **2016**, *30* (7), 5411–5418.
- (26) Gano, Z. S.; Mjalli, F. S.; Al-wahaibi, T.; Al-wahaibi, Y. The Novel Application of Hydrated Metal Halide (  $\text{SnCl}_2 \cdot 2\text{H}_2\text{O}$  ) – Based Deep Eutectic Solvent for the Extractive Desulfurization of Liquid Fuels. **2015**, *6* (5).
- (27) Tang, X. dong; Zhang, Y. fen; Li, J. jing; Zhu, Y. qiang; Qing, D. yong; Deng, Y. xin. Deep Extractive Desulfurization with Arenium Ion Deep Eutectic Solvents. *Ind. Eng. Chem. Res.* **2015**,

- 54 (16), 4625–4632.
- (28) Hadj-Kali, M. K.; Mulyono, S.; Hizaddin, H. F.; Wazeer, I.; El-Blidi, L.; Ali, E.; Hashim, M. A.; AlNashef, I. M. Removal of Thiophene from Mixtures with *N*-Heptane by Selective Extraction Using Deep Eutectic Solvents. *Ind. Eng. Chem. Res.* **2016**, *55* (30), 8415–8423.
- (29) Rodriguez, N. R.; Gerlach, T.; Scheepers, D.; Kroon, M. C.; Smirnova, I. Experimental Determination of the LLE Data of Systems Consisting of {hexane + Benzene + Deep Eutectic Solvent} and Prediction Using the Conductor-like Screening Model for Real Solvents. *J. Chem. Thermodyn.* **2017**, *104*, 128–137.
- (30) Abbott, A. P.; Boothby, D.; Capper, G.; Davies, D. L.; Rasheed, R. K. Deep Eutectic Solvents Formed between Choline Chloride and Carboxylic Acids: Versatile Alternatives to Ionic Liquids. *J. Am. Chem. Soc.* **2004**, *126* (29), 9142–9147.
- (31) Klamt, A. Conductor-like Screening Model for Real Solvents: A New Approach to the Quantitative Calculation of Solvation Phenomena. **1995**, 2224–2235.
- (32) Klamt, A.; Eckert, F. COSMO-RS: A Novel and Efficient Method for the a Priori Prediction of Thermophysical Data of Liquids. *Fluid Phase Equilib.* **2000**, *172* (1), 43–72.
- (33) Klamt, A.; Eckert, F. Erratum to “ COSMO-RS : A Novel and Efficient Method for the a Priori Prediction of Thermophysical Data of Liquids ” [ *Fluid Phase Equilib.* *172* ( *2000* ) *43 – 72* ] &. **2003**, *205*, 3812.
- (34) COSMOtherm. A Graphical User Interface to the COSMOtherm Program, User Guide. COSMOlogic GmbH & Co KG: Leverkusen, Germany 2013.
- (35) Lin, H.; Wu, D.; Liu, L.; Jia, D. Theoretical Study on Molecular Structures , Intramolecular Proton Transfer Reaction , and Solvent Effects of 1-Phenyl-3-. **2008**, *850*, 32–37.
- (36) Hizaddin, H. F.; Ramalingam, A.; Hashim, M. A.; Hadj-kali, M. K. O. Evaluating the Performance of Deep Eutectic Solvents for Use in Extractive Denitri Fi Cation of Liquid Fuels by the Conductor-like Screening Model for Real Solvents. **2014**.
- (37) Su, B.; Zhang, S.; Zhang, Z. C. Structural Elucidation of Thiophene Interaction with Ionic Liquids by Multinuclear NMR Spectroscopy. *J. Phys. Chem. B* **2004**, *108*, 19510–19517.
- (38) Sørensen, J. M.; Magnussen, T.; Rasmussen, P.; Fredenslund, A. Liquid-Liquid Equilibrium Data: Their Retrieval, Correlation and Prediction Part I: Retrieval. *Fluid Phase Equilib.* **1979**, *2* (4), 297–309.
- (39) Francisco, M.; Arce, A.; Soto, A. Ionic Liquids on Desulfurization of Fuel Oils. *Fluid Phase*

- Equilib.* **2010**, *294* (1–2), 39–48.
- (40) Rodríguez-Cabo, B.; Soto, A.; Arce, A. Desulfurization of Fuel-Oils with [C2mim][NTf2]: A Comparative Study. *J. Chem. Thermodyn.* **2013**, *57*, 248–255.
- (41) Rodríguez-Cabo, B.; Arce, A.; Soto, A. Desulfurization of Fuels by Liquid-Liquid Extraction with 1-Ethyl-3-Methylimidazolium Ionic Liquids. *Fluid Phase Equilib.* **2013**, *356*, 126–135.
- (42) Rodríguez-Cabo, B.; Francisco, M.; Soto, A.; Arce, A. Hexyl Dimethylpyridinium Ionic Liquids for Desulfurization of Fuels. Effect of the Position of the Alkyl Side Chains. *Fluid Phase Equilib.* **2012**, *314*, 107–112.
- (43) Ma, M.; Reza, M.; Mokhtarani, B. Novel Liquid E Liquid Equilibrium Data for Six Ternary Systems Containing IL, Hydrocarbon and Thiophene at 25 C. *Fluid Phase Equilib.* **2016**, *412*, 21–28.
- (44) McKetta, J. J. *Encyclopedia of Chemical Processing and Design: Volume 21 - Expanders to Finned Tubes*, 1st ed.; M. Dekker, 1984.
- (45) Mokhtarani, B.; Mansourzareh, H.; Mortaheb, H. R. Phase Behavior of Nitrate Based Ionic Liquids with Thiophene and Alkanes. *Ind. Eng. Chem. Res.* **2014**, *53* (3), 1256–1261.
- (46) Alonso, L.; Arce, A.; Francisco, M.; Soto, A. Phase Behaviour of 1-Methyl-3-Octylimidazolium Bis[trifluoromethylsulfonyl]imide with Thiophene and Aliphatic Hydrocarbons: The Influence of N-Alkane Chain Length. *Fluid Phase Equilib.* **2008**, *263* (2), 176–181.

## 5.6 Appendix Chapter 5

## DES structure

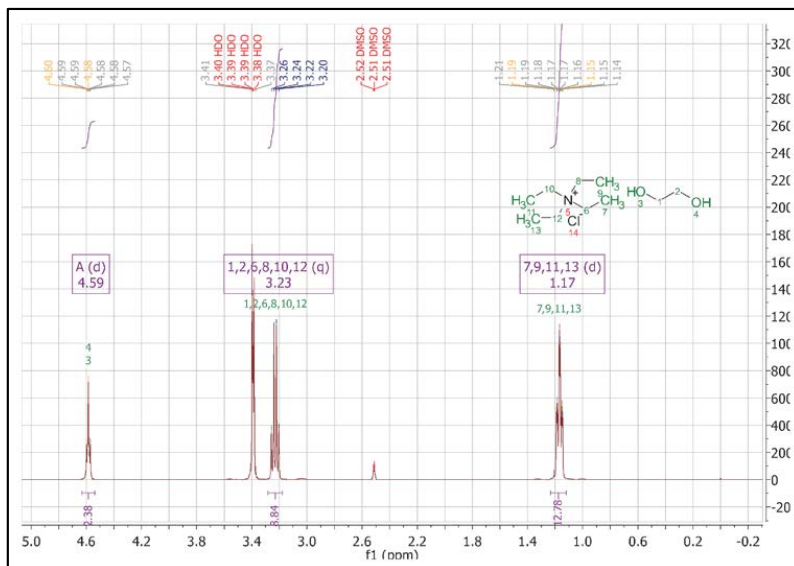


**Figure 9:**  $^1\text{H}$  NMR spectrum of TEACl:EG constituted of tetraethylammonium chloride and ethylene glycol in a 1:2 molar ratio

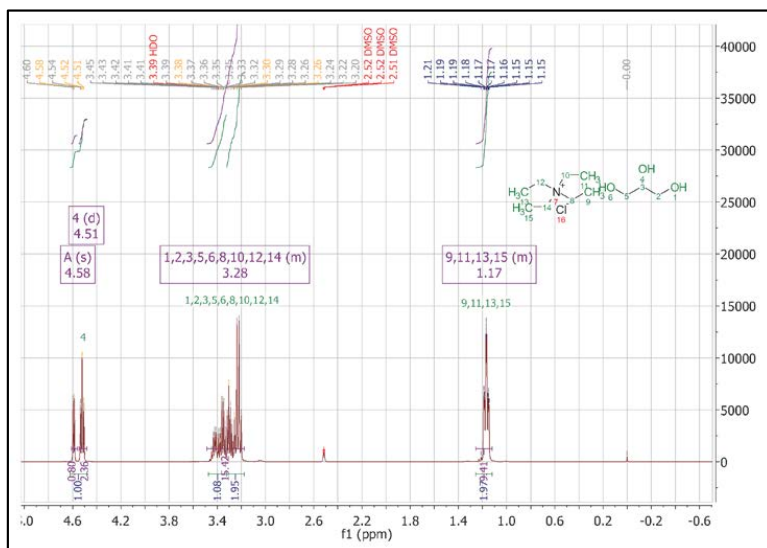


**Figure 10:**  $^1\text{H}$  NMR spectrum of TEACl:Gly constituted of tetraethylammonium chloride and glycerol in a 1:2 molar ratio







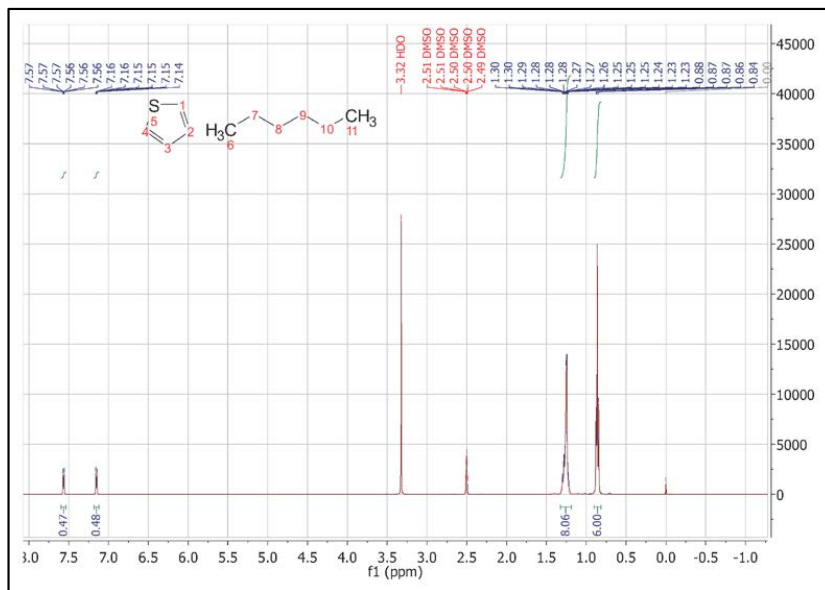
Absence of DES in the *n*-alkane rich phase

Figure 15: A sample from the aliphatic-rich phase of the system {*n*-hexane + thiophene + THABr:EG}

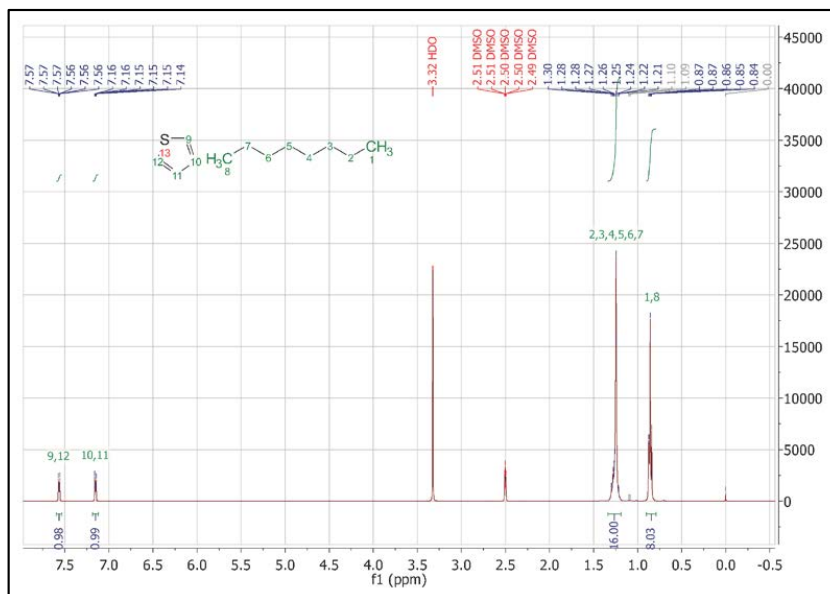


Figure 16: A sample from the aliphatic-rich phase of the system {*n*-octane + thiophene + THABr:EG}

## Experimental LLE data

**Table 6:** Experimental LLE Data in weight fractions for the pseudo-ternary systems  $\{n\text{-alkane} + \text{thiophene} + \text{DES}\}$  at 298 K and atmospheric pressure.  $\beta$  and  $S$  are the calculated distribution and selectivity values, respectively. The DES concentration ( $w_3$ ) in both phases can be calculated from mass balance.

Aliphatic phase				DES phase							
$w_1$	STD	$w_2$	STD	$w_1$	STD	$w_2$	STD	$\beta$	Error	$S$	Error
<b><math>\{n\text{-hexane (1)} + \text{thiophene (2)} + \text{TEACl:EG (3)}\}</math></b>											
0.9359	$\pm 0.0016$	0.0641	$\pm 0.0016$	0.0054	$\pm 0.0019$	0.0328	$\pm 0.0021$	0.512	$\pm 0.035$	87.994	$\pm 31.633$
0.8803	$\pm 0.0021$	0.1197	$\pm 0.0021$	0.0044	$\pm 0.0019$	0.0551	$\pm 0.0034$	0.461	$\pm 0.029$	91.567	$\pm 40.428$
0.8160	$\pm 0.0019$	0.1840	$\pm 0.0019$	0.0049	$\pm 0.0014$	0.0813	$\pm 0.0026$	0.442	$\pm 0.015$	73.321	$\pm 21.628$
0.7665	$\pm 0.0063$	0.2335	$\pm 0.0063$	0.0053	$\pm 0.0028$	0.1003	$\pm 0.0031$	0.430	$\pm 0.018$	61.816	$\pm 33.154$
0.7083	$\pm 0.0063$	0.2917	$\pm 0.0063$	0.0039	$\pm 0.0017$	0.1171	$\pm 0.0019$	0.402	$\pm 0.011$	72.154	$\pm 31.940$
0.6464	$\pm 0.0040$	0.3536	$\pm 0.0040$	0.0027	$\pm 0.0006$	0.1373	$\pm 0.0035$	0.388	$\pm 0.011$	92.676	$\pm 21.776$
0.5667	$\pm 0.0029$	0.4333	$\pm 0.0029$	0.0118	$\pm 0.0025$	0.1652	$\pm 0.0044$	0.381	$\pm 0.010$	18.326	$\pm 3.858$
0.4563	$\pm 0.0046$	0.5437	$\pm 0.0046$	0.0052	$\pm 0.0009$	0.1927	$\pm 0.0066$	0.343	$\pm 0.012$	30.833	$\pm 5.647$
0.3417	$\pm 0.0037$	0.6583	$\pm 0.0037$	0.0033	$\pm 0.0009$	0.2109	$\pm 0.0057$	0.320	$\pm 0.009$	33.296	$\pm 9.299$
0.2316	$\pm 0.0049$	0.7684	$\pm 0.0049$	0.0175	$\pm 0.0007$	0.2791	$\pm 0.0104$	0.363	$\pm 0.014$	4.813	$\pm 0.275$
<b><math>\{n\text{-hexane (1)} + \text{thiophene (2)} + \text{TEACl:Gly (3)}\}</math></b>											
0.9403	$\pm 0.0018$	0.0597	$\pm 0.0018$	0.0008	$\pm 0.0001$	0.0135	$\pm 0.0004$	0.226	$\pm 0.009$	257.734	$\pm 37.059$
0.8786	$\pm 0.0047$	0.1214	$\pm 0.0047$	0.0013	$\pm 0.0009$	0.0263	$\pm 0.0010$	0.217	$\pm 0.012$	145.239	$\pm 100.429$
0.8178	$\pm 0.0027$	0.1822	$\pm 0.0027$	0.0006	$\pm 0.0001$	0.0382	$\pm 0.0016$	0.210	$\pm 0.009$	276.892	$\pm 45.503$
0.7540	$\pm 0.0052$	0.2460	$\pm 0.0052$	0.0009	$\pm 0.0004$	0.0488	$\pm 0.0019$	0.198	$\pm 0.009$	171.839	$\pm 86.262$
0.6904	$\pm 0.0027$	0.3096	$\pm 0.0027$	0.0014	$\pm 0.0009$	0.0624	$\pm 0.0052$	0.202	$\pm 0.017$	101.361	$\pm 64.406$
0.6337	$\pm 0.0043$	0.3663	$\pm 0.0043$	0.0010	$\pm 0.0003$	0.0701	$\pm 0.0030$	0.191	$\pm 0.009$	124.598	$\pm 37.945$
0.5054	$\pm 0.0072$	0.4946	$\pm 0.0072$	0.0012	$\pm 0.0004$	0.0874	$\pm 0.0030$	0.177	$\pm 0.007$	77.065	$\pm 24.281$
0.3759	$\pm 0.0049$	0.6241	$\pm 0.0049$	0.0007	$\pm 0.0002$	0.1022	$\pm 0.0015$	0.164	$\pm 0.003$	88.027	$\pm 20.021$
0.2565	$\pm 0.0078$	0.7435	$\pm 0.0078$	0.0006	$\pm 0.0001$	0.1143	$\pm 0.0013$	0.154	$\pm 0.002$	62.634	$\pm 9.500$
0.1261	$\pm 0.0052$	0.8739	$\pm 0.0052$	0.0004	$\pm 0.0001$	0.1137	$\pm 0.0016$	0.130	$\pm 0.002$	42.681	$\pm 6.870$
<b><math>\{n\text{-hexane (1)} + \text{thiophene (2)} + \text{THABr:EG (3)}\}</math></b>											
0.947	$\pm 0.001$	0.053	$\pm 0.001$	0.110	$\pm 0.002$	0.049	$\pm 0.001$	0.935	$\pm 0.016$	8.05	$\pm 0.19$
0.896	$\pm 0.002$	0.104	$\pm 0.002$	0.114	$\pm 0.001$	0.094	$\pm 0.001$	0.902	$\pm 0.017$	7.06	$\pm 0.15$
0.845	$\pm 0.003$	0.155	$\pm 0.003$	0.127	$\pm 0.003$	0.138	$\pm 0.002$	0.888	$\pm 0.018$	5.90	$\pm 0.19$
0.795	$\pm 0.004$	0.205	$\pm 0.004$	0.140	$\pm 0.005$	0.178	$\pm 0.002$	0.868	$\pm 0.021$	4.92	$\pm 0.22$
0.746	$\pm 0.004$	0.254	$\pm 0.004$	0.156	$\pm 0.005$	0.220	$\pm 0.003$	0.869	$\pm 0.019$	4.15	$\pm 0.15$
0.697	$\pm 0.003$	0.303	$\pm 0.003$	0.168	$\pm 0.004$	0.259	$\pm 0.004$	0.854	$\pm 0.016$	3.54	$\pm 0.11$
0.602	$\pm 0.007$	0.398	$\pm 0.007$	0.194	$\pm 0.006$	0.323	$\pm 0.004$	0.810	$\pm 0.018$	2.52	$\pm 0.10$
0.489	$\pm 0.003$	0.511	$\pm 0.003$	0.231	$\pm 0.003$	0.417	$\pm 0.003$	0.816	$\pm 0.007$	1.73	$\pm 0.03$
<b><math>\{n\text{-hexane (1)} + \text{thiophene (2)} + \text{THABr:Gly (3)}\}</math></b>											
0.949	$\pm 0.001$	0.051	$\pm 0.001$	0.058	$\pm 0.001$	0.040	$\pm 0.001$	0.789	$\pm 0.018$	12.99	$\pm 0.34$
0.896	$\pm 0.002$	0.104	$\pm 0.002$	0.060	$\pm 0.001$	0.078	$\pm 0.001$	0.750	$\pm 0.016$	11.29	$\pm 0.28$
0.840	$\pm 0.002$	0.160	$\pm 0.002$	0.066	$\pm 0.001$	0.115	$\pm 0.001$	0.717	$\pm 0.009$	9.09	$\pm 0.13$
0.781	$\pm 0.001$	0.219	$\pm 0.001$	0.075	$\pm 0.003$	0.154	$\pm 0.003$	0.705	$\pm 0.016$	7.38	$\pm 0.34$
0.730	$\pm 0.004$	0.270	$\pm 0.004$	0.079	$\pm 0.001$	0.187	$\pm 0.001$	0.691	$\pm 0.011$	6.37	$\pm 0.15$

0.672	±0.006	0.328	±0.006	0.084	±0.001	0.217	±0.001	0.662	±0.013	5.31	±0.13
0.582	±0.004	0.418	±0.004	0.099	±0.002	0.277	±0.001	0.662	±0.007	3.89	±0.09
0.477	±0.004	0.523	±0.004	0.112	±0.001	0.348	±0.001	0.665	±0.005	2.82	±0.04
0.367	±0.003	0.633	±0.003	0.128	±0.002	0.438	±0.003	0.692	±0.006	1.99	±0.04
0.250	±0.004	0.750	±0.004	0.133	±0.001	0.556	±0.002	0.742	±0.005	1.40	±0.02
<b>{<i>n</i>-hexane (1) + thiophene (2) + MTPPBr:EG (3)}</b>											
0.9397	±0.0002	0.0603	±0.0002	0.0035	±0.0002	0.0314	±0.0008	0.521	±0.014	140.381	±7.927
0.8805	±0.0006	0.1195	±0.0006	0.0038	±0.0002	0.0617	±0.0013	0.517	±0.012	119.478	±5.869
0.8206	±0.0008	0.1794	±0.0008	0.0042	±0.0002	0.0921	±0.0031	0.513	±0.018	100.916	±6.165
0.7597	±0.0023	0.2403	±0.0023	0.0044	±0.0002	0.1189	±0.0032	0.495	±0.014	85.662	±4.214
0.6996	±0.0012	0.3004	±0.0012	0.0046	±0.0002	0.1443	±0.0035	0.480	±0.012	73.511	±3.755
0.6380	±0.0013	0.3620	±0.0013	0.0049	±0.0003	0.1676	±0.0059	0.463	±0.016	60.748	±4.620
0.5167	±0.0027	0.4833	±0.0027	0.0053	±0.0002	0.2149	±0.0039	0.445	±0.009	43.423	±2.024
0.3950	±0.0018	0.6050	±0.0018	0.0054	±0.0003	0.2581	±0.0073	0.427	±0.012	31.032	±2.149
0.2694	±0.0025	0.7306	±0.0025	0.0054	±0.0002	0.3060	±0.0097	0.419	±0.013	20.928	±1.043
0.1388	±0.0007	0.8612	±0.0007	0.0048	±0.0002	0.3708	±0.0107	0.431	±0.012	12.365	±0.633
<b>{<i>n</i>-hexane (1) + thiophene (2) + MTPPBr:Gly (3)}</b>											
0.9468	±0.0002	0.0532	±0.0002	0.0010	±0.0001	0.0016	±0.0002	0.031	±0.004	29.303	±4.982
0.8975	±0.0003	0.1025	±0.0003	0.0018	±0.0003	0.0089	±0.0001	0.087	±0.001	43.940	±7.700
0.8478	±0.0002	0.1522	±0.0002	0.0033	±0.0017	0.0195	±0.0008	0.128	±0.005	33.017	±17.194
0.7970	±0.0007	0.2030	±0.0007	0.0064	±0.0015	0.0304	±0.0002	0.150	±0.001	18.690	±4.335
0.7449	±0.0018	0.2551	±0.0018	0.0069	±0.0020	0.0404	±0.0009	0.158	±0.004	17.016	±4.949
0.6911	±0.0018	0.3089	±0.0018	0.0097	±0.0012	0.0483	±0.0003	0.156	±0.001	11.089	±1.319
0.5777	±0.0014	0.4223	±0.0014	0.0117	±0.0012	0.0595	±0.0006	0.141	±0.001	6.954	±0.736
0.4575	±0.0018	0.5425	±0.0018	0.0107	±0.0020	0.0697	±0.0011	0.128	±0.002	5.482	±1.033
0.3188	±0.0013	0.6812	±0.0013	0.0113	±0.0015	0.0808	±0.0007	0.119	±0.001	3.336	±0.432
0.1720	±0.0016	0.8280	±0.0016	0.0142	±0.0012	0.0974	±0.0009	0.118	±0.001	1.423	±0.120
<b>{<i>n</i>-octane (1) + thiophene (2) + TEACl:EG (3)}</b>											
0.9438	±0.0009	0.0562	±0.0009	0.0007	±0.0001	0.0394	±0.0027	0.701	±0.050	1009.107	±239.651
0.8894	±0.0015	0.1106	±0.0015	0.0013	±0.0001	0.0756	±0.0016	0.684	±0.017	468.651	±26.304
0.8339	±0.0023	0.1661	±0.0023	0.0008	±0.0001	0.1056	±0.0029	0.636	±0.020	684.834	±35.172
0.7771	±0.0022	0.2229	±0.0022	0.0008	±0.0001	0.1279	±0.0060	0.574	±0.027	534.369	±44.518
0.7166	±0.0116	0.2834	±0.0116	0.0008	±0.0001	0.1418	±0.0107	0.502	±0.043	438.989	±46.223
0.6471	±0.0094	0.3529	±0.0094	0.0009	±0.0001	0.1823	±0.0067	0.517	±0.024	366.067	±29.354
0.4907	±0.0634	0.5093	±0.0634	0.0010	±0.0001	0.2200	±0.0036	0.437	±0.055	207.484	±38.391
0.3822	±0.0087	0.6178	±0.0087	0.0011	±0.0001	0.2549	±0.0012	0.413	±0.006	149.781	±5.654
0.2634	±0.0034	0.7366	±0.0034	0.0011	±0.0001	0.2884	±0.0054	0.392	±0.007	93.604	±5.038
0.1357	±0.0023	0.8643	±0.0023	0.0011	±0.0001	0.3264	±0.0030	0.378	±0.004	46.952	±1.555
<b>{<i>n</i>-octane (1) + thiophene (2) + TEACl:Gly (3)}</b>											
0.9386	±0.0024	0.0614	±0.0024	0.0005	±0.0002	0.0221	±0.0012	0.360	±0.024	670.526	±310.857
0.8777	±0.0024	0.1223	±0.0024	0.0005	±0.0003	0.0431	±0.0018	0.353	±0.016	598.505	±318.519
0.8192	±0.0023	0.1808	±0.0023	0.0004	±0.0001	0.0621	±0.0018	0.343	±0.011	734.025	±255.877
0.7535	±0.0100	0.2465	±0.0100	0.0002	±0.0001	0.0635	±0.0356	0.323	±0.181	794.213	±638.889
0.6993	±0.0031	0.3007	±0.0031	0.0005	±0.0003	0.0918	±0.0037	0.305	±0.013	470.686	±306.882
0.6375	±0.0062	0.3625	±0.0062	0.0003	±0.0001	0.1051	±0.0022	0.290	±0.008	621.898	±58.619
0.5150	±0.0071	0.4850	±0.0071	0.0003	±0.0001	0.1323	±0.0095	0.273	±0.020	454.961	±83.899

0.3725	±0.0108	0.6275	±0.0108	0.0004	±0.0001	0.1545	±0.0102	0.246	±0.017	261.523	±100.350
0.2638	±0.0101	0.7362	±0.0101	0.0003	±0.0001	0.1700	±0.0082	0.231	±0.012	212.781	±35.349
0.1300	±0.0017	0.8700	±0.0017	0.0002	±0.0001	0.1787	±0.0048	0.205	±0.006	137.090	±15.163
<b>{<i>n</i>-octane (1) + thiophene (2) + THABr:EG (3)}</b>											
0.948	±0.002	0.052	±0.002	0.079	±0.002	0.051	±0.001	0.981	±0.033	11.71	±0.47
0.898	±0.002	0.102	±0.002	0.087	±0.001	0.098	±0.001	0.961	±0.016	9.95	±0.18
0.851	±0.002	0.149	±0.002	0.094	±0.003	0.145	±0.003	0.976	±0.024	8.87	±0.34
0.802	±0.002	0.198	±0.002	0.105	±0.001	0.186	±0.001	0.941	±0.010	7.18	±0.11
0.747	±0.009	0.253	±0.009	0.114	±0.002	0.221	±0.002	0.873	±0.032	5.73	±0.24
0.693	±0.004	0.307	±0.004	0.128	±0.001	0.267	±0.001	0.869	±0.011	4.72	±0.07
0.593	±0.008	0.407	±0.008	0.152	±0.002	0.335	±0.002	0.822	±0.017	3.20	±0.09
0.486	±0.006	0.514	±0.006	0.186	±0.002	0.409	±0.003	0.797	±0.011	2.08	±0.04
<b>{<i>n</i>-octane (1) + thiophene (2) + THABr:Gly (3)}</b>											
0.946	±0.001	0.054	±0.001	0.043	±0.006	0.043	±0.001	0.794	±0.022	17.30	±2.50
0.891	±0.001	0.109	±0.001	0.050	±0.004	0.081	±0.002	0.747	±0.020	13.35	±1.04
0.839	±0.002	0.161	±0.002	0.052	±0.006	0.121	±0.004	0.752	±0.027	12.08	±1.36
0.780	±0.001	0.220	±0.001	0.061	±0.005	0.163	±0.011	0.741	±0.048	9.50	±0.98
0.727	±0.003	0.273	±0.003	0.061	±0.001	0.188	±0.001	0.688	±0.007	8.21	±0.20
0.671	±0.002	0.329	±0.002	0.065	±0.005	0.225	±0.001	0.684	±0.006	7.04	±0.54
0.582	±0.002	0.418	±0.002	0.075	±0.005	0.281	±0.001	0.673	±0.004	5.21	±0.36
0.473	±0.002	0.527	±0.002	0.085	±0.005	0.350	±0.004	0.665	±0.008	3.69	±0.21
0.363	±0.001	0.637	±0.001	0.099	±0.004	0.443	±0.005	0.696	±0.008	2.55	±0.10
0.251	±0.001	0.749	±0.001	0.112	±0.002	0.557	±0.006	0.744	±0.008	1.66	±0.04
<b>{<i>n</i>-octane (1) + thiophene (2) + MTPPBr:EG (3)}</b>											
0.9411	±0.0002	0.0589	±0.0002	0.0011	±0.0001	0.0324	±0.0004	0.550	±0.007	465.487	±9.082
0.8837	±0.0006	0.1163	±0.0006	0.0012	±0.0001	0.0624	±0.0011	0.537	±0.010	386.066	±24.367
0.8242	±0.0011	0.1758	±0.0011	0.0014	±0.0001	0.0940	±0.0005	0.535	±0.004	313.582	±4.139
0.7672	±0.0011	0.2328	±0.0011	0.0014	±0.0001	0.1195	±0.0021	0.514	±0.009	272.718	±12.999
0.7077	±0.0013	0.2923	±0.0013	0.0015	±0.0001	0.1452	±0.0019	0.497	±0.007	227.202	±4.226
0.6472	±0.0021	0.3528	±0.0021	0.0017	±0.0001	0.1701	±0.0028	0.482	±0.008	186.496	±3.931
0.5228	±0.0067	0.4772	±0.0067	0.0020	±0.0001	0.2189	±0.0043	0.458	±0.011	117.125	±4.670
0.4008	±0.0118	0.5992	±0.0118	0.0023	±0.0001	0.2656	±0.0037	0.443	±0.011	75.676	±4.189
0.2707	±0.0054	0.7293	±0.0054	0.0025	±0.0001	0.3108	±0.0035	0.427	±0.006	45.824	±1.990
0.1422	±0.0039	0.8578	±0.0039	0.0022	±0.0001	0.3446	±0.0136	0.409	±0.016	26.442	±1.632
<b>{<i>n</i>-octane (1) + thiophene (2) + MTPPBr:Gly (3)}</b>											
0.9416	±0.0005	0.0584	±0.0005	0.0002	±0.0001	0.0075	±0.0003	0.129	±0.005	655.854	±54.330
0.8826	±0.0012	0.1174	±0.0012	0.0002	±0.0001	0.0181	±0.0003	0.160	±0.003	556.040	±33.127
0.8236	±0.0015	0.1764	±0.0015	0.0002	±0.0001	0.0320	±0.0019	0.194	±0.012	673.641	±43.058
0.7632	±0.0019	0.2368	±0.0019	0.0004	±0.0001	0.0512	±0.0016	0.218	±0.007	422.471	±159.854
0.7036	±0.0008	0.2964	±0.0008	0.0003	±0.0001	0.0697	±0.0104	0.245	±0.037	509.679	±99.672
0.6347	±0.0057	0.3653	±0.0057	0.0002	±0.0001	0.0438	±0.0377	0.189	±0.163	513.380	±515.731
0.5131	±0.0033	0.4869	±0.0033	0.0005	±0.0001	0.1118	±0.0199	0.198	±0.035	259.692	±86.144
0.3764	±0.0042	0.6236	±0.0042	0.0006	±0.0004	0.1152	±0.0076	0.178	±0.012	113.155	±82.571
0.2519	±0.0023	0.7481	±0.0023	0.0004	±0.0002	0.1376	±0.0205	0.187	±0.028	118.565	±64.961
0.1281	±0.0009	0.8719	±0.0009	0.0003	±0.0001	0.1579	±0.0304	0.182	±0.035	107.890	±49.972

## DES regeneration

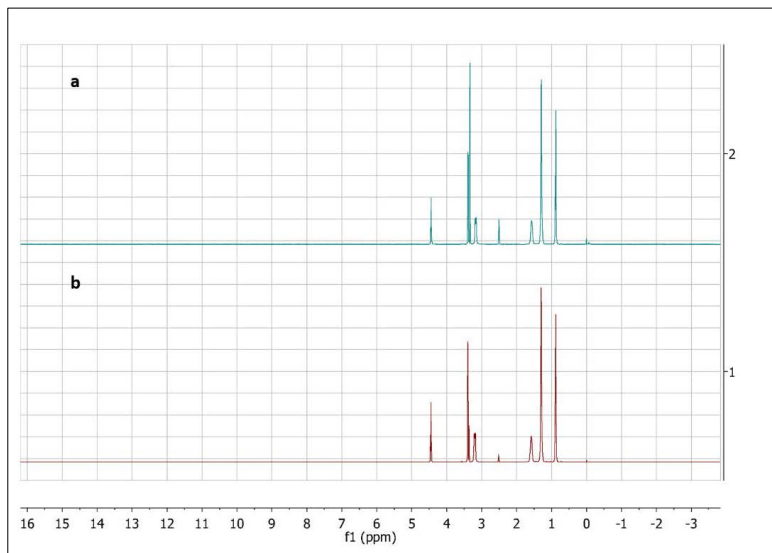


**Figure 17:**  $^1\text{H-NMR}$  spectra of: (a) the fresh THABr:EG and (b) the regenerated THABr:EG

---

## 6 PREDICTION OF THE LIQUID-LIQUID EQUILIBRIUM DATA OF {*n*-ALKANES + THIOPHENE + DES} SYSTEMS USING THE PERTURBATED CHAIN-STATISTICAL ASSOCIATING FLUID THEORY (PC-SAFT)

*This chapter has been partially published in: S. E. E Warrag, C. Pototzki, N. R. Rodriguez, M. van Sint Annaland, M. C. Kroon, C. Held, G. Sadowski, C. J. Peters, "Oil Desulfurization Using Deep Eutectic Solvents as Sustainable and Economical Extractants via Liquid-Liquid Extraction: Experimental and PC-SAFT Predictions" Fluid Phase Equilibria, 2018, 467, 33-44*

*In this chapter, the phase behavior of the 12 ternary systems of {*n*-alkane + thiophene + DES} was predicted using the Perturbed-Chain Statistical Associating Fluid Theory (PC-SAFT). It was found that PC-SAFT serves as an appropriate approach for the predictive solvent screening in order to obtain the thermodynamically optimal DESs.*

## 6.1 Introduction

Thermodynamics is the branch of science that relates the properties of a given system to parameters that are readily measured, and thus provides a good knowledge of the system behavior and a maximum return of information for any investment in laboratory experiments. In thermodynamics, relationships known as equations of state (EOS) are mathematical models between two or more state variables such as temperature, pressure, volume, internal energy or others that describe the state of the system under any given conditions. EOSs are widely used for the calculation of thermophysical properties, phase behavior, and phase equilibrium of pure components and of mixtures. Knowledge of these thermophysical properties over a wide range of temperature, pressure, and composition is crucial since they are the raw materials “feed” of chemical process design. Process simulation is becoming a more and more important tool for the design, scale-up and optimization of chemical processes. And therefore, accurate models for the description of the thermodynamic properties (in particular phase equilibria) and kinetic data are critical for the success and further development of novel chemical processes.

The first appearance of the thermodynamic modeling is dated back to 1873 when Van der Waal proposed the first EOS at his doctorate thesis entitled “*On the Continuity of the Gaseous and Liquid State*”.<sup>1</sup> The Van der Waals (vdw) EOS was the origin of a well-known class of equations of state called the *cubic equations of state* such as Peng Robinson (PR),<sup>2</sup> Soave-Redlich-Kwong (SRK),<sup>3</sup> Patel-Teja,<sup>4</sup> and others. However, the limited prediction capability of traditional cubic EOSs outside the range where their parameters were fitted is evident. On the contrary, molecular models based on statistical mechanics are gaining popularity because they are independent of the thermodynamic conditions, in other words, more predictive. The molecular-based models are intended to cover extended temperature and pressure ranges to include subcritical, near-critical and supercritical conditions. In addition, improve the predictability of fluids of variable molecular size from small spherical molecules (e.g., gases) to long-chain molecules (e.g., heavy hydrocarbons and polymers) as well as to fluids whose molecules exhibit non-polar, polar and hydrogen-bonding interactions.

In 1990, Chapman *et al.*<sup>5</sup> developed a molecular-based model, the so-called SAFT “Statistical Associating Fluid Theory”. SAFT was built to account for non-idealities in fluids, such as molecular shape and association on a molecular basis. And thus, it can be defined as an approach in which the different microscopic contributions that control the macroscopic properties of the fluid are explicitly considered in order to provide an accurate prediction of the thermophysical properties. The statistical basis of SAFT made it a robust equation that can be refined and extended systematically.

It is known that the Helmholtz free energy is invariably used in statistical thermodynamics as the basis for the derivation of equations of states. Since most properties of interest, such as system

pressure, can be obtained by proper differentiation of it. In SAFT equations the residual Helmholtz energy is calculated as follows:<sup>5</sup>

$$a^{res} = a^{seg} + a^{chain} + a^{assoc} \quad (1)$$

where  $a^{seg}$  is the Helmholtz energy of the segment, including both hard-sphere reference and dispersion terms,  $a^{chain}$  is the contribution from chain formation and  $a^{assoc}$  is the contribution from the association. In the last decades, various SAFT models were proposed such as Simplified-SAFT, Soft-SAFT, Perturbed Chain-SAFT, Variable Range-SAFT and others.<sup>6</sup> In the mentioned models, the chain and association terms did not change significantly in different SAFT versions, however, the attraction (segment) term varied. Due to the high predictability of the SAFT (and its different versions), it was one of the objectives of this chapter to predict the liquid-liquid equilibrium of the ternary system  $\{n\text{-alkane} + \text{thiophene} + \text{DES}\}$  presented in *Chapter 5* using one of the SAFT versions, in particular, the Perturbated Chain-SAFT (PC-SAFT)<sup>7</sup>.

In this chapter, PC-SAFT was used for the prediction of the LLE data of the 12 ternary systems:

- $\{n\text{-hexane} + \text{thiophene} + \text{tetraethylammonium chloride: ethylene glycol (TEACl:EG) (1:2)}\}$ ,
- $\{n\text{-hexane} + \text{thiophene} + \text{tetraethylammonium chloride: glycerol (TEACl:Gly) (1:2)}\}$ ,
- $\{n\text{-hexane} + \text{thiophene} + \text{tetrahexylammonium bromide :ethylene glycol (THABr:EG) (1:2)}\}$ ,
- $\{n\text{-hexane} + \text{thiophene} + \text{tetrahexylammonium bromide: glycerol (THABr:Gly) (1:2)}\}$ ,
- $\{n\text{-hexane} + \text{thiophene} + \text{methyltriphenylphosphonium bromide: ethylene glycol (MTPPBr:EG) (1:3)}\}$ ,
- $\{n\text{-hexane} + \text{thiophene} + \text{methyltriphenylphosphonium bromide: glycerol (MTPPBr:Gly) (1:3)}\}$ ,
- $\{n\text{-octane} + \text{thiophene} + \text{tetraethylammonium chloride: ethylene glycol (TEACL:EG) (1:2)}\}$ ,
- $\{n\text{-octane} + \text{thiophene} + \text{tetraethylammonium chloride: glycerol (TEACL:Gly) (1:2)}\}$ ,
- $\{n\text{-octane} + \text{thiophene} + \text{tetrahexylammonium bromide :ethylene glycol (THABr:EG) (1:2)}\}$ ,
- $\{n\text{-octane} + \text{thiophene} + \text{tetrahexylammonium bromide : glycerol (THABr:Gly) (1:2)}\}$ ,
- $\{n\text{-octane} + \text{thiophene} + \text{methyltriphenylphosphonium bromide: ethylene glycol (MTPPBr:EG) (1:3)}\}$ ,
- $\{n\text{-octane} + \text{thiophene} + \text{methyltriphenylphosphonium bromide: glycerol (MTPPBr:Gly) (1:3)}\}$ .

The PC-SAFT pseudo-pure component approach was applied, in which a DES was considered as a pseudo-pure compound, and its pure-component parameters were obtained by fitting to experimental liquid density data. The binary interaction parameters were fitted to experimental binary LLE data for



the systems {*n*-alkane + DES} and {thiophene + DES} at 298.2 K and atmospheric pressure, while the LLE data of the ternary systems {*n*-alkane + thiophene + DES} were fully predicted.

## 6.2 PC-SAFT

PC-SAFT<sup>7</sup> is a thermodynamic model for the calculation of the residual Helmholtz energy of a system based on the hard-chain reference system. Various perturbations to the hard-chain system can be considered. As outlined earlier, PC-SAFT is a modified version of SAFT (see eq. (1)) in which the segment term  $a^{\text{seg}}$  is a contribution of hard sphere reference  $a^{\text{HS}}$  and a contribution from chain formation  $a^{\text{chain}}$  combined and renamed as the hard-chain reference contribution  $a^{\text{hc}}$ . The dispersion term is independently quantified as  $a^{\text{dis}}$ . And  $a^{\text{assoc}}$ , the contribution from the association, is not changed in PC-SAFT. Then, the residual Helmholtz energy  $a^{\text{res}}$  of a system is then composed of the hard-chain reference contribution  $a^{\text{hc}}$ , and contributions caused by dispersion  $a^{\text{disp}}$  and association  $a^{\text{assoc}}$  the PC-SAFT equation reads:

$$a^{\text{res}} = a^{\text{hc}} + a^{\text{disp}} + a^{\text{assoc}} \quad (2)$$

Three pure-component parameters for each component *i* are needed for a non-polar and non-associating fluids. In the PC-SAFT framework, molecules are considered as chains containing a number of  $m_i^{\text{seg}}$  spherical segments of equal diameter  $\sigma_i$ . Dispersion attractions are characterized by the dispersion-energy parameter  $u_i/k_B$ , where  $k_B$  is the Boltzmann constant. If the component is able to interact via association attractions by hydrogen bonding, two more parameters are needed, the association-energy parameter  $\varepsilon^{A_i B_i}/k_B$  and the association-volume parameter  $\kappa^{A_i B_i}$ . Additional to these five pure-component parameters, the number of association sites  $N_i^{\text{assoc}}$  that can form hydrogen bonds has to be estimated, which is most commonly done based on the molecular structure of the component.

Please note, that the temperature-dependent segment diameter  $d_i$  has been applied according to the original PC-SAFT publication.<sup>7</sup> For mixtures, combining rules have to be used in order to describe the segment diameter  $\sigma_{ij}$  and the dispersion-energy parameter  $u_{ij}$ , and in this work Berthelot-Lorentz combining rules were applied according to Eqs. (3) and (4).

$$\sigma_{ij} = \frac{1}{2}(\sigma_i + \sigma_j) \quad (3)$$

$$u_{ij} = (1 - k_{ij})\sqrt{u_i u_j} \quad (4)$$

In Eq. (4), the binary interaction parameter  $k_{ij}$  is introduced for any corrections of the cross-dispersion energy from the geometric mean of its pure-component contributions. In this work, all binary interaction parameters  $k_{ij}$  were assumed to be temperature independent. For cross-associating systems, the

combination rules from Wolbach and Sandler<sup>8</sup> for the association-energy parameter  $\varepsilon^{A_i B_j}$  and association-volume parameter  $\kappa^{A_i B_j}$  as presented in Eqs. (5) and (6) were applied.

$$\varepsilon^{A_i B_j} = \frac{1}{2} (\varepsilon^{A_i B_i} + \varepsilon^{A_j B_j}) \quad (5)$$

$$\kappa^{A_i B_j} = \sqrt{\kappa^{A_i B_i} \kappa^{A_j B_j}} \left( \frac{2\sqrt{\sigma_i \sigma_j}}{\sigma_i + \sigma_j} \right)^3 \quad (6)$$

No adjustable binary parameter was used in this work in Eqs. (5) and (6).

### 6.2.1 Modeling approach

Recently, two different PC-SAFT modeling strategies for DES were compared: the pseudo-pure component approach and the individual-component approach.<sup>9,10</sup> In the first strategy, a DES is considered as a pseudo-pure compound, and its pure-component parameters are usually fitted to density data of a DES. Experimental vapor pressures of DESs are usually not available. In the second strategy, the individual components of the DESs are modeled separately, and the pure-component parameters of the individual components were fitted to the density of aqueous solutions containing the pure components.<sup>9,10</sup> The pseudo-pure component approach is a simple and pragmatic method; however, it requires new PC-SAFT pure-component parameters for every DES. In contrast, the pure-component parameters (for the individual-component approach) are fitted to pure-component data or to data of aqueous binary solutions containing one DES constituent and water. Because the individual components of the DESs in this work are solid at ambient conditions and show very low aqueous solubility, the pure-component parameters could not be obtained by these standard procedures. Hence, the individual-component strategy was not applied and the pseudo-pure component approach was used in this work. According to a previous study, temperature-dependent density data for a DES mixture is required for parameter estimation.<sup>11</sup>

The pure-component PC-SAFT parameters of the DESs under investigation (TEACl:EG, TEACl:Gly, THABr:EG, THABr:Gly, MTPPBr:EG, and MTPPBr:Gly,) are not yet available in the literature. Therefore, the pure-component parameters were determined by fitting to density data of the pure DES measured in this work. For the modeling, the DESs were considered as non-spherical molecules with the ability to exert self-association interactions. The association scheme for the DESs under investigation was chosen to be the 2B scheme, according to the findings of previous studies on modeling DESs with PC-SAFT.<sup>9,10</sup> Further, the 2B association scheme was also applied by several researchers who modeled DESs with SAFT-based approaches.<sup>9-15</sup> Cross-association has not been considered in this work as the *n*-alkane (*n*-hexane and *n*-octane) were assumed to be non-associating fluids. Thiophene is a weakly polar compound (with dipole moment  $\mu \approx 0.53$  D). Therefore, it was considered as non-associating fluid as well. Nevertheless, cross-dispersion among all pairs existing in the ternary systems (*n*-alkane/thiophene, DES/thiophene, DES/*n*-alkane) was taken into account, and

binary interaction parameters ( $k_{ij}$ ) for the pairs DES/thiophene, DES/*n*-hexane, and DES/*n*-octane were obtained by fitting to LLE data measured in this work (see Chapter 5, section 5.3.1). For the pair thiophene/*n*-hexane, literature vapor-liquid equilibria<sup>16</sup> (VLE) data were used to fit the  $k_{ij}$  values. For the pair thiophene/*n*-octane, excess enthalpies data<sup>17</sup> were used to fit the  $k_{ij}$  value.

The accuracy of the calculated data compared to experimentally obtained data was evaluated through the percentage average relative deviation (ARD). The ARD between calculated and experimental data is defined as

$$ARD = \frac{1}{n^{exp}} \cdot \sum_{i=1}^{n^{exp}} \left| \frac{y_i^{exp} - y_i^{calc}}{y_i^{exp}} \right| \cdot 100\% \quad (7)$$

$n_{exp}$  is the number of experimental points,  $y_{exp,i}$  the experimentally determined value and  $y_{calc,i}$  the calculated value.

### 6.3 Results and discussion

#### 6.3.1 Pure components

As mentioned in the previous section, the PC-SAFT pseudo-pure component approach requires fitting the pure-component parameters of the DESs to the experimental density data. For this purpose, the temperature dependence of the specific density ( $\rho$ ) was measured in the temperature range of 298.2 – 323,2 K for all the prepared DESs. The experimental values of the specific density are shown graphically in Figure 1 and the numerical values of  $\rho$  can be found Table 1. The pure-component parameters of the DESs were adjusted using the following objective function (OF):

$$OF = \sum_{i=1}^{n^{exp}} \left( \frac{y_i^{exp} - y_i^{calc}}{y_i^{exp}} \right)^2 \quad (8)$$

within an own FORTRAN code and an IMSL-implemented Levenberg-Marquardt algorithm. Again,  $n_{exp}$  is the number of experimental points,  $y_{exp,i}$  the experimentally determined value and  $y_{calc,i}$  the PC-SAFT calculated value.

PC-SAFT pure-component parameters for thiophene,<sup>18</sup> *n*-hexane,<sup>7</sup> and *n*-octane<sup>7</sup> were taken from literature and are listed in Table 2. The parameters for the DESs fitted in this work are shown in Table 2 and the accuracy of the calculation of pure densities was estimated using the ARD (see Table 2).

As can be seen from Figure 1 and Table 2, the PC-SAFT calculated and experimentally determined densities of the pure DESs are in very good agreement. The ARD values are comparable to

other works dealing with modeling density of ionic liquids or DESs with PC-SAFT.<sup>9,11</sup> Thus, the determined PC-SAFT pure-component parameters of the DESs are apparently validated, which further confirms the use of density data to fit pseudo-DES PC-SAFT parameters.

**Table 1:** Experimental density data of the studied DESs at different temperatures and 1.01 bar. The densities with the superscripts a were taken from literature (Rodriguez et. al. 2016).<sup>19</sup> The densities of the other four were measured in this work

T(K)	$\rho(\text{g}\cdot\text{cm}^{-3})$					
	THABr:EG	THABr:Gly	TEACl:EG	TEACl:Gly	MTPPBr:EG	MTPPBr:Gly
293.15	1.0078 <sup>a</sup>	1.0458 <sup>a</sup>	1.0523	1.124	na	na
298.15	1.0045 <sup>a</sup>	1.0426 <sup>a</sup>	1.0494	1.1210	1.2491	1.2958
303.15	1.0013 <sup>a</sup>	1.0393 <sup>a</sup>	1.0466	1.1181	1.2457	1.2924
308.15	0.9983 <sup>a</sup>	1.0360 <sup>a</sup>	1.0437	1.1151	1.2422	1.2889
313.15	0.9951 <sup>a</sup>	1.0327 <sup>a</sup>	1.0409	1.1123	1.2388	1.2853
318.15	0.9919 <sup>a</sup>	1.0295 <sup>a</sup>	1.0381	1.1094	1.2354	1.2817
323.15	0.9886 <sup>a</sup>	1.0263 <sup>a</sup>	1.0353	1.1066	1.2319	1.2781
328.15	0.9854 <sup>a</sup>	1.0231 <sup>a</sup>	1.0325	1.1038	na	na
333.15	0.9822 <sup>a</sup>	1.0200 <sup>a</sup>	1.0297	1.1010	na	na
338.15	0.9789 <sup>a</sup>	1.0168 <sup>a</sup>	1.0269	1.0982	na	na
343.15	0.9757 <sup>a</sup>	1.0137 <sup>a</sup>	1.0241	1.0954	na	na

\*Standard uncertainty in temperature  $u(T) = 0.01$  K,  $u(p) = 0.02$  bar and in density  $u(\rho) = 0.0005$  g·cm<sup>-3</sup>

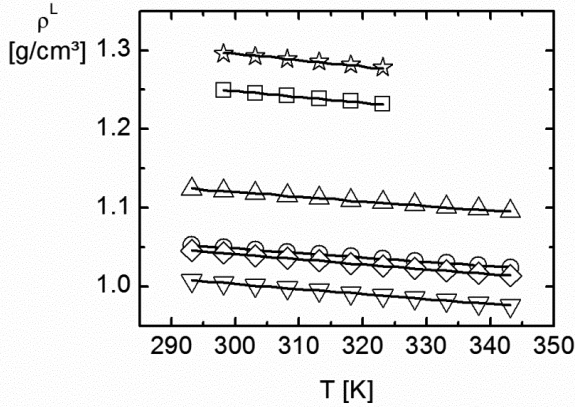


**Figure 1:** Liquid densities  $\rho^L$  of pure DESs as a function of temperature. Circles: tetraethylammonium chloride:ethylene glycol (1:2), triangles: tetraethylammonium chloride:glycerol (1:2), squares: methyltriphenylphosphonium bromide:ethylene glycol (1:3), stars: methyltriphenylphosphonium bromide:glycerol (1:3), triangles upside down: tetrahexylammonium bromide:ethylene glycol (1:2), and diamonds: tetrahexylammonium bromide:glycerol (1:2). The symbols are experimental data, and the solid lines are the PC-SAFT modeling results using the parameters listed in Table 2.

**Table 2:** PC-SAFT pure-component parameters for thiophene,<sup>18</sup> *n*-hexane<sup>7</sup>, *n*-octane<sup>7</sup> and DESs including percent average relative deviation (ARD (%)) between PC-SAFT calculated pure-DES densities and experimental data.

Component	$M$ (g/mol)	$m_i^{seg}$ (-)	$\sigma_i$ (Å)	$u_i/k_B$ (K)	$\varepsilon^{A_iB_i}/k_B$ (K)	$\kappa^{A_iB_i}$ (-)	$N_i^{assoc}$ (-)	$ARD_\rho$ (%)
Thiophene	84.14	2.4970	3.5395	291.44	-	-	-	-
<i>n</i> -Hexane	86.18	3.0576	3.7983	236.77	-	-	-	-
<i>n</i> -Octane	114.23	3.8176	3.8373	242.78	-	-	-	-
TEACl:EG	96.27	2.6385	3.8252	548.32	4265	0.01	1/1	0.03
TEACl:Gly	116.38	2.5881	4.0117	551.83	4969	0.01	1/1	0.04
MTPPBr:EG	135.86	2.5972	3.9918	397.20	4809	0.01	1/1	0.05
MTPPBr:Gly	158.38	3.8734	3.6788	440.88	4632	0.03	1/1	0.06
THABr:EG	185.00	4.2966	4.0680	418.92	4787	0.03	1/1	0.04
THABr:Gly	205.11	3.6961	4.3950	467.78	4897	0.02	1/1	0.04

### 6.3.2 Binary systems

The binary interaction parameters of all pairs were adjusted to thermodynamic data. The binary interaction parameter between thiophene and *n*-hexane was fitted to isothermal VLE data reported by

Sapei *et al.*<sup>16</sup> As can be seen in Figure 2, PC-SAFT calculations of the VLE are in good accordance with the experimental data using the pure-component parameters from Table 2 and the  $k_{ij}$  value from Table 3, which was found to be close to zero. The binary interaction parameter between thiophene and *n*-octane was fitted to excess enthalpies reported by Didaoui-Nemouchi and Ait Kaci<sup>20</sup> at 303.15 K. Applying a small  $k_{ij}$  value allowed reasonably well correlating the experimental excess enthalpies with PC-SAFT (see Figure 3). The  $k_{ij}$  values of the pairs thiophene/*n*-hexane and thiophene/*n*-octane are very similar, which is an expected result. Binary interaction parameters for the pairs DES/thiophene, DES/*n*-hexane and DES/*n*-octane were fitted to the binary LLE data, which are given in *chapter 5, section 5.3.1*. The results are not illustrated graphically but listed as ARD values in Table 3. All the resulting  $k_{ij}$  values are also given in Table 3. The ARD values refer to either  $h^E$  or LLE (mass fraction in the DES-rich phase  $w_i^{DES}$ ,  $i=\{n\text{-hexane}, n\text{-octane}, \text{thiophene}\}$ ) according to equation (7). It can be observed from Table 3 that all ARD values are below 1 %, which is a satisfactory result especially for temperature-dependent experimental data such as LLE, VLE, or  $h^E$ , considering the fact that temperature-independent fit parameters were used.

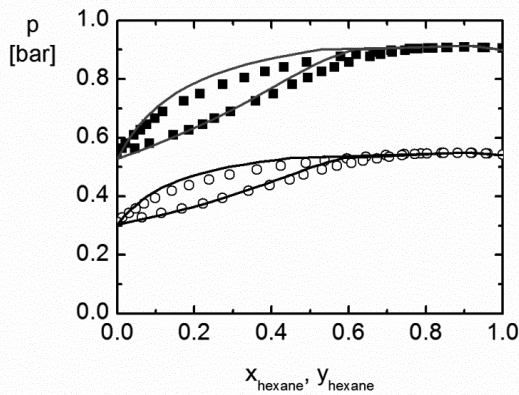


**Figure 2:** Isothermal VLE of the binary system thiophene/*n*-hexane at (circles) 323.15 K and (squares) 338.15 K. The symbols are literature data<sup>16</sup>, and the lines are PC-SAFT modeling results using the pure-component parameters from Table 2 and the binary interaction parameter  $k_{ij} = 0.03$ .

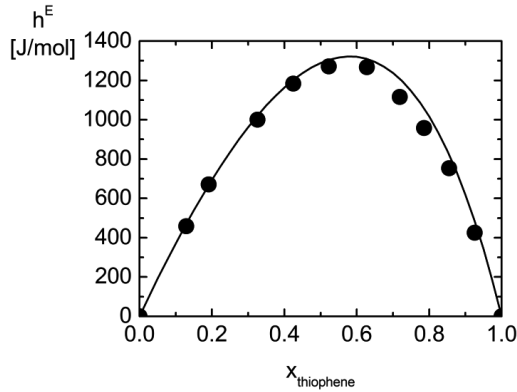


**Figure 3:** Excess enthalpy  $h^E$  of the binary system thiophene/*n*-octane at 303.15 K. The solid symbols are literature data<sup>20</sup>, and the solid lines are the PC-SAFT modeling results using the pure-component parameters from Table 2 and the binary interaction parameter  $k_{ij} = 0.032$ .

**Table 3:** Binary interaction parameters between all components considered in this work. All parameters are temperature independent. For the  $k_{ij}$  obtained by fitting to LLE, VLE, or  $h_E$  data, the percent average relative deviation (ARD (%)) is given.\*

Component i	Component j	$k_{ij}$	Data*	ARD (%)
<b>TEACl:EG</b>	Thiophene	-0.0195	LLE	0.60
	<i>n</i> -Hexane	-0.0221	LLE	0.01
	<i>n</i> -Octane	-0.00627	LLE	0.00
<b>TEACl:Gly</b>	Thiophene	0.0151	LLE	0.25
	<i>n</i> -Hexane	0.0418	LLE	0.11
	<i>n</i> -Octane	0.0386	LLE	0.08
<b>MTPPBr:EG</b>	Thiophene	0.02488	LLE	0.01
	<i>n</i> -Hexane	0.07985	LLE	0.00
	<i>n</i> -Octane	0.0841	LLE	0.21
<b>MTPPBr:Gly</b>	Thiophene	0.00572	LLE	0.11
	<i>n</i> -Hexane	-0.0203	LLE	0.09
	<i>n</i> -Octane	0.033	LLE	0.85
<b>THABr:EG</b>	Thiophene	0	n/a	n/a
	<i>n</i> -Hexane	-0.0069	LLE	0.05
	<i>n</i> -Octane	-0.002	LLE	0.01

<b>THABr:Gly</b>	Thiophene	0.0313	LLE	0.02
	<i>n</i> -Hexane	0.0268	LLE	0.02
	<i>n</i> -Octane	0.027	LLE	0.02
<b>Thiophene</b>	<i>n</i> -Hexane	0.03	VLE	2.19
	<i>n</i> -Octane	0.032	$h^E$	5.36

\* LLE data were obtained in this work, VLE data <sup>16</sup> and  $h^E$  data <sup>20</sup> were taken from literature.

### 6.3.3 Ternary systems

With the pure-component parameters and the binary interaction parameters obtained in previous sections, LLE data of ternary systems containing thiophene, *n*-alkane and one DES were predicted with PC-SAFT. The accuracy of the PC-SAFT predictions is measured by means of the deviations between the experimental and predicted thiophene distribution coefficient  $\beta_{thiophene}$  and the selectivity  $S$ . The experimentally obtained  $\beta_{thiophene}$  and  $S$  are reported in Chapter 5

$$\beta_{thiophene} = \frac{w_{thiophene}^{DES\ phase}}{w_{thiophene}^{n-alkane\ phase}} \quad (9)$$

$$S = \frac{\beta_{thiophene}}{\beta_{n-alkane}} = \frac{w_{thiophene}^{DES\ phase} \cdot w_{n-alkane}^{n-alkane\ phase}}{w_{thiophene}^{n-alkane\ phase} \cdot w_{n-alkane}^{DES\ phase}} \quad (10)$$

Figures 4-9 show the experimentally determined and predicted  $\beta_{thiophene}$  and  $S$  of all ternary systems of  $\{n\text{-alkane} + \text{thiophene} + \text{DES}\}$ . As highlighted in Chapter 5, it becomes clear that selectivity strongly decreases with increasing thiophene concentration. In contrast, the distribution coefficients of thiophene are rather constant upon increasing the thiophene concentration.

From a thermodynamic point-of-view, DESs are very appropriate to extract thiophene from *n*-alkanes at low thiophene concentrations. Comparing these experimental findings with the PC-SAFT predictions, it is obvious that PC-SAFT allows validating this observation quantitatively. PC-SAFT can be used to screen the best DES for the extraction of thiophene from *n*-alkanes. Ethylene glycol-based DESs showed higher distribution coefficients than the glycerol-based DESs, which can be predicted quantitatively correctly with PC-SAFT. Further, PC-SAFT predicts correctly the system  $\{n\text{-hexane} + \text{thiophene} + \text{MTPPB:EG}\}$  that showed high distribution coefficients and simultaneously high selectivities. Also, even the behavior of the systems  $\{n\text{-alkane} + \text{thiophene} + \text{THABr:EG}$  or  $\text{THABr:Gly}\}$  are predicted correctly, for which relatively high distribution coefficients but extremely low selectivities were observed from experiments and PC-SAFT predictions.

Among all systems studied, the best PC-SAFT prediction results were obtained for the systems  $\{n\text{-hexane} + \text{thiophene} + \text{TEACl:EG}\}$  and  $\{n\text{-hexane} + \text{thiophene} + \text{TEACl:Gly}\}$ , shown in Figure 4. Overall, predictions agree with the experimentally determined values. Even when the experimental data



is not matched exactly, the behavior of  $\beta_{thiophene}$  and  $S$  are predicted qualitatively correct. Thus, PC-SAFT using the pseudo-pure component approach for DESs is an accurate modeling approach for the prediction of the separation of thiophene from  $n$ -alkanes with the help of DESs.

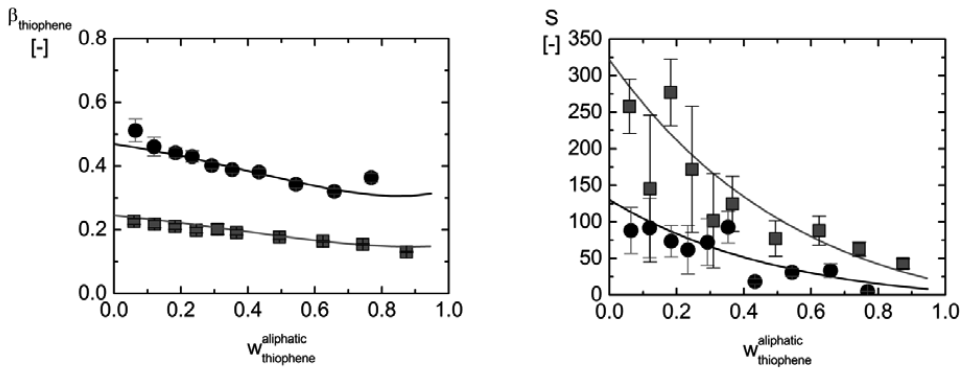


**Figure 4:** Distribution coefficient of thiophene  $\beta_{thiophene}$  and selectivity  $S$  of thiophene over  $n$ -hexane in ternary systems. Circles:  $\{n\text{-hexane} + \text{thiophene} + \text{TEACl:EG}\}$ , squares:  $\{n\text{-hexane} + \text{thiophene} + \text{TEACl:Gly}\}$ . Symbols represent experimentally determined values and lines PC-SAFT calculations.

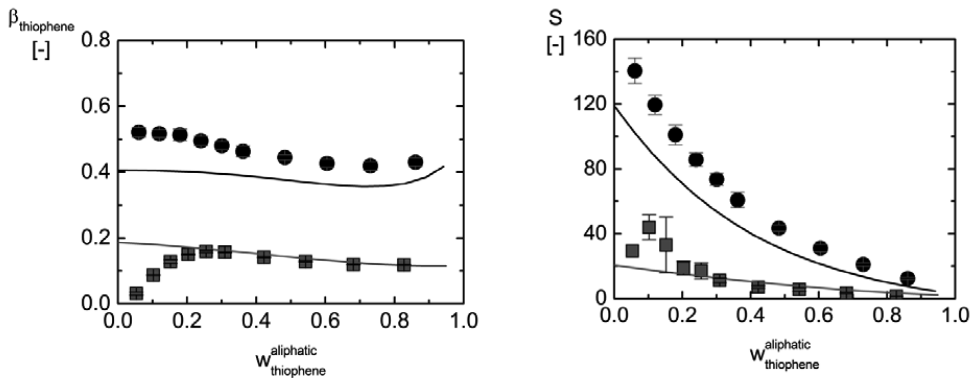


**Figure 5:** Distribution coefficient of thiophene  $\beta_{thiophene}$  and selectivity  $S$  of thiophene over  $n$ -hexane in ternary systems. Circles:  $\{n\text{-hexane} + \text{thiophene} + \text{MTPPBr:EG}\}$ , squares:  $\{n\text{-hexane} + \text{thiophene} + \text{MTPPBr:Gly}\}$ . Symbols represent experimentally determined values and lines PC-SAFT calculations.

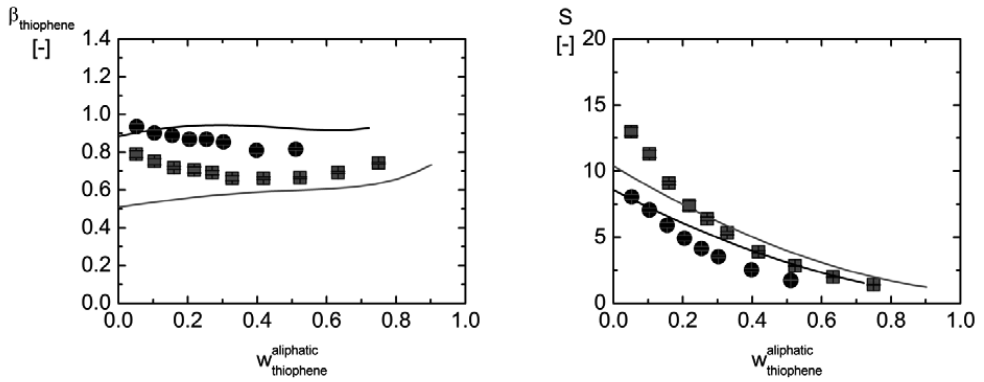


**Figure 6:** Solute distribution coefficient of thiophene  $\beta_{thiophene}$  and selectivity  $S$  of  $n$ -hexane and thiophene in ternary systems. Circles:  $\{n\text{-hexane} + \text{thiophene} + \text{THABr:EG}\}$ , squares:  $\{n\text{-hexane} + \text{thiophene} + \text{THABr:Gly}\}$ . Symbols represent experimentally determined values and lines PC-SAFT calculations.

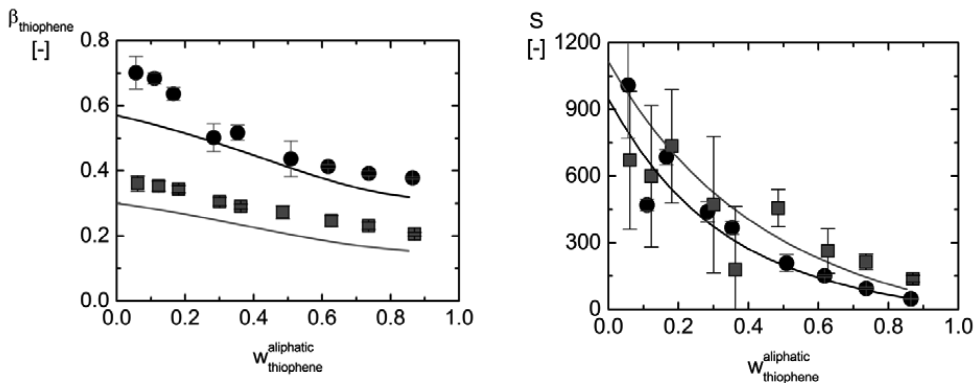


**Figure 7:** Distribution coefficient of thiophene  $\beta_{thiophene}$  and selectivity  $S$  of thiophene over  $n$ -octane in ternary systems. Circles:  $\{n\text{-octane} + \text{thiophene} + \text{TEACl:EG}\}$ , squares:  $\{n\text{-octane} + \text{thiophene} + \text{TEACl:Gly}\}$ . Symbols represent experimentally determined values and lines PC-SAFT calculations.

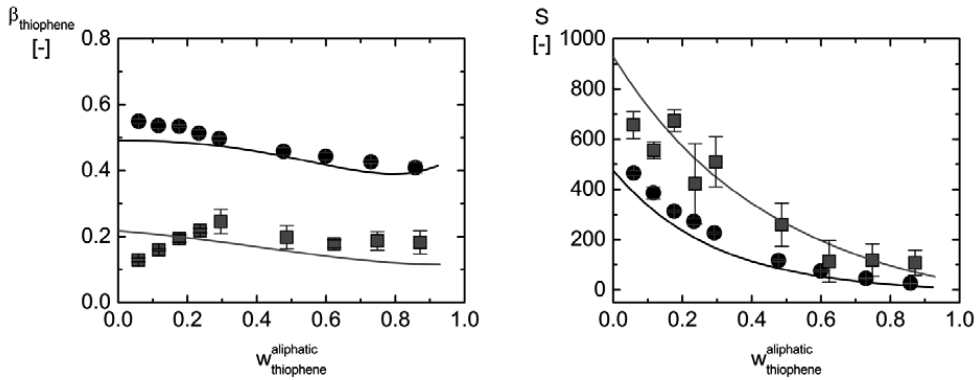


**Figure 8:** Distribution coefficient of thiophene  $\beta_{thiophene}$  and selectivity  $S$  of thiophene over n-octane in ternary systems. Circles: {n-octane + thiophene + MTPPBr:EG}, squares: {n-octane + thiophene + MTPPBr:Gly}. Symbols represent experimentally determined values and lines PC-SAFT calculations.

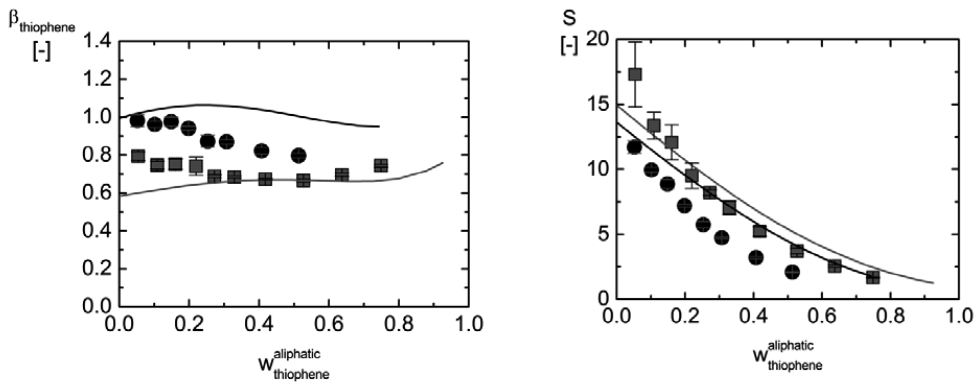


**Figure 9:** Distribution coefficient of thiophene  $\beta_{thiophene}$  and selectivity  $S$  of thiophene over n-octane in ternary systems. Circles: {n-octane + thiophene + THABr:EG}, squares: {n-octane + thiophene + THABr:Gly}. Symbols represent experimentally determined values and lines PC-SAFT calculations.

For the purpose of comparison, Figure 10 show the predicted and the experimentally obtained  $\beta_{thiophene}$  and  $S$  values of all {n-alkane + thiophene + DES} systems at  $w_{thiophene}^{n-alkane} = 0.5$ . In this case, experimentally obtained means that, the experimental data was interpolated to  $w_{thiophene}^{n-alkane} = 0.5$ . It is shown that in all cases ethylene-glycol based DESs are better extracting agents (higher  $\beta_{thiophene}$ ) than glycerol based DESs. Comparing the results obtained for the TEACl-based DESs and THABr-based

DESS, it can be observed that the longer the alkyl chain length on the HBA, the higher the thiophene distribution coefficient, but the lesser the selectivity. Therefore, the use of a long alkyl chain would lead to a lower solvent:feed ratio but rather increased extractor size. Moreover, it was observed that the distribution coefficients were low for all systems. Practically, this behavior would result in a high number of extraction stages.

Again, the overall good agreement between the predictions and the experimentally determined values can be clearly observed. Here, the best PC-SAFT prediction results were obtained for the systems  $\{n\text{-hexane} + \text{thiophene} + \text{TEACl:EG or TEACl:Gly}\}$  regarding  $\beta_{\text{thiophene}}$ . The best prediction results regarding  $S$  were obtained for the systems  $\{n\text{-alkanes} + \text{thiophene} + \text{THABr:EG or THABr:Gly}\}$ .

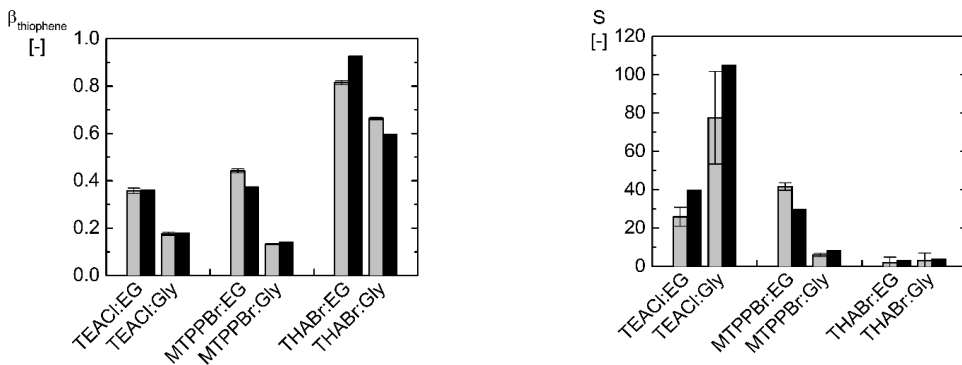


**Figure 10:** Distribution coefficient of thiophene  $\beta_{\text{thiophene}}$  and selectivity  $S$  of thiophene over  $n$ -hexane in ternary systems  $\{n\text{-hexane} + \text{thiophene} + \text{DES}\}$  at  $w_{\text{thiophene}}^{\text{aliphatic}} = 0.5$ . Gray: interpolated between experimentally determined values, black: PC-SAFT calculations.

#### 6.4 Conclusions

In this chapter the phase behavior of the 12 ternary systems of  $\{n\text{-alkane} + \text{thiophene} + \text{DES}\}$  was predicted using the Perturbed-Chain Statistical Associating Fluid Theory (PC-SAFT). The DESs under investigation were: (i) tetraethylammonium chloride: ethylene glycol (1:2), (ii) tetraethylammonium chloride: glycerol (1:2), (iii) Tetrahexylammonium bromide: ethylene glycol (1:2), (iv) Tetrahexylammonium bromide: ethylene glycol (1:2), (v) methyltriphenylphosphonium bromide:ethylene glycol (1:3), and (vi) methyltriphenylphosphonium bromide: glycerol (1:3). It was found that the distribution coefficient of thiophene and the selectivity of thiophene over the  $n$ -alkane in the ternary systems containing DESs can be qualitatively well predicted using PC-SAFT. PC-SAFT captured qualitatively the main observations outlined in *Chapter 4*, that the longer the alkyl chain length on the HBA, the higher the thiophene distribution coefficient, but the lesser the selectivity for both

alkanes *n*-hexane and *n*-octane. Moreover, higher selectivities and slightly lower distribution ratios were obtained when thiophene was extracted from *n*-octane instead of *n*-hexane. It can be concluded that DESs are promising candidates for extractive desulfurization of fuels, and that PC-SAFT serves as an appropriate approach for the predictive solvent screening in order to obtain the thermodynamically optimal DESs.

## 6.5 References

- (1) Van Der Waals, J. D.; Rowlinson, J. S. *On the Continuity of the Gaseous and Liquid States*; Dover Publications: New York, 2004.
- (2) Peng, D. Y.; Robinson, D. B. A New Two-Constant Equation of State. *Ind. Eng. Chem. Fundam.* **1976**, *15* (1), 59–64.
- (3) Soave, G. Equilibrium Constants from a Modified Redlich-Kwong Equation of State. *Chem. Eng. Sci.* **1972**, *27* (6), 1197–1203.
- (4) Patel, N. C.; Teja, A. S. A New Cubic Equation of State for Fluids and Fluid Mixtures. *Chem. Eng. Sci.* **1982**, *37* (3), 463–473.
- (5) Chapman, W. G.; Gubbins, K. E.; Jackson, G.; Radosz, M. New Reference Equation of State for Associating Liquids. *Ind. Eng. Chem. Res.* **1990**, *29* (8), 1709–1721.
- (6) Economou, I. G. Statistical Associating Fluid Theory : A Successful Model for the Calculation of Thermodynamic and Phase Equilibrium Properties of Complex Fluid Mixtures. *Ind. Eng. Chem.* **2002**, *41*, 953–962.
- (7) Gross, J.; Sadowski, G. Perturbed-Chain SAFT : An Equation of State Based on a Perturbation Theory for Chain Molecules. *Ind. Eng. Chem. Res.* **2001**, *40*, 1244–1260.
- (8) Wolbach, J. P.; Sandler, S. I. Using Molecular Orbital Calculations To Describe the Phase Behavior of Cross-Associating Mixtures. *Ind. Eng. Chem. Res.* **1998**, *37*, 2917–2928.
- (9) Zubeir, L. F.; Held, C.; Sadowski, G.; Kroon, M. C. PC-SAFT Modeling of CO<sub>2</sub> Solubilities in Deep Eutectic Solvents. *J. Phys. Chem. B* **2016**.
- (10) Verevkin, S. P.; Sazonova, A. Y.; Frolkova, A. K.; Zaitsau, D. H.; Prikhodko, I. V.; Held, C. Separation Performance of BioRenewable Deep Eutectic Solvents. *Ind. Eng. Chem. Res.* **2015**, *54* (13), 3498–3504.
- (11) Dietz, C. H. J. T.; van Osch, D. J. G. P.; Kroon, M. C.; Sadowski, G.; van Sint Annaland, M.; Gallucci, F.; Zubeir, L. F.; Held, C. PC-SAFT Modeling of CO<sub>2</sub> Solubilities in Hydrophobic Deep Eutectic Solvents. *Fluid Phase Equilib.* **2017**, *448*, 94–98.
- (12) Haghbakhsh, R.; Raeissi, S.; Parvaneh, K.; Shariati, A. The Friction Theory for Modeling the Viscosities of Deep Eutectic Solvents Using the CPA and PC-SAFT Equations of State. *J. Mol. Liq.* **2018**, *249*, 554–561.
- (13) Animasahun, O. H.; Khan, M. N.; Peters, C. J. Prediction of the CO<sub>2</sub> Solubility in Deep Eutectic Solvents: A Comparative Study between PC-SAFT and Cubic Equations of State. In *Abu Dhabi International Petroleum Exhibition & Conference*; Society of Petroleum Engineers, 2017.

- 
- (14) Haghbakhsh, R.; Raeissi, S. Modeling the Phase Behavior of Carbon Dioxide Solubility in Deep Eutectic Solvents with the Cubic Plus Association Equation of State. *J. Chem. Eng. Data* **2017**, Article AS, acs.jced.7b00472.
- (15) Haghbakhsh, R.; Parvaneh, K.; Raeissi, S.; Shariati, A. A General Viscosity Model for Deep Eutectic Solvents: The Free Volume Theory Coupled with Association Equations of State. *Fluid Phase Equilib.* **2017**, Article in, 1–10.
- (16) Sapei, E.; Zaytseva, A.; Uusi-Kyyny, P.; Keskinen, K. I.; Aittamaa, J. Vapor–Liquid Equilibrium for Binary System of Thiophene + N -Hexane at (338.15 and 323.15) K and Thiophene + 1-Hexene at (333.15 and 323.15) K. *J. Chem. Eng. Data* **2006**, 51 (6), 2203–2208.
- (17) Wolbach, J. P.; Sandler, S. I. Using Molecular Orbital Calculations To Describe the Phase Behavior of Hydrogen-Bonding Fluids. *Ind. Eng. Chem. Res.* **1997**, 36, 4041–4051.
- (18) Caßens, J. Modellierung Thermodynamischer Eigenschaften Pharmazeutischer Substanzen in Lösungsmitteln Und Lösungsmittelgemischen, Technische Universität Dortmund, 2013.
- (19) Rodriguez, N. R.; Requejo, P. F.; Kroon, M. C. Aliphatic–Aromatic Separation Using Deep Eutectic Solvents as Extracting Agents. *Ind. Eng. Chem. Res.* **2015**, 54 (45), 11404–11412.
- (20) Didaoui-Nemouchi, S.; Kaci, A. A. ENTHALPIES MOLAIRES D'EXCES DES MELANGES BINAIRES THIOPHENE ET DIETHYLSULFIDE AVEC N-ALCANES. *J. Therm. Anal. Calorim.* **2002**, 69, 669–680.

## 7 EXTRACTION OF THIOPHENE FROM {*n*-HEXANE + THIOPHENE} MIXTURES USING DEEP EUTECTIC SOLVENTS: A SENSITIVITY ANALYSIS

*In this chapter, a sensitivity analysis of the liquid extraction column using Aspen Plus<sup>®</sup> is reported. The influences of varying the solvent-to-feed ratio and the number of equilibrium stages on: (i) the thiophene recovery, (ii) the *n*-alkane recovery, (iii) the mass fraction of thiophene in the extract stream, and (iv) the mass fraction of *n*-alkane in the raffinate stream, were studied at 298 K and atmospheric pressure. The sensitivity analysis was done for the extraction of thiophene from {*n*-hexane + thiophene} mixtures using four different DESs: TEACl:EG (1:2), TEACl:Gly (1:2), THABr:EG (1:2), and THABr:Gly (1:2). TEACl:EG was found to be the best option meeting the product specifications.*



## 7.1 Introduction

Sensitivity analyses play an essential role in assessing the robustness of findings or conclusions based on the primary analysis of a data set. They are a critical way to assess the influence of key variations on the overall conclusions of a study. In this thesis, the liquid-liquid equilibrium (LLE) data of the ternary systems {*n*-alkane + thiophene + DES} were experimentally determined at 298.2 K and atmospheric pressure (see *Chapter 5*). The results suggested that DESs are potential candidates for desulfurization of oil fuels. The LLE data can be further utilized to optimize the design parameters of liquid-liquid extraction processes (e.g. solvent-to-feed ratio and the number of equilibrium stages) to achieve the targeted extraction efficiency. In this chapter, a sensitivity analysis on the performance of a liquid extraction column was performed using Aspen Plus<sup>®</sup>. The influences of varying the solvent-to-feed ratio and the number of equilibrium stages on: (i) the thiophene recovery, (ii) the *n*-alkane recovery, (iii) the mass fraction of the thiophene in the extract stream, and (iv) the mass fraction of the *n*-alkane in the raffinate stream, were studied at 298.2 K and atmospheric pressure. The sensitivity analysis was done for the extraction of thiophene from {*n*-hexane + thiophene} mixtures using four different DESs, tetraethylammonium chloride:ethylene glycol (TEACl:EG) (1:2), tetraethylammonium chloride:glycerol (TEACl:Gly) (1:2), tetrahexylammonium bromide:ethylene glycol (THABr:EG) (1:2), and tetrahexylammonium bromide:glycerol (THABr:Gly) (1:2). These DESs were selected in order to further compare the role of the hydrogen bond acceptor (HBA) (TEACl-based DES vs THABr-based DES) and the role of the hydrogen bond donor (HBD) (polyols) on the process design parameters.

## 7.2 Procedure

Similar to ILs, DESs are not available in Aspen Plus<sup>®</sup> databanks. Thus, DESs should be first introduced to the software using a “user-defined” function. In this work the implementation of DESs in Aspen Plus<sup>®</sup> was adopted from the literature.<sup>1</sup> Given the LLE data of the ternary systems {*n*-hexane + thiophene + TEACl:EG}, {*n*-hexane + thiophene + TEACl:Gly}, {*n*-hexane + thiophene + THABr:EG}, and {*n*-hexane + thiophene + THABr:Gly}, the binary interaction parameters can be obtained by regression using the appropriate thermodynamic model. Based on previous studies,<sup>1-4</sup> the Non-Random Two-Liquid (NRTL) model was found to correlate well with experimental LLE data for the DES containing systems. Therefore, the NRTL model was also used in this work and the binary interaction parameters were calculated (see the Appendix, Table 2). Then, a sensitivity analysis of the liquid-liquid extraction column was performed using Aspen Plus<sup>®</sup>. A schematic diagram of the extraction column is shown in Figure 1, and the input data for the extractor and desired product specifications are listed in Table 1. The thiophene recovery and the *n*-hexane recovery were defined as follows:

$$\text{thiophene recovery (\%)} = \frac{\text{Mass flow of the thiophene in the extract}}{\text{Mass flow of the thiophene in the feed}} \quad (1)$$

$$n\text{-hexane recovery (\%)} = \frac{\text{Mass flow of the hexane in the raffinate}}{\text{Mass flow of the hexane in the feed}} \quad (2)$$

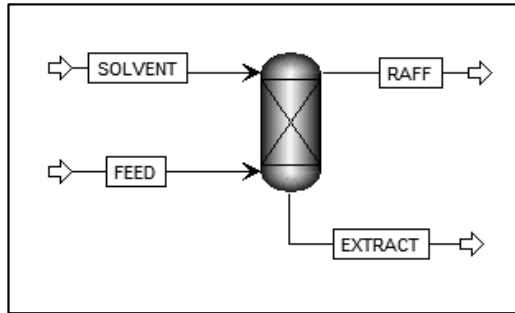


**Figure 1:** The simulated extraction column

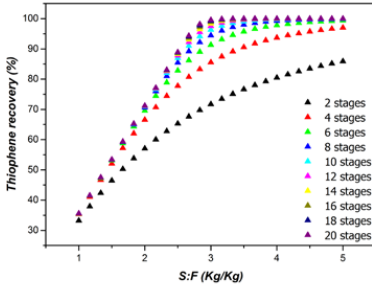
**Table 1:** Input data for the extraction column and the desired product specifications

<i>Temperature (K)</i>	298.2
<i>Pressure (Bar)</i>	1
<i>Feed (tonnes/hr)</i>	300
<i>Thiophene in the feed (wt%)</i>	10
<i>n-Hexane in the feed</i>	90
<i>Solvent purity (wt%)</i>	100
<i>Desired thiophene recovery (wt%)</i>	≥98
<i>Desired n-hexane recovery (wt%)</i>	≥98
<i>Desired thiophene purity (wt%)</i>	≥99
<i>Desired n-hexane purity (wt%)</i>	≥99

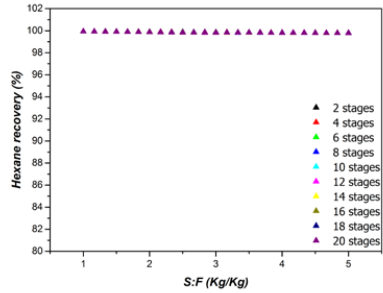
### 7.3 Results and discussion

The obtained results of the sensitivity analysis are shown in Figures 2-5 for the extraction thiophene from {*n*-hexane + thiophene} mixtures with TEACl:EG (1:2), TEACl:Gly (1:2), THABr:EG (1:2), and THABr:Gly (1:2), respectively.

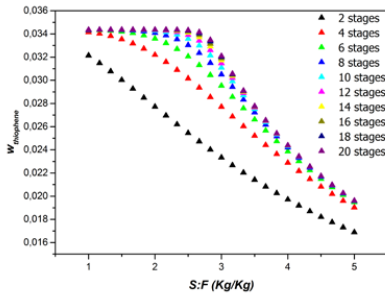
(a)



(b)



(c)



(d)

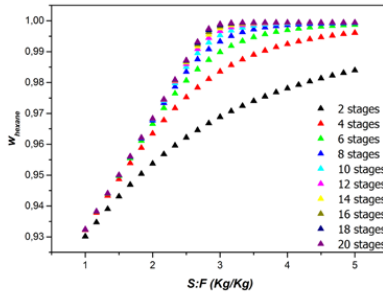
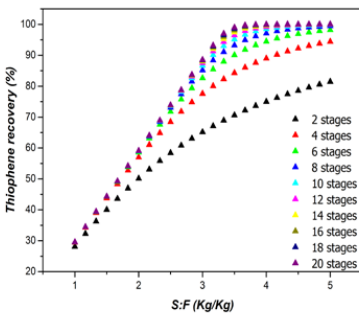
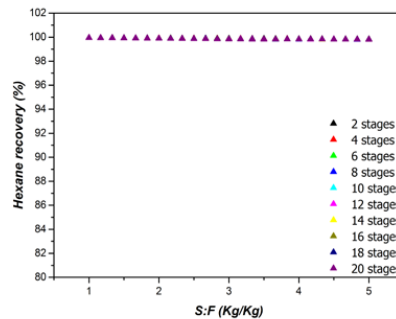


**Figure 2:** Sensitivity analysis for the ternary system {*n*-hexane + thiophene + TEACl:EG}. Figures (a) and Figure (b) show the thiophene recovery and the *n*-hexane recovery, respectively, as a function of the solvent-to-feed ratio and the number of equilibrium stages. Figure (c) shows the composition of thiophene in the extract and, Figure (d) shows the composition of *n*-hexane in the raffinate, as a function of the solvent-to-feed ratio and the number of equilibrium stages. The extraction was performed at 298.2 K and 1 bar.

(a)

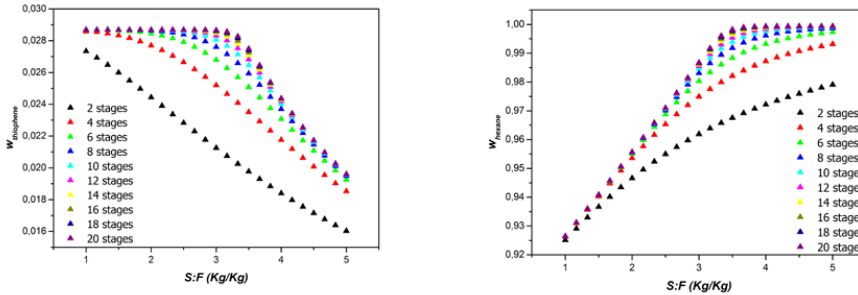


(b)



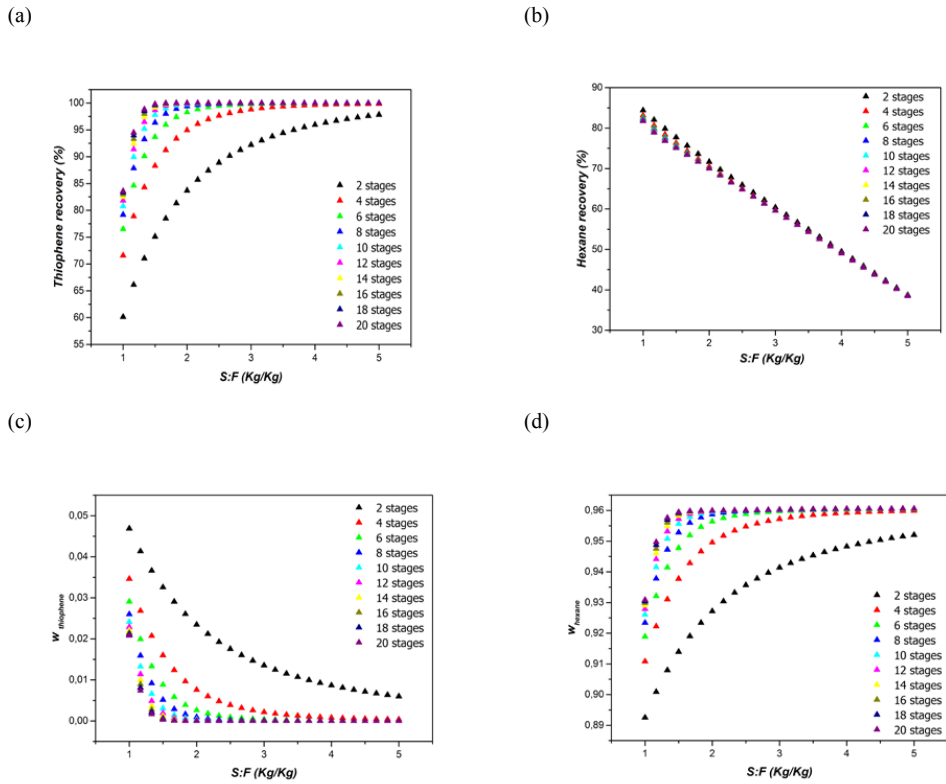
(c)

(d)

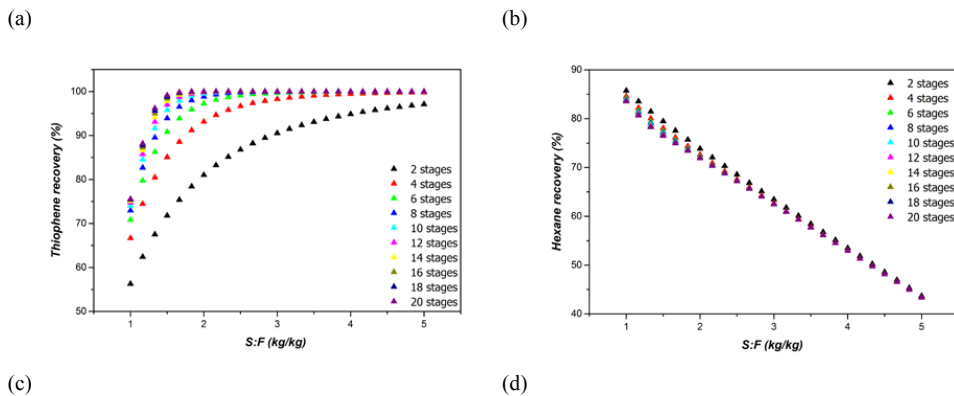


**Figure 3:** Sensitivity analysis for the ternary system  $\{n\text{-hexane} + \text{thiophene} + \text{TEACl:Gly}\}$ . Figures (a) and Figure (b) show the thiophene recovery and the  $n$ -hexane recovery, respectively, as a function of the solvent-to-feed ratio and the number of equilibrium stages. Figure (c) shows the composition of thiophene in the extract and, Figure (d) shows the composition of  $n$ -hexane in the raffinate, as a function of the solvent-to-feed ratio and the number of equilibrium stages. The extraction was performed at 298.2 K and 1 bar.

From Figures 2a and 3a it can be observed that the thiophene recovery was enhanced by increasing the solvent-to-feed ratio and the number of equilibrium stages. Furthermore, due to the high selectivity of both DESs “TEACl:EG and TEACl:Gly” full recovery of the  $n$ -hexane can be obtained (see Figures 2b and 3b). Moreover, it can be seen that the  $n$ -hexane recovery was not influenced by both the solvent-to-feed ratio or the number of equilibrium stages. The mass fraction of the thiophene in the extract decreased with increasing solvent-to-feed ratios and increased with increasing the number of equilibrium stages, as shown in Figures 2c and 3c. Moreover, the raffinate purity (Figures 2d and 3d) was promoted by increasing both the solvent-to-feed ratio and the number of equilibrium stages. Using TEACl:EG, in an extraction column of 10 equilibrium stages or more with a solvent-to-feed ratio of 3 or more can fulfill the desired product specifications. While for TEACl:Gly, a solvent-to-feed ratio of 4 or more and 10 equilibrium stages are needed for the fulfillment of the product specification. For the same thiophene recovery and the same number of stages a higher amount of solvent was needed when TEACl:Gly was used. This result was expected because the thiophene distribution ratio of the TEACl:Gly is lower.



**Figure 4:** Sensitivity analysis for the ternary system {*n*-hexane + thiophene + THABr:EG}. Figures (a) and Figure (b) show the thiophene recovery and the *n*-hexane recovery, respectively, as a function of the solvent-to-feed ratio and the number of equilibrium stages. Figure (c) shows the composition of thiophene in the extract and, Figure (d) shows the composition of hexane in the raffinate, as a function of the solvent-to-feed ratio and the number of equilibrium stages. The extraction was performed at 298.2 K and 1 bar.



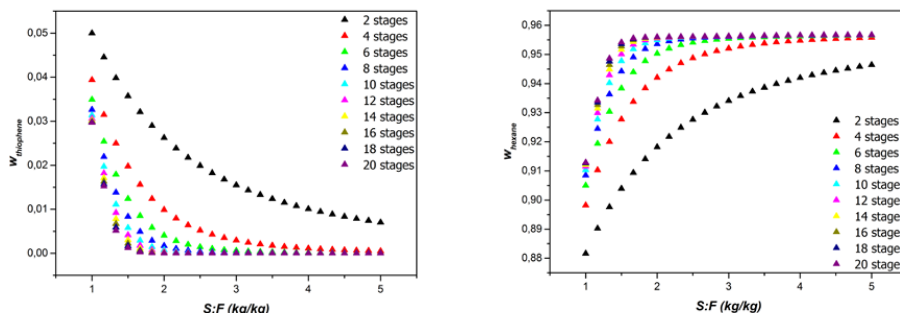


**Figure 5:** Sensitivity analysis for the ternary system  $\{n\text{-hexane} + \text{thiophene} + \text{THABr:Gly}\}$ . Figures (a) and Figure (b) show the thiophene recovery and the *n*-hexane recovery, respectively, as a function of the solvent-to-feed ratio and the number of equilibrium stages. Figure (c) shows the composition of thiophene in the extract and, Figure (d) shows the composition of *n*-hexane in the raffinate, as a function of the solvent-to-feed ratio and the number of equilibrium stages. The extraction was performed at 298.2 K and 1 bar.

Figure 4a shows the thiophene recovery as a function of the solvent-to-feed ratio and the number of stages for the THABr:EG. It was observed that a solvent-to-feed ratio of only 1.3 is required to achieve a recovery of aromatics of 98% using an extraction column of 16 stages. As shown in the figure, the increase in both the number of equilibrium stages and the solvent-to-feed ratio increases the aromatics recovery. However, the highest *n*-hexane recovery that can be reached with this DES is lower than 85% (see Figure 4b). This can be attributed to the low selectivity of this DES. The *n*-hexane recovery is decreased by an increase in the solvent-to-feed ratio, while it was hardly affected by the number of equilibrium stages.

Figure 4c and 4d show the content of the thiophene in the extract and the content of the *n*-hexane in the raffinate, respectively. As can be observed, the thiophene content in the extract decreases with the solvent-to-feed ratio and with the number of equilibrium stages. The opposite is true for the *n*-hexane concentration in the raffinate, that is positively affected by an increase of the solvent-to-feed ratio and the number of equilibrium stages.

Regarding the results of the THABr:Gly, shown in Figure 5, the trends observed for the thiophene recovery, the *n*-hexane recovery, the mass fraction of the thiophene in the extract and the *n*-hexane concentration in the raffinate are similar compared to the DES THABr:EG. Nevertheless, a solvent-to-feed ratio of 1.5 is required using an extraction column of 14 stages or more for a thiophene recovery above 98%, while the highest *n*-hexane recovery that can be reached is 86%. As expected, for the same aromatic recovery, THABr:Gly requires a larger amount of solvent than THABr:EG. This is because the aromatic distribution ratio of the THABr:EG is higher.

From the above sensitivity analysis, the influence of the HBA (TEACl-based DES vs THABr-based DES) on the process design parameters can be compared. The longer the alkyl-chain length of the cation of the HBA, the lower the solvent-to-feed ratio and the higher the number of required equilibrium

stages. Also, due to the higher solubility of the *n*-alkane in the longer alkyl chain length DESs, and therefore lower selectivity, full recovery of the *n*-alkane cannot be reached. The resulted raffinate requires further purification in order to meet the desired product specifications. Furthermore, the usage of ethylene glycol DESs results in a lower required solvent-to-feed ratio compared to the glycerol-based DESs. However, due to the higher selectivity of the glycerol-based DESs, a better *n*-alkane recovery can be obtained.

According to the described specifications (see Table 1), among the four DESs studied, the DES TEACl:EG was found to be the best candidate for this extraction. Due to the following: (i) almost full recovery of both thiophene and the *n*-alkane in the extract and raffinate phase, respectively, (ii) in the ideal scenario, the purity of the raffinate can be greater than 99%. This is very beneficial, because this implies that the raffinate phase does not require any additional separation process. Additionally, the *n*-alkane content of the extract phase is negligible; therefore, the extract, essentially thiophene and DES, can be directly separated in the flash and the DES can further be recycled. In *Chapter 5*, on lab scale, it was proven that DESs can be successfully recovered via rotary evaporator under vacuum. In principle, lowering the pressure, lowers the boiling points of compounds resulting in evaporation of the thiophene. this validates our assumption of full recovery of the DES using a flash on an industrial scale.

Catalytic hydrodesulfurization (HDS) has been the conventional approach applied by oil refineries to capture sulfur and sulfur compounds. This approach is based on hydrotreating the sulfur-containing fuel under elevated temperatures (573.2–673.2 K), as well as elevated pressures (3.5–7.0 MPa), which results in high hydrogen consumption, and an expensive and energy-intensive method. Additionally, hydrogen in fuels considerably lowers its cetan number.<sup>5</sup> Therefore, the proposed desulfurization method “extractive desulfurization using DESs” might overcome the mentioned disadvantages, since the extraction is conducted at milder operating conditions and no hydrogen is required.

It should be noted that, the results of the sensitivity analysis presented in this chapter are only preliminary assuming a very simple oil model of {*n*-alkane + thiophene}. Also, only four DESs were studied. Experimental investigations are needed in order to find DESs with higher distribution ratios but still high selectivities. Moreover, extensive characterization of the DESs is highly needed in order to accurately define the DESs in simulation software such as Aspen Plus®. Nevertheless, the desulfurization of fuel using DESs is a promising approach with a widely open future for further optimization.

#### 7.4 Conclusions

In this chapter, a sensitivity analysis of the liquid extraction column for the separation of thiophene from {*n*-hexane + thiophene} mixtures using DESs, was performed via Aspen Plus®. Four different DESs: TEACl:EG (1:2), TEACl:Gly (1:2), THABr:EG (1:2), and THABr:Gly (1:2) were

---

selected for this extraction. The solvent-to-feed ratio and the number of equilibrium stages was varied in a systemic way and their influences on: (i) the thiophene recovery, (ii) the *n*-alkane recovery, (iii) the mass fraction of the thiophene in the extract stream, and (iv) the mass fraction of the *n*-alkane in the raffinate stream, were reported. It was found that the higher the thiophene distribution ratio, the lower the amount of solvent required for the targeted recovery. Moreover, it was also found that the higher the selectivity, the higher the *n*-alkane recovery as well as the purity of the raffinate. The *n*-alkane recovery was found to be very sensitive to the selectivity of the DES. Essentially, for highly selective DESs, almost full recovery of the *n*-alkane can be obtained. Furthermore, an extract almost *n*-alkane-free can be obtained which be directly sent to a flash column to recycle the solvent. TEACl:EG was found to be the best option compared to the other three DESs, because the desired product specifications can be fulfilled in an extraction column of 10 equilibrium stages or more with a solvent-to-feed ratio of 3 or more.



---

## 7.5 References

- (1) Rodriguez, N. R. *Azeotrope Breaking Using Deep Eutectic Solvents* Azeotrope Breaking Using Deep Eutectic Solvents, Technische Universiteit Eindhoven, 2016.
- (2) Warrag, S. E. E.; Rodriguez, N. R.; Nashef, I. M.; van Sint Annaland, M.; Siepmann, J. I.; Kroon, M. C.; Peters, C. J. Separation of Thiophene from Aliphatic Hydrocarbons Using Tetrahexylammonium-Based Deep Eutectic Solvents as Extracting Agents. *J. Chem. Eng. Data* **2017**, *62* (9), 2911–2919.
- (3) Hadj-Kali, M. K.; Mulyono, S.; Hizaddin, H. F.; Wazeer, I.; El-Blidi, L.; Ali, E.; Hashim, M. A.; AlNashef, I. M. Removal of Thiophene from Mixtures with *N*-Heptane by Selective Extraction Using Deep Eutectic Solvents. *Ind. Eng. Chem. Res.* **2016**, *55* (30), 8415–8423.
- (4) Rodriguez, N. R.; Requejo, P. F.; Kroon, M. C. Aliphatic–Aromatic Separation Using Deep Eutectic Solvents as Extracting Agents. *Ind. Eng. Chem. Res.* **2015**, *54* (45), 11404–11412.
- (5) Talibi, M.; Hellier, P.; Balachandran, R.; Ladommatos, N. Effect of Hydrogen-Diesel Fuel Co-Combustion on Exhaust Emissions with Verification Using an in-Cylinder Gas Sampling Technique. *Int. J. Hydrogen Energy* **2014**, *39* (27), 15088–15102.

## 7.6 Appendix chapter 7

The experimentally obtained LLE data were correlated using the non-random two liquid (NRTL) model. The root mean square deviation (RMSD %) from the experimental data was calculated as:

$$\text{RMSD}(\%) = 100 * \sqrt{\frac{(w_{\text{hex}}^{\text{exp}} - w_{\text{hex}}^{\text{cal}})^2 + (w_{\text{thio}}^{\text{exp}} - w_{\text{thio}}^{\text{cal}})^2 + (w_{\text{DES}}^{\text{exp}} - w_{\text{DES}}^{\text{cal}})^2}{2MN}} \quad (3)$$

where  $w_i^{\text{exp}}$  and  $w_i^{\text{cal}}$  are the experimentally obtained and the calculated mass fractions of the compound  $i$ , respectively.  $M$  is the number of tie-lines and  $N$  is the number of compounds.

The LLE data were regressed using Aspen Plus. The estimated values of the binary parameters and the deviation for the experimental data are presented in Table 2.

**Table 2:** The binary interaction parameters for the NRTL model and the root mean square deviation (RMSD %) from the experimentally determined ternary LLE

Component i	Component j	$a_{ij}$ (J.K <sup>-1</sup> .mol <sup>-1</sup> )	$a_{ji}$ (J.K <sup>-1</sup> .mol <sup>-1</sup> )	$b_{ij}$ (J.mol <sup>-1</sup> )	$b_{ji}$ (J.mol <sup>-1</sup> )	$c_{ij}$	RMSD (%)
<i>n</i> -Hexane	Thiophene	-0.1	0.9	101.8	477.5	0.3	3.2
<i>n</i> -Hexane	TEACl:EG	2.1	2.7	477.5	641.8	0.3	
Thiophene	TEACl:EG	1.1	0.4	315.2	137.0	0.3	
<i>n</i> -Hexane	Thiophene	5.5	-12.2	-1826.1	4138.2	0.2	0.7
<i>n</i> -Hexane	TEACl:Gly	17.7	-79.9	-1616.3	25630.4	0.2	
Thiophene	TEACl:Gly	0.4	-29.1	3757.0	8960.3	0.2	
<i>n</i> -Hexane	Thiophene	-6.9	25.0	-5672.4	21400.7	0.3	0.3
<i>n</i> -Hexane	THABr:EG	5.0	-1.3	2304.7	1834.5	0.3	
Thiophene	THABr:EG	50.4	4.1	15098.7	1505.1	0.3	
<i>n</i> -Hexane	Thiophene	5.7	25.4	-2017.4	-6880.4	0.3	0.2
<i>n</i> -Hexane	THABr:Gly	10.8	8.2	-3023.6	-1704.8	0.3	
Thiophene	THABr:Gly	64.8	-14.2	-14772.6	4116.0	0.3	

## 8 CONCLUSIONS & RECOMMENDATIONS

*In this chapter, the main conclusions are summarized. Moreover, some recommendations are given for future development of this research.*

## 8.1 Conclusions

In this thesis, the performance of DESs to capture impurities from oil and gas was investigated. The main objective was to propose novel solutions to some industrial challenges in the purification of oil and gas. Particularly capturing mercury, CO<sub>2</sub> capture and oil desulfurization were investigated from a thermodynamic point of view.

DESs were considered as extractants of elemental mercury (Hg<sup>0</sup>) from oil. Four DESs were prepared; choline chloride:urea, choline chloride:ethylene glycol, choline chloride: levulinic acid, and betaine: levulinic acid, all in molar ratios of 1:2. The DESs were first tested for their thermal stability by observing their degradation, and for their transport properties by determining glass transition temperatures and measuring viscosities. The densities and viscosities of the DESs were determined at temperatures from 298.2 to 333.2 K and atmospheric pressure. Next, the extraction efficiency for the system [dodecane + Hg<sup>0</sup> + DES] was determined by direct solvent-feed extraction in ratios of 1:1 and 2:1 at T = 303.2 and 333.2 K and atmospheric pressure. All four DESs were found to be very good extraction solvents with extraction efficiencies exceeding 80% for 1:1 and 2:1 solvent:feed ratios and Gibbs free energies of transfer from *n*-dodecane to DES being negative (i.e., favorable) with a magnitude from about 4 to 14 kJ mol<sup>-1</sup>.

DESs were also assessed as absorbents for CO<sub>2</sub>. Two DESs composed of tetrahexylammonium bromide as a hydrogen bond acceptor (HBA) and either ethylene glycol or glycerol as a hydrogen bond donor (HBD) with molar ratios of HBA:HBD equal to 1:2. The CO<sub>2</sub> uptakes in the DESs were measured using a magnetic suspension balance (MSB) at 293.2 K and 298.2 K and pressures up to 2 MPa. It was observed that the CO<sub>2</sub> solubility increased with pressure and decreased with temperature, as expected. The Henry's law constants and the enthalpy of absorption were calculated for the investigated DESs and compared to the relevant literature. THABr:Gly showed the highest Henry's law constant among all other solvents, and therefore the lowest solubility, while the Henry's law constant of THABr:EG was found to be comparable to those of the hydrophobic DESs. Furthermore, the enthalpy of absorption was found to be comparable to those of the physical solvents. In spite of the low CO<sub>2</sub> solubilities observed in the studied DESs, the results are promising and with further research and optimization DESs can be a low-cost and sustainable alternative for CO<sub>2</sub> capture.

Extractive desulfurization of oil using DESs was also studied in this work. Six different DESs were evaluated for their extraction properties of sulfur compounds from *n*-alkane hydrocarbons via liquid-liquid equilibrium (LLE). The oil models were: {*n*-hexane + thiophene} and {*n*-octane + thiophene}. The selected DESs were: (i) tetraethylammonium chloride:ethylene glycol (TEACl:EG) with molar ratio of 1:2, (ii) tetraethylammonium chloride:glycerol (TEACl:Gly) with molar ratio of 1:2, (iii) tetrahexylammonium bromide:ethylene glycol (THABr:EG) with molar ratio of 1:2 and (iv) tetrahexylammonium bromide:glycerol (THABr:Gly) with molar ratio of 1:2, (v) methyltriphenylphosphonium bromide:ethylene glycol (MTPPBr:EG) with molar ratio of 1:3 and (vi) methyltriphenylphosphonium bromide:glycerol (MTPPBr:Gly) with molar ratio of 1:3. The objective

of this study was to provide insights on: (i) the LLE  $\{n\text{-alkane} + \text{thiophene} + \text{DES}\}$  systems, (ii) the effect of type/length of the  $n\text{-alkane}$ , (iii) the influences and/or characteristics of the HBAs different chain length of the alkyl group and the functional group on the ammonium cation, (iv) and HBDs type of the polyol and on the extraction of thiophene from  $\{n\text{-alkane} + \text{thiophene}\}$  mixture. First, the solubility of the thiophene,  $n\text{-hexane}$  and  $n\text{-octane}$  in the DESs at 298.2 K and atmospheric pressure was determined. Then, the liquid–liquid equilibrium (LLE) data of the ternary systems  $\{n\text{-hexane} + \text{thiophene} + \text{DESs}\}$  and  $\{n\text{-octane} + \text{thiophene} + \text{DESs}\}$  were measured at 298.2 K and atmospheric pressure. Further, the solute distribution ratios and the selectivities were calculated from the experimental LLE data.

The solute distribution coefficients obtained for the ethylene glycol-based DESs are always higher than those of glycerol based-DESs. The thiophene distribution coefficients were independent of the thiophene concentration. This means that the thiophene concentration in the system does not affect the extraction efficiency of the considered DESs. Also, the longer the alkyl chain length of the HBA, the higher the thiophene distribution coefficient. Moreover, it was found that, for the same DES, roughly similar distribution coefficients and lower selectivities were obtained for the  $\{n\text{-hexane} + \text{thiophene} + \text{DES}\}$  system compared to the  $\{n\text{-octane} + \text{thiophene} + \text{DES}\}$  system.

The Conductor-like Screening Model for Real Solvents (COSMO-RS) was used to better understand the extraction mechanism of thiophene. Based on the  $\sigma$ -profiles, it was observed that the dominant interaction between thiophene and DESs is the electrostatic interaction, with negligible and/or absent hydrogen bonding interaction. Regeneration of the DESs has been successfully achieved by means of vacuum evaporation. On the basis of the obtained distribution coefficients and selectivities, DESs were found to be competitors for the desulfurization of fuels to ILs with almost similar performance but lower price.

The Perturbed-Chain Statistical Associating Fluid Theory (PC-SAFT) was used to predict the phase behavior of the 12 measured ternary systems. It was found that the distribution coefficient of thiophene and the selectivity of thiophene over the  $n\text{-alkane}$  in the ternary systems containing DESs can be qualitatively well predicted using PC-SAFT. PC-SAFT captured “qualitatively” the main observations, particularly that, the longer the alkyl chain length on the HBA, the higher the thiophene distribution coefficient, but the lower the selectivity for both alkanes ( $n\text{-hexane}$  and  $n\text{-octane}$ ). Moreover, higher selectivities and slightly lower distribution ratios were obtained when thiophene was extracted from  $n\text{-octane}$  instead of  $n\text{-hexane}$ . It can be concluded that DESs are promising candidates for extractive desulfurization of fuels, and that PC-SAFT serves as an appropriate approach for predictive solvent screening in order to obtain a thermodynamically optimal DES.

Last but not the least, a sensitivity analysis of the liquid extraction column for the separation of thiophene from  $\{n\text{-hexane} + \text{thiophene}\}$  mixtures using DESs, was performed via Aspen Plus®. Four different DESs: TEACl:EG (1:2), TEACl:Gly (1:2), THABr:EG (1:2), and THABr:Gly (1:2) were

selected for this study. The solvent-to-feed ratio and the number of equilibrium stages was varied in a systemic way and their influences on: (i) the thiophene recovery, (ii) the *n*-alkane recovery, (iii) the mass fraction of the thiophene in the extract stream, and (iv) the mass fraction of the *n*-alkane in the raffinate stream, were reported. It was found that the higher the thiophene distribution ratio, the lower the amount of solvent required for the targeted recovery. Moreover, it was also found that the higher the selectivity, the higher the *n*-alkane recovery as well as the purity of the raffinate. The *n*-alkane recovery was found to be very sensitive to the selectivity of the DES. Essentially, for highly selective DESs, almost full recovery of the *n*-alkane can be obtained. Furthermore, an extract almost *n*-alkane-free can be obtained which can be directly sent to a flash column to recycle the solvent. TEACl:EG was found to be the best solvent compared to the other three DESs, because the desired product specifications can be fulfilled in an extraction column of 10 equilibrium stages or more with a solvent-to-feed ratio of 3 or more.

## 8.2 Recommendations

Throughout this thesis “Capturing Impurities from Oil and Gas Using Deep Eutectic Solvents”, one might observe that the application of DESs as a separating agent for targeted impurities is indeed promising. However, the DESs selected for each application was based on either previous literature or an educated guess that a particular DES might work until further proven by experiment. There are still many gaps that need to be filled in the future of the DES research.

A DES is known to have negligible vapor pressure as result of a combination of entropic effects and a wide variety of intermolecular interactions. Understanding the nature of these intermolecular interactions would significantly help to systematically select the constituents of a DES for a particular application. Molecular dynamics (MD) could provide detailed information about the molecular interactions within the DES and its physicochemical properties. It could also predict the suitability of the DES for a specific application with a great accuracy. It might be challenging, however possible, to develop force fields that can be applied to all intermolecular interactions associated with DESs and thus improve the accuracy of the predicted properties. Experimental data are highly desirable. Very few (MD) studies have been reported in the literature, that have mostly focused on the formation and the physicochemical properties of choline chloride/urea DES.<sup>1-6</sup> It is highly recommended to enrich this type of studies in the DES research field.

Experimental studies on DES physicochemical properties are still scarce. There is also lack of safety, health and environmental studies. Long term stabilities and corrosivities of DESs have hardly been assessed, hampering industrial application. Additionally, there is also an absence of systematic studies to determine the effects of the salt and hydrogen-bond-donor type and the molar ratio in the mixture on the physicochemical properties of the DESs.

Regarding the applicability of DESs in mercury capture, in this thesis only four DESs were assessed. There is a plenty of room to further extend this study. For example, studying the effect of the halide anion of the salt (e.g. Br<sup>-</sup> containing salts), different molar ratios of the HBA and the HBD, and the recyclability of the DES. The emergence of hydrophobic DESs,<sup>7</sup> might also open the door for the investigation of the removal of mercury from wastewater streams of power plants.

Regarding, the CO<sub>2</sub> capture, only two out of virtually infinite combinations of HBAs and HBDs were applied. However, there is an exponential increase on the publications on CO<sub>2</sub> capture appearing in the literature. The influence of the DES' constituents and conditions on the binary phase behavior is extensively studied, although there is not (yet?) a standard approach or IUPAC standard DES available for comparison and reproducibility reasons. Combined experimental and modeling approaches are required to develop and design novel DESs with specific physicochemical properties for dedicated applications involving CO<sub>2</sub> capture, and in this respect there is still a lot of work to be done. Moreover, the influence of other species present in natural gas, such as N<sub>2</sub>, H<sub>2</sub>O, H<sub>2</sub>S and others is extremely important. So far, selectivity studies are fully absent, and the gas solubility measurements mainly focus on CO<sub>2</sub> only (only a few studies on SO<sub>2</sub> solubilities are also available). Phase equilibria of multi-

component DES + CO<sub>2</sub> systems are also very interesting for other applications (besides CO<sub>2</sub> capture), including the use of supercritical CO<sub>2</sub> as an extracting agent for the recovery of products from DESs

Extractive desulfurization of oil using DESs showed promising results. Therefore, further research is recommended. Based on the results obtained, many factors were found to influence the extraction efficiency. I encourage further studies on the following:

- (i) The nature of the DES HBA and HBD and the type of interactions between the DES and the sulfur compound.
- (ii) Oil contains a series of hydrocarbons ranging from C<sub>1</sub> up to more than C<sub>100</sub>. It was already clear that the carbon number would affect the selectivity, thus further research is encouraged. Hydrocarbons are known to follow the “principle of congruence”. It would be interesting to test this phenomena on the extractive desulfurization of oil using DESs, as it could save tremendous effort on the DES selection.
- (iii) Oil also contains a large variety of organosulfur compounds, including thiols (R-S), sulfides (R-S-R), and sulfur-containing aromatics (“thiophene’s family”); a thorough research on the different species is recommended, especially the ones with strong steric hindrance, such as dibenzothiophene.
- (iv) Furthermore, oil contains aromatics, such as benzene, toluene, etc. They have a strong affinity to DESs.<sup>8-10</sup> Studying the selectivity of the DES for sulfur compounds in the presence of aromatic compounds is of great interest.

In order to apply the DES on an industrial scale, long-term use stability of the solvent should be investigated. For example, the number of the re-use experiments for the same DES and the extraction efficiency losses should be investigated. Thereafter, pilot plant experiments, including the solvent recovery process, should be performed.

To conclude, as sustainable solvents, DESs are expected to play a significant role in the future. The economic value, efficiency, cleanness and renewability of DESs are all very attractive properties for large scale investment in the field of oil and gas processing.



## ABOUT THE AUTHOR

Samah Esam-Eldin Warrag was born on May 8<sup>th</sup>, 1990 in Florida (United States). In November 2006, she started her Bachelor degree (B.Sc.) in chemical engineering at the University of Khartoum (Sudan). She was one of the top students during all her studying years and she graduated, in June 2011, with First Class “Honors”. Her graduation research project titled “Production of *n*- Butanol from Molasses via Fermentation” achieved a distinction mark.

In November 2011, she moved to Qatar to work in a research laboratory “Fuel Characterization Lab”, as a research assistant, at Texas A&M University at Qatar, a branch campus of Texas A and M University. She worked in a research project focused on the formulation and characterization of new generations of synthetic fuels obtained from natural gas via gas-to-liquid (GTL) technology under the supervision of Prof. N. Elbashir.

September 2012, Samah was admitted to the Master of Science in Chemical Engineering Program at Texas A&M University at Qatar. Her M.Sc. thesis entitled “Multiphase Equilibrium of Fluids confined in Fischer-Tropsch Catalytic Systems” under the joint supervision of Prof. Nimir O. Elbashir and Prof. Marcelo Castier. She received the Richard E. Ewing award for excellence in student research for her M.Sc. thesis in April 2014. And she got her M.Sc. degree “with Honors” in May 2014.

Upon her graduation, in September 2014, she moved to the United Arab Emirates and joined the Petroleum Institute (PI), Abu Dhabi. She was appointed as a research assistant in a collaborative project at the Petroleum Institute (PI) and at the University of Minnesota from the Petroleum Institute Research Center (PIRC) through a grant entitled “Advanced PVT-Properties and Molecular Modeling of Complex Fluids in Support of Safe and Green Hydrocarbon Production” under the supervision of Prof. Cor J. Peters and Prof. Ilja J. Siepmann. The experimental activities of this project were conducted at Eindhoven University of Technology (TUE) where Samah started her PhD under the supervision of Prof. Maaïke C. Kroon in the Separation Technology Group (SEP). The research results have been disseminated in peer-reviewed scientific journals and presented at international conferences. In May 2016, she moved to the Process Intensification Group (SPI) in TUE to continue her PhD research under the supervision of Prof. Martin van Sint Annaland.

## CONTRIBUTIONS AND PUBLICATIONS

### Publications in peer-reviewed journals

- 1- **S. E. E Warrag**, D. J. G. P. van Osch, E. O. Fetisov, D. B. Harwood, M. C. Kroon, J. I. Siepmann, C. J. Peters” Mercury Capture from Petroleum Using Deep Eutectic Solvents”, *Submitted to the Journal of Industrial & Engineering Chemistry Research*, **2018**.
- 2- **S. E. E Warrag**, C. J. Peters, M. C. Kroon” Deep Eutectic Solvents for Highly Efficient Separations in Oil and Gas Industries” *Current Opinion in Green and Sustainable Chemistry*, **2017**, 5, 55–60.
- 3- **S. E. E Warrag**, N. R. Rodriguez, I. M. Nashef, M. Annaland, M. C. Kroon, C. J. Peters, “Separation of Thiophene from Aliphatic Hydrocarbons Using Tetrahexylammonium-Based Deep Eutectic Solvents as Extracting Agents” *Journal of Chemical & Engineering Data*, **2017**, 62, 2911–2919.
- 4- **S. E. E Warrag**, C. Pototzki, N. R. Rodriguez, M. Annaland, M. C. Kroon, C. Held, G. Sadowski, C. J. Peters, “Oil Desulfurization Using Deep Eutectic Solvents as Sustainable and Economical Extractants via Liquid-Liquid Extraction: Experimental and PC-SAFT Predictions” *Fluid Phase Equilibria*, **2018**, 467, 33-44.
- 5- **S. E. E Warrag**, I. Adeyemi, N. R. Rodriguez, I. M. Nashef, M. Annaland, M. C. Kroon, C. J. Peters, “Effect of the Type of Ammonium Salt on the Extractive Desulfurization of Fuels using Deep Eutectic Solvents” *Journal of Chemical & Engineering Data*, **2018**, 63, 1088-1095.
- 6- E. O. Fetisov, D. B. Harwood, I. Kuo, **S. E. E. Warrag**, M. C. Kroon, C. J. Peters, and J. I. Siepmann, “ First-Principles Molecular Dynamics Study of a Deep Eutectic Solvent: Choline Chloride/Urea and Its Mixture with Water” *Journal of Physical Chemistry B*, **2018**, 122, 1245-1254.
- 7- **S. E. E. Warrag**, M. C. Kroon, C. J. Peters” Mercury Capture from Petroleum Using Deep Eutectic Solvents”, *Patent ref. no.: A149669WO*.
- 8- **S. E. E. Warrag**, Muhammad N. Khan, M. C. Kroon, C. J. Peters” *The Solubility of CO<sub>2</sub> in Tetrahexylammonium Bromide based-Deep Eutectic Solvents” To be submitted to the Journal of Chemical Engineering Data.*

## Contributions in conferences:

1. **S. E. E Warrag**, N. R. Rodriguez, M. Annaland, J. I. Siepmann, M. C. Kroon, C. J. Peters, “Oil Desulfurization Using Deep Eutectic Solvents via Liquid-Liquid Extraction” *American Institute of Chemical Engineers (AIChE)*, **2017**, Minneapolis, Minnesota.
2. **S. E. E Warrag**, N. R. Rodriguez, M. Annaland, J. I. Siepmann, M. C. Kroon, C. J. Peters, “Separation of Thiophene from Aliphatic Hydrocarbons Using Tetrahexylammonium-Based Deep Eutectic Solvents as Extracting Agents”, *29th European Symposium on Applied Thermodynamics (ESAT)*, **2017**, Bucharest, Romania.
3. J. I. Siepmann, E. O. Fetisov, D. B. Harwood, **S. E. E Warrag**, C. J. Peters,” First Principles Molecular Dynamics Simulations of Deep Eutectic Solvent Systems” *American Institute of Chemical Engineers (AIChE)*, **2015**, Salt Lake City, Utah.

## ACKNOWLEDGEMENTS

The American writer Rita Brown once wrote that “the recipe for happiness is very simple: someone to love, something to do, and something to look forward to”. In my opinion, these three ingredients of happiness can be achieved once you define what are your goals and dreams in life. To me and since really long time ago, I decided that I want to be a teacher one day, following the footprint of my father who will always be my role model. Thus, my road map was clear that started with completing my B.Sc. degree, then my M.Sc. degree and here I am closing my Ph.D. degree and looking forward to start teaching career. I must say that I had a unique journey flying between two countries, United Arab Emirates “the Petroleum Institute (PI)” and the Netherlands “Eindhoven University of Technology (TU/e)”. I would like to deeply thank everyone who contributed to make this journey very wonderful and rewarding. I would like to express my sincere appreciation to everyone who supported me, helped me and inspired me. I have truly learned from each of you.

In the first place, I would like to thank my 1<sup>st</sup> co-promoter, Prof. Cor Peters for giving me the opportunity to do my Ph.D. I sincerely appreciate your strong trust and confidence in me. You have continued to trust me and support me from the day I joined your project and until this moment. Prof. Cor, I will never forget our very early morning meetings at PI. Our discussions with lovely morning coffee resulted in a Ph.D. thesis.

Also, I would like to deeply thank my 2<sup>nd</sup> co-promoter, Prof. Maaïke Kroon. Maaïke, I was really lucky to have the chance to be one of your students in the SEP group. Your kind, peaceful and supportive personality made you a wonderful professor. Maaïke, you have supported me immeasurably. You were always pushing me to innovate and publish papers. You trusted me and helped in every way possible and this is absolutely not strange for a person like you. You have also introduced me to Prof. Martin van Sint Annaland “My promoter”. Prof. Martin, no words can be enough to thank you for adopting me in your team ‘SPI’. You were always willing to help and support to the best you can and I sincerely appreciate that. Thank you professors!

I would like to thank Prof. Ilja Siepmann and his students Evgenii Fetisov and David Harwood for their great contribution to this thesis. I learned a lot from you. Also, teams from different universities have made this work successful. The team in TU Dortmund, I would like to acknowledge Prof. Gabriele Sadowski, Prof. Christoph Held and Clarissa Pototzki. The team in Masdar Institute, I would like to thank Prof. Inas Nashef and Dr. Idowu Adeyemi “Azeez”. And from the PI, I would like to thank Prof. Donald Reinalda, Naveed, Sabbir, Olamide, and Ruth.

Flying to Eindhoven for 6 month every year was always full of science, fun and many wonderful friends. I started in the SEP lab not knowing anything, everyone in SEP taught me something in the lab. I will start with Wilko, you have always been my problem solver. Our times with the Mercury analyzer and the GC are unforgettable. I really like how you make everything in life “not only in the lab” simple and full of fun. I enjoyed our 3 pm dutch coffee. Please keep your forever smile shining. Thank you Wilko for everything. Lawien, in 2015, you were not only in the office next door, but also in the house next door. I enjoyed a lot our evening walks back home after a long day. I enjoyed a lot your mum cookies, our arabic conversations and our TGA times. You always make fun of me “and of everything”, but I do like it. You are always ready to help everyone in the team with your knowledge, experience or even few words of encouragement. I wish you all the best in life. Adriaan “the gentle man”, I admire how you may give all your time helping others, you actually spend more than 2 hours teaching me on the NMR software. Dannie, working with you was super fun, I appreciate your great support. Our mercury experiments were really a nice opportunity to get to know a great person like you. I’m dead sure you will achieve all your goals because you’re very brilliant and hard worker. I wish all the best in life. Nerea, no words can describe how beautiful soul you are. Together we made 3 publications in 4 months of experiments, this has only one justification that you are awesome!. You write everything in lists and bullets in excel sheets, papers and tissue papers too!. You’re unique in everything and you will have a unique future too. All the best Nerea!. Carin “the always smiling lady” I wish if I knew you earlier before. You were my adopted sister in the SPI group. I enjoyed a lot our membrane conversations and I had really wonderful times with you and Michela. Thank you Carin for everything you did to me. I wish you all the best and keep smiling!. Maybe, we met in Abu Dhabi in my first visit to PI. You were so friendly, warm and kind and this is typically you. The list of the SEP team is getting longer, but still I would like to endlessly acknowledge, the loveliest couple “Sona & Ali” I’m keeping all your gifts, Laura, Mamoun and especially Caroline, each one of you added something to my journey. From the SPI, I would like to acknowledge Prof. Fausto Gallucci and Judith. Judith, thank you forever for all your help. You are very efficient and superfast answering emails. It’s amazing how you solve each and every administrative problem, without you, I wouldn’t have completed on time.

My family “parents and siblings”, no word could be enough to thank you. Dad, you have been no. 1 supporter. Your trust and confidence in me were my driving force to achieve my life goals. Thank you for your never-ending support and thank you for being my forever reference. My grandparents, thank you for none-stop prayers.

Last but indeed not least, Ashraf, we have met in the low times of this journey. You have always been my other pair of eyes looking at life differently. Your funny and dynamic spirit have added a spicy taste to my days. You stood by me and supported me to reach this moment. I still remember how you were always trying so hard “with your tough schedules” to come and see me. Trust me, these few hours

we met, made my days lovely. Also not forgetting our long phone calls, listening to all my stories were my relieve, your words were like the cold breeze to my heart. You have always been my home finder in every time I move, until you held my hands and took me to our forever home. All this has only one translation: "love". Thank you for your love, patience, endless support and thank you for completing me.

*Samah Esam-Eldin Warrag,*

*Eindhoven 2018*

